GEMS & GEMOLOGY

VOLUME XXXV SUMMER 1999

THE QUARTERLY JOURNAL OF THE GEMOLOGICAL INSTITUTE OF AMERICA

GEMS & GEMOLOGY
SUMMER 1999 VOLUME 35 NO. 2

TABLE OF CONTENTS


pg. 83

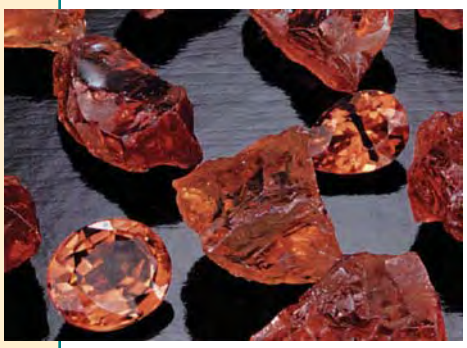
pg. 109

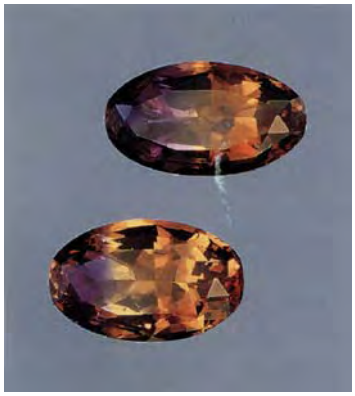
pg. 130

pg. 145

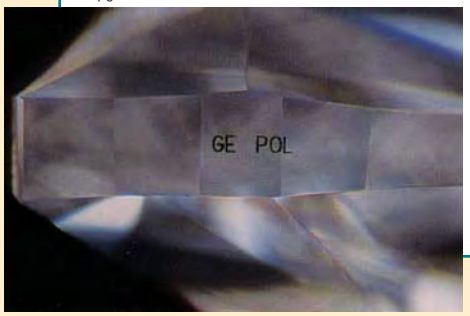

EDITORIAL

79 **Nothing Is as Simple as It Seems**
Alice S. Keller

80 **LETTERS**

FEATURE ARTICLES

82 **On the Identification of Various Emerald Filling Substances**
Mary L. Johnson, Shane Elen, and Sam Muhlmeister

108 **Sapphire and Garnet from Kalalani, Tanga Province, Tanzania**
Antonin V. Seifert and Jaroslav Hyrsl

122 **Russian Synthetic Ametrine**
Vladimir S. Balitsky, Taijin Lu, George R. Rossman, Irina B. Makhina, Anatolii A. Mar'in, James E. Shigley, Shane Elen, and Boris A. Dorogovin

REGULAR FEATURES

135 **1999 Challenge Winners**
136 **Gem Trade Lab Notes**
142 **Gem News**
156 **Thank You, Donors**
157 **Book Reviews**
160 **Gemological Abstracts**

ABOUT THE COVER: Emeralds typically contain numerous fractures when recovered, and yet consumers have high expectations for their clarity as well as color. As a result, the overwhelming majority of emeralds on the market today have undergone some form of clarity enhancement. The proliferation of filler substances in recent years has raised widespread concern in the trade about their identity and durability. The lead article in this issue reviews the history of emerald clarity enhancement and the current situation in the trade. It then focuses on possible methods of distinguishing among different clarity-enhancement substances.

The emerald cabochon in this Sabi-finish gold necklace weighs 77.68 ct. Courtesy of Henry Dunay Designs Inc., New York.

Photo © Harold & Erica Van Pelt—Photographers, Los Angeles, California.

Color separations for Gems & Gemology *are by Pacific Color, Carlsbad, California. Printing is by Fry Communications Inc., Mechanicsburg, Pennsylvania*

 ISSN 0016-626X

NOTHING IS AS SIMPLE AS IT SEEMS

Someone asked me recently if gemologists really used the infrared, EDXRF, and Raman spectra that we now publish in most *Gems & Gemology* articles. Twenty years ago, a good gemologist could identify almost any gem material, and most enhancement processes, with straightforward gemological testing—refractive index, specific gravity, optic character, and the like. Twenty years ago, we did quite well (some tell me) without all of this advanced instrumentation. A new material like cubic zirconia could be addressed quickly and efficiently. The major issues were gem localities, cause of color, and interesting new inclusions. Twenty years ago, we did not have commercial quantities of flux and hydrothermal synthetic sapphires, gem-quality synthetic diamonds, or bleached and impregnated 'B' jade, and few questions were asked about the filler used in 'oiled' emeralds.

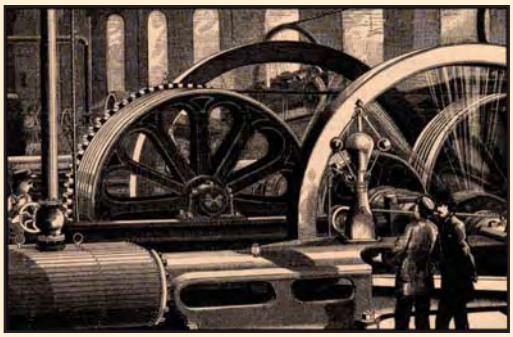

"Impressive. What does it do?"

Think about it. Ask yourself how many gem materials presented to you in a simple white parcel paper you could identify conclusively—the material, whether natural or synthetic, the presence and nature of any treatment—with the same basic equipment gemologists used almost exclusively twenty years ago. The stone is green. The question no longer is 'simply' whether it is emerald, peridot, tourmaline, or the like. But rather, once you know it's emerald, is it a natural stone or a flux or hydrothermal synthetic? Could there be an overgrowth? Is it filled? How extensively? With what? Twenty years ago, the grading of near-colorless diamonds required primarily determination of color, clarity, and finish along with the plotting of inclusions. Now, it must first be determined whether it is diamond or a convincing imitation, and—if diamond—whether it is natural or synthetic. Then, is it fracture-filled? And eventually, perhaps, does it show evidence of 'lightening' by the GE process?

Carefully executed standard gemological practices can still provide identification for many stones and essential information for most others. Once the determination of, for example, R.I. and S.G. has narrowed the field, microscopic features often will reveal strong indications of natural or synthetic origin, or whether the stone has been treated. Yet even the field of microscopy has changed. In many cases where standard inclusions or color zoning cannot conclusively identify 'flawless' synthetic rubies and sapphires, growth structure analysis can make the distinction, but this requires a new level of technical knowledge and skill with a microscope.

The article on the identification of emerald fillers in this issue is a good case in point. As the authors note, there are tens of thousands of potential emerald fillers. They studied 39 known and possible filler substances—and found that to make even basic distinctions between 'presumed natural' oils and artificial resins required a combination of techniques, such as microscopy and infrared or Raman spectroscopy. Even the advanced techniques cannot always resolve the challenges posed by emeralds that have undergone more than one generation of treatment (a common practice) or have been filled with mixtures of substances.

Yes, the articles have become more technical and sometimes can be daunting. And, no, the 21st century gemologist does not have to be a spectroscopist, chemist, or physicist. However, he or she should develop some understanding of how sophisticated techniques in spectroscopy, chemistry, and physics can contribute to the gem identification process. As new materials and treatments have become more advanced and difficult to detect, the means of identification have become more complicated as well. Like all good professionals, gemologists must know the limitations of their knowledge and the outside resources that are available when they reach these limitations. An awareness of the capabilities of advanced testing methods available in modern gem testing laboratories is a must. Because, indeed, nothing is as simple as it seems.

Alice S. Keller
EDITOR, Akeller@gia.edu

LETTERS

Heat Exposure May Affect Reflectance Testing of Synthetic Moissanite

In the Winter 1997 *Gems & Gemology* article by K. Nassau et al., "Synthetic Moissanite: A New Diamond Substitute," it was noted that testing with a reflectivity meter "can also give diagnostic results" for identifying this material, provided great care is taken with the instrument (see p. 273). Recently, however, scientists at C3 Inc., the company that manufactures and distributes synthetic moissanite to the gem trade, discovered that exposure of gem-quality synthetic moissanite to high temperatures for extended periods of time can result in thin oxide films on the surface that may cause a shift in the measured surface reflectance. While such coatings are beneficial to electronics applications of silicon carbide, they can create substantial errors when the material is tested on gemstone reflectance meters, potentially causing synthetic moissanite to be mistaken for diamond.

Most commercial reflectance testers bounce an infrared beam off the surface to be tested and onto a detector that records the intensity of the reflected beam. If the surface is composed of a single (homogeneous) well-polished material, then the light reflected can be related to the refractive index of that material. If, however, a thin film of another material coats the surface of the gemstone, the reflectance signal will no longer be related in a simple way to the refractive index of the underlying bulk material (see, e.g., E. Hecht and A. Zajac, *Optics*, Addison Wesley Publishing Co., Reading, MA, 1979, p. 311).

In the case of synthetic moissanite (silicon carbide, or SiC), a stable, uniform, thin surface film of silicon dioxide (SiO_2) is produced when the gem material is heated sufficiently in an oxygen-containing atmosphere. The resulting change in surface reflectance strongly depends on the thickness and composition of the oxide film (figure 1). As the thickness of the film increases, the measured surface reflectance drops through the arbitrarily chosen reflectance values for moissanite, diamond, cubic zirconia, and yttrium aluminum garnet (YAG). In fact, when the oxide film reaches a certain thickness, the surface will become antireflective and will register as zero on a reflectance meter. The exact thickness of the oxide film that produces the erroneous diamond reflectance measurement will vary according to the precise wavelength of the infrared beam and the incidence angle used by the reflectance tester.

We performed some simple experiments to confirm the predicted reflectance behavior. We tested about 30 faceted synthetic moissanites on three standard reflectance testers (Presidium, DiamondEye, and Jemeter Digital 90) and with the C3 Tester Model 590, and verified that they measured as moissanite. (With a thermal conductivity probe, the same samples registered as "diamond.") The stones were then heated in air for varying times using a furnace. Although the times and temperatures used were more extreme than those encountered in typical jewelry fabrication, they were still well below those required to cause damage (e.g., surface pitting visible at 50×–100× magnification) to the stones. The stones were re-measured on the reflectance testers. Depending on the time and temperature of heating, the treated samples of synthetic moissanite measured incorrectly as diamond, cubic zirconia, or YAG; longer exposure to the heat treatment produced lower values of surface reflectance as the oxide film grew thicker. The results given by the different reflectance meters were in general agreement. A surface reflectance measurement equivalent to that of diamond was produced by a 40- to 60-nm-thick film of oxide, which is very difficult to detect using commonly available means; no visible changes in the appearance of the heated stones could be seen. Note that, after treatment, all of the faceted synthetic moissanites still

Figure 1. The surface reflectance of synthetic moissanite is reduced by the thermal growth of an oxide film. The measured reflectance value may equal that of diamond or any lower-R.I. gem material, depending on the thickness of the oxide coating (as shown here for a 45° incident beam angle).

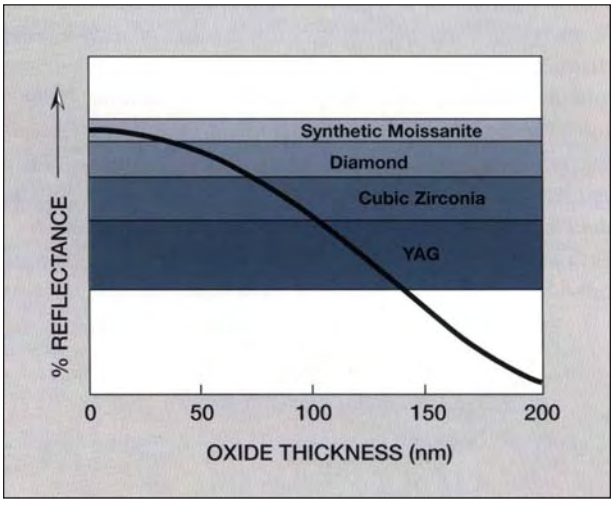

tested as "diamond" with a thermal conductivity probe, but they were correctly identified by the C3 Tester Model 590 as synthetic moissanite. Other distinguishing gemological features (e.g., doubling of the back facets) also remained the same.

The oxide film produced by the high-temperature treatment was extremely robust and could not be removed by solvents, ultrasonic cleaning, or by most acids. However, use of standard hydrofluoric-acid-based glass etchants for silicon dioxide did restore the surface reflectance readings to their initial values.

Testing of faceted synthetic moissanites (about 20 samples) that had been subjected to normal jewelry operations, such as the re-tipping of prongs on a ring, did not produce any modifications to the surface reflectance unless the samples were heated excessively. Given the very slight amount of oxidation required to produce a substantial measurement error, it is conceivable that such a film might be grown inadvertently during jewelry manufacturing or repair. C3 has no plans to manufacture or sell faceted synthetic moissanite that has a modified surface reflectance. Nevertheless, because the possibility exists that intentional or unintentional surface reflectance modifications may occur, C3 does not recommend the use of reflectance testing as an independent means for distinguishing synthetic moissanite gemstones from diamond.

Mark Kellam, Ph.D.
Director of Technology, C3 Inc.
Morrisville, North Carolina

Comments on the Sources of Blue Diamonds

I read with great interest the article "Characterizing Natural-Color Type IIb Blue Diamonds," by J. M. King et al., which appeared in your Winter 1998 issue. The intricate scientific information on a difficult subject such as color and electron resonance is well presented and explained; however, some inaccuracies have crept into the section on history and geographic origin.

Although it is customary to speak of "Golconda diamonds," in actuality there are no observed mines or diamond occurrences at or near the city of Golconda. The famous Indian diamonds, including the Koh-i-Nur, were found in the peripheral areas of the ancient Golconda Kingdom, in the valley of the lower course of the Krishna River. This is a distance of 120 miles (193 km) from Golconda. This city was the capital of the ancient kingdom, where all diamonds found in the surrounding region were traded. The old fortress of Golconda still exists, and is located 10 miles west of Hyderabad.

Note also, in the last paragraph on page 249, that it should be the *Helam* mine near Swartsruggens, and Sierra Leone is better described as being in West Africa.

Nonetheless, I think that this is a very authoritative paper, and it gets my vote for most valuable article of the year.

Dr. A. J. A. (Bram) Janse
Diamond Exploration Consultant
Perth, Western Australia

IN MEMORIAM
D. VINCENT MANSON (1936–1999)

Gems & Gemology mourns the loss of Vince Manson, who passed away on July 3 following a year-long battle with cancer. At the time of his death, at age 63, Dr. Manson was an associate editor of *Gems & Gemology* (a position he had held for 19 years) as well as GIA's director of strategic planning. Most recently, he was chairperson of the Third International Gemological Symposium, which was held in San Diego on June 21–24. Although Dr. Manson was not able to attend the 1999 Symposium because of his illness, he learned from his many visitors of the overwhelming success of the event he had spent three years planning. He originally established the concept of the International Gemological Symposium, and also chaired the first and second Symposia in 1982 and 1991.

Vince Manson received his Bachelor of Science and Master's degrees in geology from the University of Witwatersrand in South Africa. He subsequently spent two years at the De Beers Diamond Research Laboratory in South Africa and six months doing geochemical prospecting in Nova Scotia. In 1964, he earned his Ph.D. in geology from Columbia University. For the next 12 years, Dr. Manson was curator of gems and minerals at the American Museum of Natural History in New York. He joined GIA in 1976 and was responsible for establishing the Research Department. Among his many other technical accomplishments, he served as a consultant for the widely acclaimed documentary "The Time of Man," and was coproducer for both the Time-Life film "Our Dynamic Earth" and the award-winning "Gems of the Americas."

In addition to his role as associate editor of *Gems & Gemology*, Dr. Manson is remembered for his comprehensive articles on garnet classification, which he coauthored with *G&G* technical editor Carol Stockton. The final article in this series, "A Proposed New Classification of Gem-Quality Garnets," won the journal's most valuable article award for 1985.

Vince Manson is survived by his wife Averil, sons Dirk and Scott, and four grandchildren. At the family's request, GIA has established the D. Vincent Manson Fund for Gemological Research in his honor. Admired for his vision and intellect, treasured for his wit and warmhearted laughter, he will be profoundly missed.

On the Identification Of Various Emerald Filling Substances

By Mary L. Johnson, Shane Elen, and Sam Muhlmeister

Criteria for distinguishing emerald filling substances were investigated. Thirty-nine fillers were divided into six substance categories—three "presumed natural" (essential oils [including cedarwood oil], other oils, waxes) and three "artificial resin" (epoxy prepolymers, other prepolymers [including UV-setting adhesives], polymers). Regardless of their composition, fillers with R.I.'s of 1.54 or above show flash effects in emeralds. On the basis of Raman and infrared spectroscopy, the fillers could be separated into five spectral groups, A through E. Most, but not all, commonly used artificial resins have spectra distinct from that of cedarwood oil. However, the detection of one substance in a fissure does not imply that all others are absent.

ABOUT THE AUTHORS

Dr. Johnson is manager of Research and Development, and Mr. Muhlmeister is a research associate, at the GIA Gem Trade Laboratory in Carlsbad, California. Mr. Elen is a research gemologist at GIA Research in Carlsbad.

Please see acknowledgments at the end of the article.

Gems & Gemology, **Vol. 35, No. 2, pp. 82–107**

The vast majority of emeralds on the market today have undergone clarity enhancement; identification laboratories estimate that about 90% of the emeralds they see (most of which are high quality) have been clarity enhanced in some fashion (Genis, 1997; Hänni et al., 1997). In recent years, however, there has developed a growing need to reach a consensus on acceptable trade practice regarding such clarity enhancements, and to find appropriate ways to disclose this information in the marketplace.

If clarity enhancement is a cause for concern, why is it done? For one thing, as they are recovered, most emeralds have many fissures (see, e.g., Sinkankas, 1981; Ottaway et al., 1994). In addition, there are many more potential emerald buyers with high expectations of color and clarity (see, e.g., figure 1) than there are untreated gems to satisfy this demand. Filling substances that almost match the refractive indices of the host emerald make the fissures less noticeable, especially to the unaided eye (figure 2). Even colorless fillers improve the color appearance: The light that would scatter from an unfilled fissure (and thus lighten the apparent color) is no longer visible (Ringsrud, 1983).

Major colored stone trade organizations—such as the International Colored Gemstone Association (ICA) and the American Gem Trade Association (AGTA)—as well as the international jewelry organization CIBJO, recommend that gemstone treatments be disclosed at every stage of the distribution process. However, the trade continues to debate exactly what should be disclosed and how it should be disclosed. In particular, emeralds are less salable in some markets if they are perceived to contain some filler substances such as "Opticon" (an epoxy resin) rather than others such as cedarwood oil. However, one proposal to distinguish "oiling" from enhancement with epoxy resins was voted down by ICA members as unworkable ("Congress votes. . . ,"

Figure 1. The desire for beautiful emeralds has fueled the practice of filling surface-reaching fissures with oils or resins. This jewelry demonstrates the irreplaceable beauty that emeralds provide. The 5.79 ct oval-cut emerald on the left is surrounded by 2.84 ct of diamonds, while the 5.40 ct emerald on the right is surrounded by 2.59 ct of diamonds. Rings courtesy of Henry Dunay; photo © Harold & Erica Van Pelt.

1995). In 1997, ICA decided to delay an emerald promotion due to lack of a consensus on the enhancement issue ("Review on ruby promotion," 1997).

A number of reasons have been given for the need to determine the nature of a particular filling material. First, there is the growing body of anecdotal evidence that various fillers "age" differently, thus changing the appearance of the enhanced emerald over time. For instance, Ringsrud (1998) reported that the artificial resin "palm oil" (also called "palma") turns white within a few months in about 20% of the emeralds filled with this substance. Federman (1998a) noted that "traditional" natural oils and resins (such as cedarwood oil and Canada balsam) could dehydrate or leak out. Kammerling et al. (1991) experimentally determined that Opticon treatment was somewhat more durable than cedarwood oil and Canada balsam, but that all three treatments were affected by routine cleaning and jewelry-manufacturing processes. In addition, due to the variety of growth conditions, emeralds from different localities may not respond similarly to the same filler. Last, different cultures may find some fillers more acceptable than others.

The purpose of this article is to critically evaluate the effectiveness of various methods for distinguishing among clarity-enhancement substances. The main methods currently in use are the "flash effect" (usually seen with magnification), Raman microspectrometry, and infrared spectroscopy. This investigation is part of an ongoing study of emerald fillers; other aspects of emerald enhancement will be addressed in future articles.

HISTORICAL BACKGROUND

Clarity Enhancement in Emeralds. Emeralds from all sources generally contain fissures, and emerald processing (e.g., mining, fashioning, and jewelry manufacturing) can add fractures as well. The filling of such surface-reaching features (hereafter called fissures) to make them less visible has been practiced for centuries. The first description of "oiling" of green gems (probably turquoise, but possibly emeralds) was made by Pliny the Younger in about 55 AD. At least by the 14th century, reference was being made to the oiling of emeralds in particular (Nassau, 1994).

The first references to emerald treatments and their detection in the gemological literature are much more recent. Nassau (1994) cites the sixth edition of Liddicoat's *Handbook of Gem Identification* (1962) as the first gemology book to mention oiling, although it was occasionally mentioned earlier in *Gems & Gemology* (Crowningshield, 1958, 1960–1961; Benson, 1960). Subsequently, *Gems & Gemology* published two comprehensive articles describing some of the techniques and substances used to "clarity enhance" emeralds (Ringsrud, 1983; Kammerling et al., 1991). Hänni (1988) described the detection of filled fissures.

Disclosure. We examined records from two major auction houses, Christie's and Sotheby's, and found that disclaimers regarding filling substances in emeralds were first published in November 1992 (Sotheby's, 1992a, 1992b) and November 1993 (Christie's, 1993). The clarity enhancement of a par-

ticular emerald was first noted in October 1993 (Sotheby's, 1993). Although various classes of possible filling materials—oil, natural resin, and artificial (or synthetic) resin—were noted in these early disclaimers, the specific substance categories were not disclosed for *individual* emeralds (see Box A for a discussion of filler substance classification). The disclosure statements were made more explicit in early 1997 (Federman, 1997). However, specific "types" of enhancements (e.g., "oil type") were first noted in October 1997 (Christie's, 1997a).

Clarity Enhancement Substances. Although there is almost universal agreement that most emeralds need some treatment to be salable, there is still little agreement as to which filling substances are acceptable and why one substance is preferable to another. A good filling substance should have certain properties: It should hide fissures, it should flow into the fractures (i.e., be liquid, at least initially), it should hold up over time or else be easy to restore, and it should be removable or not have any physical properties that might later harm the stone (e.g., during jewelry repair or repolishing). It should also have an R.I. similar to that of the stone being treated.

Several substances have been used by the trade to fill fissures in emeralds. M. Kostetski (pers. comm., 1999) used linseed oil as an emerald filler in the 1930s through 1960s, and C. Altobelli (pers. comm., 1999) used rapeseed oil (now usually called canola oil) from the late 1940s onwards. Crowningshield (1958) mentioned "3-in-1 penetrating" oil, whale oil, and mineral oil. Ringsrud (1983) noted clove oil in addition to Merck cedarwood oil and Merck Canada balsam. Hänni (1988) mentioned also sperm whale oil, paraffin, and an unspecified artificial resin. Kammerling et al. (1991) noted that cedarwood oil and Canada balsam were considered "traditional" filling materials, with Opticon 224 resin (generally only surface hardened) as a newer substitute. Kennedy (1998) described clarity enhancement of emeralds in Brazil: Although baby oil and cedarwood oil ("cedro") were mentioned, Brazilian goods were usually treated with "Opticon." (It is important to remember that, as Federman [1998b] cautioned, not all epoxy resins are Opticon, which is a specific substance with a registered trade name; nevertheless, "Opticon" is often misused as a generic term in the trade.) Ringsrud (1998) wrote that a "synthetic resin" known as "palm oil" was used heavily in Colombia from 1990 to 1996. Three widely discussed enhancement substances at the present time are cedarwood oil, Opticon resin, and "palm oil" (Box B).

In fall 1997, we asked 33 emerald dealers worldwide to tell us which emerald treatments they were aware of. We received 12 responses (one each from Israel, Italy, and Switzerland, and the rest from the U.S.). Each of the following substances was mentioned by at least one dealer: "natural and synthetic oils and resins," Opticon 224 resin (with or without hardener), green-colored oil, wax, paraffin, "cedarwood oil with hardener," "WD 40," Joban oil, "Yehuda treatment," Arthur Groom–Gematrat treatment, linseed oil, epoxy fillers, and plastic sealers.

To many, the most important distinction is that between oils and artificial resins. As summarized by Chalain et al. (1998): "the use of artificial resins to fill emeralds has only been significant in the last fifteen years. . . . Unlike oils, artificial resins act to 'consolidate' emeralds. . . . It is easy to replace oil that oozes out, but hard to get rid of altered resins." *The Guide* reported that 64% of the dealers surveyed at Tucson in February 1997 thought that the clarity enhancement of emeralds with colorless oil was acceptable, while fewer than 48% found "Opticon" treatment acceptable ("Survey: Emerald treatments," 1997). However, no "natural" filler currently in use is found within emeralds *in nature*; all are added during clarity enhancement (Genis, 1997).

From our discussions with members of the trade, we also know that certain fillers are used not only individually, but in mixtures as well. For example, treaters have experimented with mixtures of Canada balsam and cedarwood oil (Ringsrud 1998) to see if an "all-natural" material can replace cedarwood oil as an emerald filler. Such experiments were prompted by reports of a change in the viscosity of Merck cedarwood oil, which had been evident since the late 1980s (as reported by Johnson and Koivula, 1998b). It is also possible that mixtures of oils and artificial resins have been used.

In addition, many stones have undergone several generations of enhancement (i.e., treatment, cleaning, and re-treatment—sometimes with a new substance). Residues of earlier treatments may be left deep within an emerald. This further complicates the identification process (H. Hänni, pers. comm., 1998; C. Smith, pers. comm., 1999).

Previous Work on Characterizing Fillers. Gemological determination of clarity enhancement in emeralds has been described by GIA researchers

Kammerling et al. (1991) and Johnson et al. (1998a), as well as in several *Gems & Gemology* Gem Trade Lab Notes (see, e.g., Fryer et al., 1984; Hurwit, 1989; Kane, 1990; Kammerling, 1993; and Kammerling et al., 1995). One distinguishing feature is the "flash effect" seen with magnification in some filled emeralds, which is similar to that seen in fracture-filled diamonds (Kammerling et al., 1994).

Two relatively recent technological advances have made possible the characterization of specific filling materials within gemstones. The first was the development of a Raman spectrometer designed for gemological use (the Renishaw laser Raman microspectrometer; see, e.g., Hänni et al., 1996a). The second was the adaptation of Fourier-transform infrared (FTIR) reflectance spectroscopy to probe *within* an emerald (see, e.g., Zecchini and Maitrallet, 1998).

In 1994, the Asian Institute of Gemmological Sciences (AIGS; Bangkok, Thailand) was among the first gemological laboratories to use a Raman microspectrometer for gemological characterizations. The Raman spectra of Opticon 224 prepolymer and polymer, and several other fillers, were presented at an ICA-organized meeting in Bangkok in 1994 (K. Scarratt, pers. comm., 1999). Mr. Scarratt currently offers filler identification services at the AGTA Gemological Testing Center, in New York City.

The SSEF Swiss Gemmological Institute has been particularly open in sharing the criteria that they use for filler identification (see, e.g., Hänni et al., 1997; Hänni, 1998; SSEF Swiss Gemmological Institute, 1998; Weldon, 1998b). The techniques employed by SSEF include microscopy, observations of fluorescence, reflectance infrared spectrometry, and (since 1995) Raman microspectrometry. Hänni et al. (1996a) described four substances that are used to fill emeralds: cedarwood oil, an artificial resin, "universal oil," and a wax. Since 1988, SSEF has examined at least 13 different artificial resins (seven epoxy and other hardening resins, and six UV-setting resins; Chalain et al., 1998).

Zecchini and Maitrallet (1998) have used reflectance infrared spectroscopy to characterize eight potential emerald-filling materials and two related substances, both as loose materials and as fillers in emeralds. This research team represents a collaboration between the Université de Franche-Comté and the Service du Contrôl des Diamants, Pierres et Perles of the Paris Chamber of Commerce.

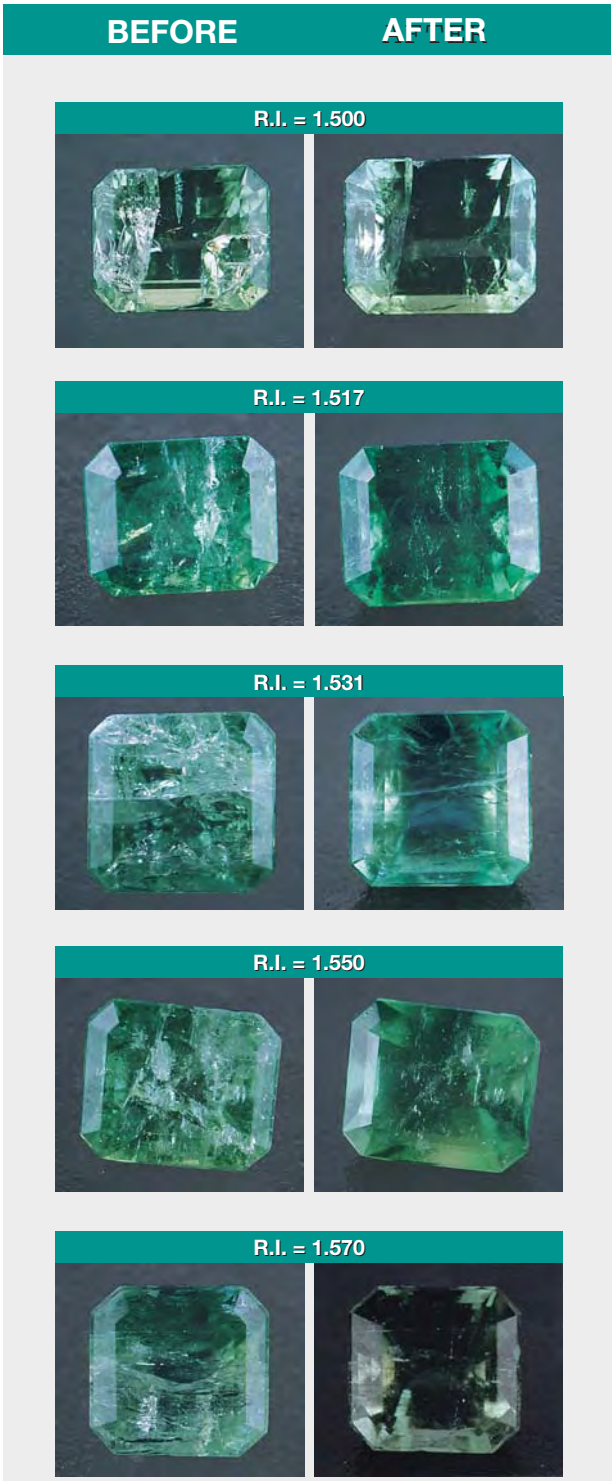

Figure 2. These before-and-after photographs illustrate that the fissures in emeralds become less visible as the R.I. of the filling material increases. Shown are fillers with R.I.'s of 1.500, 1.517, 1.531, 1.550, and 1.570. The refractive indices of the five emeralds ranged from 1.569 to 1.580. Photos by Maha DeMaggio.

BOX A: CLASSIFICATION OF FILLING SUBSTANCES: OILS, ESSENTIAL OILS, RESINS, PREPOLYMERS, AND POLYMERS

Several substances have been used in the clarity enhancement of emeralds. Some are called "oils" (e.g., Cedarwood, paraffin, whale, 3-in-1, "palma"), and some "resins" (e.g., Canada balsam, unhardened Opticon 224). Since the substances used to fill emeralds originally come from various branches of chemistry (from perfumes to polymers), with somewhat different definitions for each field, it is important to create a consistent terminology for use by gemologists.

The following definitions are taken from technical and popular dictionaries, including *Webster's Ninth New Collegiate Dictionary* (Webster's, 1987) for "everyday" English; Stecher et al. (*The Merck Index*, 1968), Alger (1989), and Brady and Clauser (1986) as general chemical and technical dictionaries; Sivry (1985) for European usage; Elias (1993) and Lee and Neville (1967) for plastics; Herout (1982) for perfumes; and Mutton (1982) for the wood products industry. Information on the trees from which certain filling materials are derived is from Lincoln (1986).

OIL

Oil originally meant olive oil, which is not generally used in emeralds today. Its common meaning is one of "numerous unctuous combustible substances that are liquid or at least easily liquefiable on warming, are soluble in ether but not in water, and leave a greasy stain on paper or cloth" (Webster's, 1987). However, *oil* means one thing to petroleum chemists, who use it to refer to long-chain hydrocarbons of a certain weight (e.g., paraffin oil); something else to cooks and nutritionists, who use it to refer to triglycerides (e.g., olive oil, sesame oil); and something else again to perfume chemists, who use it to refer to essential oils (e.g., cedarwood oil, clove oil; see below).

Essential Oils. Some compounds—such as cedarwood oil—are "essential oils." These compounds are extracted from their host plants using solvents. According to the *Polymer Science Dictionary* (Alger, 1989), "an essential oil is the predominantly volatile material isolated by some physical process from an odorous single-species botanical. Over 3000 oils have been identified. . . . Essential oils are generally liquid at room temperature; however, some are semisolid and several are solid. . . . Essential oils are made up of carbon, hydrogen, and oxygen, and occasionally nitrogen and sulfur. . . . It is not uncommon for an essential oil to contain over two hundred components."

The main components of many essential oils have been synthesized (again, including cedarwood oil—see, e.g., Stecher et al., 1968), and commercial essential oils may be partially or wholly synthetic. Because of their volatility, open containers (such as an emerald) of essential oils *cannot* be stable over time, since the fragrant components are continuously lost to the atmosphere (or they would not reach our noses, to be smelled).

Other Oils. Because "essential oils" differ from "other oils" (such as mineral and vegetable oils) in many respects (volatility, viscosity, chemistry, and infrared and Raman spectra), we have treated these as separate categories when reporting the results of our research.

RESIN

Resin originally meant pine sap. Today, *resin* can mean (at least) three different things: natural plant exudates (i.e., saps), either hardened or unhardened; hardened manufactured polymers; or the unhardened prepolymer "building blocks" that can be used to make manufactured polymers (Webster's, 1987; Stecher et al., 1968; Alger, 1989). Natural resins can harden (polymerize) over time (e.g., amber, copal). The emerald filler Canada balsam is generally considered a natural resin, and the essen-

MATERIALS AND METHODS

Almost every chemical product (including natural compounds and extracts) available in the U.S. has a Chemical Abstracts Service (CAS) registry number, and—if there is any possibility of a hazard associated with the material—a Material Safety Data Sheet (MSDS). Details about a chemical compound can be found in many databases if the CAS registry number is known; this is accessible on the World Wide Web at www.cas.org. (Another useful database, *ChemFinder*, is available at www.chemfinder.com.) The MSDS sometimes contains information on the color, odor, specific gravity, and other properties of the material.

Safety is an issue when working with any chemical substance: The MSDS discloses hazardous constituents and their associated risks. Many of the substances in this article pose slight-to-high acute (short-term) health risks. For the most part, they can affect skin, eyes, mucous membranes,

tial oil cedarwood oil is considered a resin by the wood pulp industry (Mutton, 1982).

Polymers and Prepolymers. A *polymer* is a large molecule made up of repeating units of smaller molecules. The smallest such unit is a *monomer* (figure A-1). We prefer to use the term *prepolymers* for the small units that are assembled into polymers, since they could be either monomers or a few monomers attached together. They polymerize—or harden—with the use of a chemical catalyst, illumination, heat, or time.

Specific polymers and prepolymers are named after the parts of their chemical structures that attach these units together. Epoxy resins have two carbons bonded to each other and to the same oxygen; bonds in this *epoxide* group break in order for the prepolymers to be linked. Most artificial resins used to fill emeralds (e.g., Opticon 224, Epon 828, Araldite 6010) are based on one type of epoxy molecule, diglycidyl ether of bisphenol A (DGEBA). They are introduced into the emeralds as prepolymers, and then may be polymerized later. However, UV-setting adhesives, which are also used to fill gems, are based on different chemical compounds, usually methacrylates. These also polymerize, but their infrared and Raman spectra are different from those of the epoxies.

"Synthetic" versus "Artificial" Resin. Chemists use the term *synthetic* differently from gemologists: For a chemist, a synthetic chemical is one that was made from other chemicals, regardless of whether or not it has a natural analog; in gemology, only a material with a natural analog can be called a "synthetic." Some of the "natural" filler materials we examined contained synthetic ingredients (e.g., one of the cedarwood oils; see Box B), or were stated to be completely synthetic (Sigma cinnamon oil). We know of no nondestructive technique to determine whether a filler with a "natural" composition within an emerald is "completely" natural. As a consequence, we refer to the possibly natural materials in this article as "presumed natural," since there is no way to independently guarantee that they are completely natural.

The emerald trade frequently uses the terms *resin* or *synthetic resin* to refer to epoxy prepolymers and polymers such as Opticon 224, Epon 828, and Araldite 6010. As we have seen, both *resin* and *synthetic* are ambiguous. However, *artificial resin* is an unambiguous term that can be used for both liquid prepolymers and solid polymers.

WAX

Another material sometimes encountered as a filler (or luster enhancer) in gems is wax. This term originally meant "beeswax," but it now also includes various similar substances (Webster's, 1987) with higher molecular weights, on average, than oils. Common waxes include: beeswax, spermaceti (from the sperm whale), vegetable waxes, and mineral waxes (including paraffin wax; Brady and Clauser, 1986).

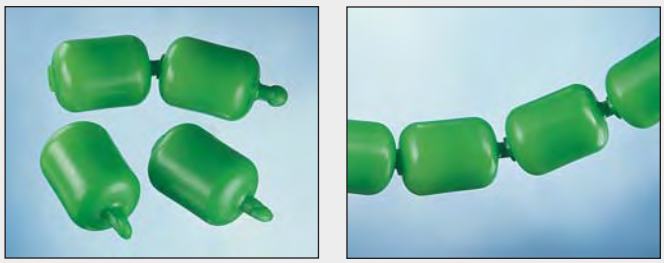

Figure A-1. Snap-Lock™ beads illustrate the concept of polymerization. Polymers are large molecules (right) made from smaller identical pieces—monomers (here, one bead) or other prepolymers (a few linked monomers; here on the left, two beads). Usually, prepolymers are liquid and polymers are solid. Photos by Maha DeMaggio.

and lungs; some can cause mutations in dividing cells; and most are flammable. Persons wishing to experiment with any of these substances should consult the relevant MSDS and follow recommended procedures scrupulously. Although most emerald filling substances present some health hazard to the experimenter, they are probably not dangerous to the ultimate consumer. (However, some people are allergic to cedarwood oil; Bleumink et al., 1973.)

Filling Substances. For this study, we chose fillers that we knew were commonly used in the trade (e.g., Baker and Merck cedarwood oils, Opticon 224 resin), some that have been used previously (e.g., clove oil; Ringsrud, 1983), some that were stated to be in use now (e.g., UV-setting adhesives; C. Osorio, pers. comm., 1998; D. Allen, pers. comm., 1998), and some that were easily available but not known to be in use (e.g., sesame oil, Epo Tek prepolymers). We selected the fillers in this last set because they

Box B: CEDARWOOD OIL, OPTICON, AND "PALM OIL" ("PALMA")

Three of the most-discussed enhancement substances at this time are cedarwood oil, Opticon 224, and "palma." Cedarwood oil from one source (Merck) and Opticon 224 were profiled by Kammerling et al. (1991).

WHAT IS CEDARWOOD OIL?

Cedarwood oil is one of the most widely accepted filling substances today, both because it is perceived as a natural oil, and because it has a higher R.I. and viscosity than other traditional oils (e.g., linseed, rapeseed oil). Detailed information about this essential oil comes from the perfume industry (see, e.g., Herout, 1982), where it is used in the production of perfumes and soaps; it is also used in medicine and microscopy, and as an insecticide (Stecher et al., 1968).

Natural sources. Cedarwood oil is extracted from several coniferous trees, especially the junipers *Juniperus virginiana* (Virginia cedarwood oil), *J. procera* (Kenya cedarwood oil), and *J. mexicana* (Texas cedarwood oil), among others; however, some cedarwood oil is still produced from the true cedar *Cedrus atlantica* (Atlas cedarwood oil; Herout, 1982). Both Texas and Atlas cedarwood oils have the same CAS registry number, 68990-83-0, while most other cedarwood oils have the CAS registry number 8000-27-9.

Composition. Cedarwood oil is primarily composed of tricyclic compounds (molecules with three carbon rings), including cedrol, cedrene, and cedrenol. All these chemicals are synthesized, and commercial cedarwood oils may contain either the synthetic or natural compounds (or both) plus other (synthetic and/or natural) ingredients (Stecher et al., 1968; Herout, 1982).

We looked at five commercially available cedarwood oils from four different sources, all of which were suggested to us by individuals in the emerald trade. These were: Baker cedarwood oil for immersion, EM (Merck) cedarwood oils for immersion and for clearing, Shemen Tov (Texas) cedarwood oil, and "aceite de cedro" from Antonio Negueruela S.A.

We inquired about the composition of each cedarwood oil from its distributor, and received replies from Russell Lance at Mallinckrodt Baker Inc., Rande Klein at EM Science (Merck), Lee Saal at Shemen Tov, and Antonio Negueruela at Antonio Negueruela S.A. Because some of the information we received was proprietary, we will not describe their responses in detail. None of the distributors manufactured the cedarwood oil themselves, and all regarded their sources as proprietary. Three distributors stated that the material was all natural, but the fourth acknowledged a considerable amount (but less than 50%) of synthetic ingredients. Another distributor mentioned that their cedarwood oil also contained rosin (tree sap from which the turpentine has been distilled, according to Brady and Clauser, 1986) and a castor oil solubilizer. None contained Canada balsam. No distributor specified which species of tree the cedarwood oil came from, or the extraction technique used. Despite the differences in composition, four of the cedarwood oils had the same CAS registry number, 8000-27-9; the Shemen Tov (Texas) cedarwood oil had CAS registry number 68990-83-0.

We also asked the distributors to explain the difference between cedarwood oil for clearing and that for immersion. They replied that these have slightly different formulations because they have different uses in biological microscopy. Cedarwood oil for immersion has a higher refractive index (see table 1 in text), and is the substance typically used to fill emeralds.

Physical and Optical Properties. These are given in table 1 in the text; all were somewhat variable. Infrared spectra (figure B-1) were similar for all but the Merck cedarwood oil for clearing, which had a spectrum closely resembling the spectra of Norland Optical Adhesives 63 and 65. Raman spectra (also in figure B-1) showed small variations in detail, with the Baker cedarwood oil the most distinctive.

In short, there are many slight differences among cedarwood oils, as this substance is not a single chemical compound and it can come from several sources. Although some of these differences

fit into substance categories commonly used as emerald fillers and they have R.I.'s close to those of emerald.

Rather than refer to each substance individually, we sought to establish categories of related materials (e.g., oil, resin). However, when we looked into the definitions of these categories, we found ambiguity, both in the meanings attributed to specific

are detectable within emeralds, we do not yet know if any are significant.

WHAT IS OPTICON?

The term *Opticon* should properly refer only to the epoxy resin Opticon 224, manufactured by Hughes Associates, Victoria, Minnesota. This artificial resin may be used in emeralds as a liquid prepolymer or a hardened polymer. The most common procedure (Kammerling et al., 1991) is to fill emeralds with liquid Opticon and brush the catalyst on the surface to provide a hardened surface layer. Because Opticon 224 is a DGEBA (see Box A) epoxy resin, it cannot be separated easily from other DGEBA resins by spectroscopic means, especially when it is within an emerald.

WHAT IS "PALM OIL" OR "PALMA"?

According to anecdotal evidence (J. Rotlewicz and R. Giraldo, pers. comm., 1998), when the viscosity of Merck cedarwood oil changed in the 1980s, Colombian emerald laboratories began using "palma" or "palm oil" instead. This substance more closely matched the R.I.'s of emerald than cedarwood oil did—disguising the fissures well—but it was distinguished from cedarwood oil by its "flash effect" (Ringsrud 1998).

At first, dealers believed from the name that this was another natural oil. "Palm oil" is "aceite" (or "azeite") "de dende" in Spanish, but castor bean oil has been translated as "aceite de palma." However, both of these substances have relatively low refractive indices (about 1.475), so they would not show a "flash effect."

The material represented as "palma" is probably an unhardened epoxy prepolymer resin. Both Araldite 6010 and Epon 828 have been proposed as the identity of "palma" (the former by A. Groom, pers. comm., 1997, and by C. Osorio, J. Rotlewicz, and R. Giraldo, pers. comms., 1998; the latter by C. Beesley, pers. comm., 1998). The R.I.'s and infrared and Raman spectra of these substances are nearly identical.

Figure B-1. The five cedarwood oils we examined had slightly different infrared and Raman spectra.

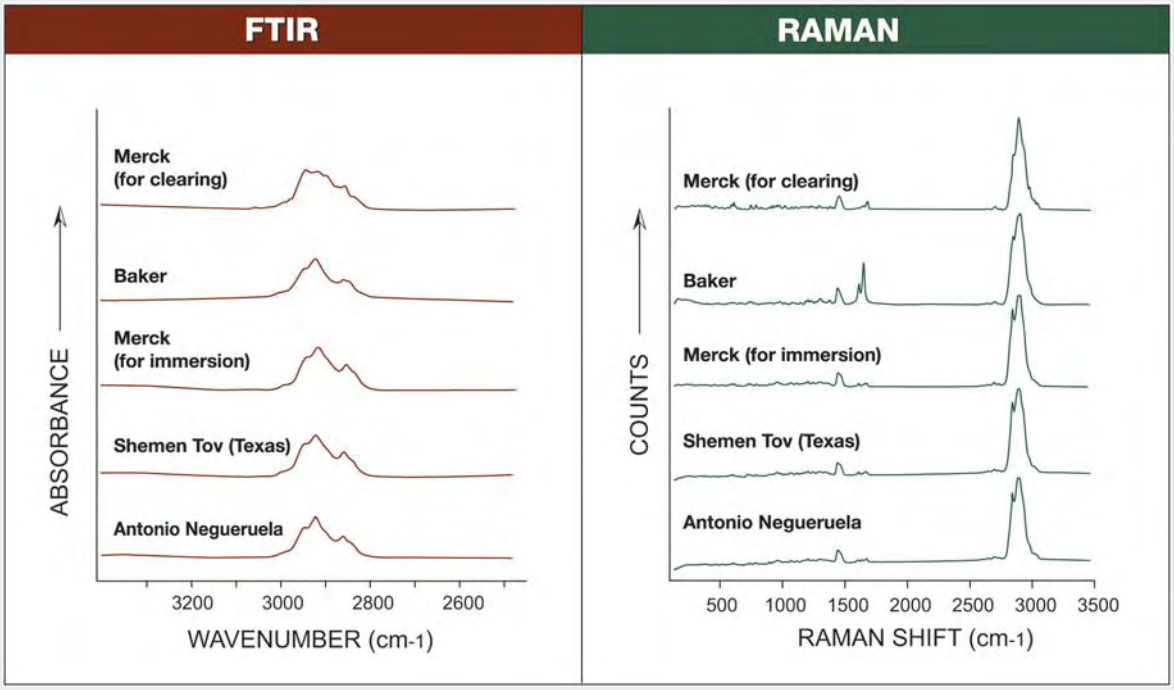

terms and in the ways these terms are applied by different branches of chemistry (again, see Box A). Nevertheless, on the basis of the MSDS information, we classified the fillers we studied into the following six *substance categories*: essential oils (including natural resins), other oils, waxes, epoxy prepolymers, other prepolymers (i.e., which have different chemistries, including UV-setting adhe-

sives), and (hardened) polymer resins. The first three categories contain both natural and manufactured substances; the last three contain only manufactured substances. The two hard polymers Super Tres and Permasafe are similar in their properties and spectra to hardened Opticon 224 (see below), so we suspect these are epoxy (DGEBA) polymers, at least in part.

The 39 materials studied are listed according to these substance categories in table 1. We examined the liquid filling substances both as droplets and as samples mounted between two glass microscope slides (Corning pre-cleaned micro slides, #2927). The solid substances were examined both as polished blocks and as KBr pellets for infrared spectroscopy. Our investigation of isolated fillers is consistent with the recommendation by Zecchini and Maitrallet (1998) that the spectra of the substances alone should be examined before the fillers are investigated within emeralds. To answer key questions about filler mixtures, however, we did study some materials within emeralds.

We observed the color of each filling substance on a white background, using daylight-equivalent fluorescent light. We determined the refractive index of each liquid by placing a drop on the hemicylinder of a Duplex II refractometer equipped with a sodium-equivalent light source; we polished small flats on blocks of the solid materials to get their R.I. values. We observed fluorescence in a darkened room using a GIA GEM short-wave/long-wave ultraviolet lamp.

We assessed the approximate specific gravity of each filler (relative to de-ionized water at 21.5°C) by inserting a few drops (or, if solid, a small fragment) of the substance below the meniscus of a small vial of water, and observing whether the material sank or floated to the surface. (Although this test is not useful to identify fillers *in* emeralds, many dealers do have access to the material that is being used to fill their stones, and this test may help confirm the identity of that filler.) All observations of viscosity were made at room temperature; the flow characteristics were observed by tilting a transparent container of the material and observing whether the surface shifted back to level on a short (like water) or a long (like honey) time scale.

Experiments with Mixtures. For two specific experiments, we investigated some properties of three groups of our own filler mixtures, both as isolated substances and within emeralds. These experiments were designed to answer two questions: (1) Does a flash effect imply an artificial resin? And (2) how well can "adulterated" cedarwood oil be detected with spectroscopic techniques?

We addressed the first question with the following substances, chosen (or mixed) for their refractive indices (table 2): the epoxy prepolymer Epo Tek 314 (R.I. = 1.500); Baker cedarwood oil (R.I. = 1.517); Sigma clove oil (R.I. = 1.531); mixtures of Epo Tek 314 and Epo Tek 302-3M (R.I.'s = 1.517, 1.531, 1.550, 1.570); and mixtures of Sigma clove oil and Sigma cinnamon oil (R.I.'s = 1.550, 1.570). We also examined the stones filled with these substances to determine the effect of filler R.I. on apparent clarity and to observe the appearance of the fillers within fissures. We addressed the second question using mixtures of two components with very different spectral characteristics: Baker cedarwood oil and Araldite 6010 (table 3).

We made 50 ml batches of each filler mixture. The proper volume of each component was determined by assuming a linear relationship between volume and refractive index. The substances were mixed shortly prior to filling the stones, and the R.I. of each mixture was measured.

From a batch of about 250 natural emeralds approximately 0.5 ct and larger, which we had selected for durability testing, we chose 18 to be cleaned, photographed, and filled. Each was first "emptied" by Arthur Groom–Gematrat in New York, using a proprietary process, and then examined with a Reichert Stereo Star Zoom microscope to check that the previous filler material had been removed. Both macro- and micro-photography were performed before and after filling on the nine stones for the first experiment; only macro-photography was done on the other nine. Refractive indices were measured and fluorescence was observed with the above-listed equipment. Care was taken with the R.I. determinations, to ensure that the R.I. liquid was not drawn (or "wicked") into the fissure. We determined the weight of each stone before and after filling (in carats, to five decimal places) using a Mettler MT5 balance.

For the first experiment (table 2), we filled one each of nine emeralds using a "Mini Oiler" (Zamrot Ashalim Engineering Ltd., Ramat Gan, Israel) for the essential-oil mixtures and a "Color Stone Oiling Unit" (Jairo Vaca Camacho, Bogotá) for the artificial-resin mixtures. In the Mini Oiler, samples were held in an evacuated container (i.e., one from which the air had been pumped out) and suspended in a

porous basket over the oil, which was heated to about 50°–60°C. The stones were then plunged into the filler, and 700 mbar overpressure (1.7 bars total pressure) was applied overnight. In the Color Stone Oiling Unit, the emeralds were placed in the bottom of the container and resin was poured over them; the chamber was heated to 50°–60°C and then pressurized to 4000 psi (about 275 bars total pressure) overnight. After the stones were cooled to room temperature, each device was brought to atmospheric pressure and the stones were removed, cleaned with alcohol, and then weighed and rephotographed.

For the second experiment, we examined the mixtures of Baker cedarwood oil and Araldite 6010 both as loose substances and as fillers within emeralds. The measured liquids were poured into brown glass bottles and stirred thoroughly. The three mixtures richest in cedarwood oil and the two richest in Araldite 6010 combined smoothly, but the four mixtures with 30 to 60 volume percent cedarwood oil "unmixed" overnight at room temperature (figure 3). The unmixed fillers were stirred again immediately prior to filling the stones. We filled nine emeralds with these mixtures, using the Zamrot Mini Oiler and the same conditions as above.

Infrared Spectroscopy and Raman Microspectrometry. We analyzed the nine emeralds filled with mixtures in table 3 with a Nicolet Magna 550 Fourier-transform (FTIR) spectrometer, using reflectance infrared spectrometry as described by Zecchini and Maitrallet (1998). For this techique, we adjusted the beam to focus within the emerald, rather than at its surface, to generate a transmission spectrum. We used a known "clean" emerald standard for comparison: a 5.01 ct crystal collected *in situ* from the wall of a mine at Muzo, Colombia, by GIA's Bill Boyajian. We also compared the results for the emeralds filled with these mixtures with those for emeralds we had filled with 100% Baker cedarwood oil or 100% Araldite 6010 as part of the durability study.

Infrared spectra of the loose fillers in tables 1 and 3 were also produced with the Nicolet Magna 550 spectrometer. Spectra were taken of thin films of the liquid fillers made by compressing a drop of the filler between two glass microscope slides, each about 1 mm thick. This collection geometry was chosen so that the strongest infrared-active absorptions would not be too intense to show any features. The IR spectra of solid fillers were obtained using the KBr pressed-powder technique.

Spectra were collected over the range 6000–400 cm^{-1}. We chose a spectral resolution of about 4 cm^{-1}; in general, absorption peaks in polymers are wider than this (5 to 30 cm^{-1}), so peaks can be reported to the nearest cm^{-1} without loss of accuracy (Bower and Maddams, 1989, p. 18). We also examined different resolutions for FTIR spectra of some representative fillers and found no differences in peak position and width for 4 cm^{-1} as compared to 1 cm^{-1} resolution. Because the glass slides had only broad, low background absorption in the region of interest (3200–2400 cm^{-1})—that is, the region in which emeralds are transparent—infrared absorption related to the glass itself did not interfere with the collection of important data, and we observed that the spectra of the loose fillers were practically identical to those taken of the same fillers in emeralds as reported in table 3.

Raman spectra were produced of all the "loose" fillers (both isolated and as mixtures) and of fillers in selected fissures of the filled emeralds in tables 2 and 3. We used a Renishaw 2000 Ramascope laser Raman microspectrometer, with a 514.5 nm argon laser source and five summed 10-second scans on each point. We placed a drop of each liquid filler on a clean piece of aluminum foil, and then analyzed it in the spectral range 100–3500 cm^{-1}. For the loose fillers, we used low (20×) magnification to prevent selective volatilization of the filler substances. In the filled emeralds (tables 2 and 3), we recorded the spectra of fillers in selected fissures at 50× magnification, in the same spectral range. Our Raman spectra had a resolution of about 1 cm^{-1}.

RESULTS

Physical and Optical Characteristics of Loose Filling Materials. All of the substances tested were found to have many properties in common. In some cases, we saw slight differences that might be useful to help determine the substance category or specific filler used in a particular emerald. Properties are listed for the fillers, grouped by substance category, in table 1; significant differences are discussed below.

Color. The Joban oil and green Opticon 224 resin were moderate green, and the Negueruela cedarwood oil was very light green. The rest were colorless or very light, light, or moderate yellow.

TABLE 1. Description and gemological properties of the emerald-filling materials examined for this study.

Substance category	Filler[a]	Source[b]	Used in the trade?[c]	Color	R.I.[d]	Long-wave UV fluorescence	Short-wave UV fluorescence	Relative viscosity[e]	S.G.[f]	IR group, spectrum[g]	Raman group, spectrum[g]
"PRESUMED NATURAL" SUBSTANCES											
ESSENTIAL OILS OR NATURAL RESINS	Cedarwood oil for clearing	Merck	N.R.	Light yellow	1.509	Inert	Inert	Flows sluggishly	Floats	C, 11l	C, 12l
	Cedarwood oil for immersion	Baker	Yes	Yellow	1.517	Strong yellowish white	Weak yellowish green	Flows sluggishly	Floats	C, 11n	C, 12n
	Cedarwood oil	Negueruela	Yes	Very light green	1.518	Moderate white	Inert	Semi-solid	Floats	C, 11n	C, 12o
	Cedarwood oil for immersion	Merck	Yes	Very light yellow	1.520	Weak yellowish green	Inert	Flows sluggishly	Floats	C, 11n	C, 12o
	(Texas) cedarwood oil	Shemen Tov	Yes	Light yellow	1.520	Inert	Inert	Flows sluggishly	Floats	C, 11n	C, 12o
	Canada balsam (natural resin)	Sigma	Yes	Yellow	1.521	Strong yellowish white	Very weak yellowish green	Flows sluggishly	Floats	C, 11n	C, 12n
	Clove bud oil	Spectrum	N.R.	Very light yellow	1.531	Very weak yellowish green	Weak yellowish green	Flows easily	Sinks	D, 11p	D, 12q
	Clove oil	Sigma	Rarely	Light yellow	1.531	Very weak greenish yellow	Weak yellowish green	Flows easily	Sinks	D, 11p	D, 12q
	Clove stem oil	Spectrum	N.R.	Yellow	1.537	Very weak yellowish green	Weak yellowish green	Flows easily	Sinks	D, 11p	D, 12q
	Cinnamon oil (synthetic)	Sigma	N.R.	Yellow	1.589	Inert	Inert	Flows easily	Sinks	D, 11q	E, 12r
	Cinnamon oil (cassia)	Spectrum	N.R.	Yellow	1.589	Very weak green	Inert	Flows easily	Sinks	D, 11p	None
OTHER OILS											
Mineral oil	*Mineral oil*	Spectrum	Yes	Colorless	1.478	Inert	Inert	Flows easily	Floats	B, 11f	B, 12f
	Paraffin oil	Schroeder	Yes	Colorless	1.478	Inert	Inert	Flows easily	Floats	B, 11f	B, 12f
Mineral(?) oil	*"Isocut" fluid*	Buehler	N.R.	Colorless	1.449	Inert	Inert	Flows easily	Floats	B, 11g	None
Vegetable oil	*Sesame oil*	Health Valley	No	Light yellow	1.474	Inert	Inert	Flows easily	Floats	B, 11g	B, 12g
	Azeite de Dende (palm [tree] oil)	Mavalério	No	Yellow	1.473	Moderate greenish yellow	Very weak greenish yellow	Flows easily	Floats	B, 11g	B, 12g
	Castor oil	Spectrum	N.R.	Colorless	1.479	Moderate yellowish green	Very weak yellowish green	Flows easily	Floats	B, 11g	B, 12g
Mineral(?) oil plus vegetable(?) dye	*Joban oil*	Real Gems	Yes	Green	1.478	Moderate yellowish green	Weak yellowish green	Flows easily	Floats	B, 11g	B, 12g
WAX	Paraffin wax	Spectrum	Yes	Colorless	About 1.52	Inert	Inert	Solid	Floats	B, 11h	B, 12h

[a] *Fillers in boldface type have R.I.'s greater than 1.54 and should show a flash effect; fillers in* italics *have R.I.'s less than 1.500 and should not enhance clarity as effectively as others in the table.*

[b] *Sources: Baker (Mallinckrodt Baker Inc., Phillipsburg, NJ); Buehler (Buehler Ltd., Lake Bluff, IL); Centro Gemológico (Centro Gemológico para la Investigación de la Esmeralda, Bogotá, Colombia); CIBA-GEIGY Corp., Hawthorn, NY; Conservator's Emporium, Reno, NV; Epo Tek (Epoxy Technology, Billerica, MA); Health Valley Co., New York City; Hughes (Hughes Associates, Victoria, MN); Liquid Resins (Liquid Resins International Ltd., Olney, IL); Malavério (Indústria de Productos Alimentícios Malavério Ltda., Proporinha, Brazil); Merck (EM Science, Gibbstown, NJ); Negueruela (Antonio Negueruela S.A., Madrid, Spain); Norland (Norland Products Inc., New Brunswick, NJ); Real Gems (Real Gems Inc., New York City); Schroeder J. Schroeder Pharm., Geneva, Switzerland); Shell (Shell Oil Co., Houston, TX); Shemen Tov (Shemen Tov Corp., West Orange, NJ); Sigma (Sigma Chemical Corp., St. Louis, MO); Spectrum Chemical Manufacturing Corp., Gardena, CA; Treatment World (Treatment World Emerald Gemológico Universal, Bogotá, Colombia).*

[c] *N.R. = not reported.*

[d] *The R.I. of the filler increased (by about 0.03) on curing for the three cases we examined (Opticon 224, Epo Tek UVO114, Norland type 65).*

[e] *Flows easily = flows like water; flows sluggishly = flows like honey. These were evaluated at room temperature (21.5ÞC).*

TABLE 1 (cont'd). Description and gemological properties of the emerald-filling materials examined for this study.

Substance category	Filler[a]	Source[b]	Used in the trade?[c]	Color	R.I.[d]	Long-wave UV fluorescence	Short-wave UV fluorescence	Relative viscosity[e]	S.G.[f]	IR group, spectrum[g]	Raman group, spectrum[g]
ARTIFICIAL RESINS											
EPOXY PREPOLYMERS											
	Epo Tek 314	Epo Tek	N.R.	Colorless	1.500	Weak yellowish green	Very weak yellowish green	Flows sluggishly	Sinks	C, 11m	C, 12m
	HXTAL	Conservator's Emporium	N.R.	Colorless	1.501	Inert	Inert	Flows sluggishly	Sinks	B, IIi	B/C, 12i
	Epo Tek 301	Epo Tek	N.R.	Colorless	1.538	Weak to moderate greenish white	Very weak yellowish green	Flows sluggishly	Sinks	A, 11c	A, 12a
	Opticon Resin 224	Hughes	Yes	Colorless	1.550	Inert	Inert	Flows sluggishly	Sinks	A, 11c	A, 12c
	Opticon Resin (green)	Hughes	N.R.	Green	1.550	Weak greenish yellow	Inert	Flows easily	Sinks	A, 11c	A, 12c
	Araldite 506	Sigma	N.R.	Colorless	1.551	Weak yellowish green	Very weak yellowish green	Flows sluggishly	Sinks	A, 11c	A, 12c
	Araldite 502	Sigma	N.R.	Very light yellow	1.559	Weak yellowish green	Strong yellow	Flows sluggishly	Sinks	A, 11c	A, 12c[h]
	Araldite 6005	Sigma	N.R.	Colorless	1.570	Weak yellowish green	Inert	Flows sluggishly	Sinks	A, 11c	A, 12c
	Araldite 6010	CIBA-GEIGY	Yes	Very light yellow	1.572	Weak yellowish green	Inert	Flows sluggishly	Sinks	A, 11c	A, 12c
	Epon 828	Shell	Yes	Light yellow	1.575	Weak yellowish green	Weak greenish yellow	Flows sluggishly	Sinks	A, 11c	A, 12c
	Epo Tek 302-3M	Epo Tek	N.R.	Colorless	1.577	Very weak yellowish green	Inert	Flows sluggishly	Sinks	A, 11b	A, 12b
OTHER PREPOLYMERS											
	Liquid Resin (green cap formula)	Liquid Resins	N.R.	Colorless	1.481	Inert	Inert	Flows easily	Sinks	C, 11o	C, 12p
UV-setting	Epo Tek UVO114	Epo Tek	N.R.	Colorless	1.527	Moderate green	Green	Flows sluggishly	Sinks	A, 11c	A, 12a
	Norland Optical Adhesive type 65	Norland	Yes	Colorless	1.501	Weak greenish yellow	Inert	Flows easily	Sinks	C, 11j	C, 12j
	Norland Optical Adhesive type 63	Norland	N.R.	Colorless	1.519	Strong blue	Inert	Flows easily	Sinks	C, 11j	C, 12j
POLYMERS											
	Permasafe	Centro Gemológico	Yes	Very light yellow	1.565	Strong blue-white	Weak blue	Solid	1.11	A, 11e	A, 12e
	Super Tres	Treatment World	Yes	Light yellow	1.570	Strong bluish white	Moderate grayish blue	Solid	1.11	A, 11e	A, 12e
	Opticon Resin 224 (cured)	Hughes	Yes	Very light yellow	1.580	Strong light blue	Moderate light blue	Solid	Sinks	A, 11d	A, 12d
UV-setting	Norland Optical Adhesive type 65 (cured)	Norland	Yes	Colorless	1.529	Moderate blue	Weak green	Solid	Sinks	C, 11k	C, 12k
	Epo Tek UVO114 (cured)	Epo Tek	N.R.	Light yellow	1.553	Strong blue	Moderate blue	Solid	Sinks	A, 11a	A, 12d

[f] S.G. is reported relative to water: floats—S.G. less than 1.0; sinks—S.G. greater than 1.0. Both Permasafe and Super Tres had hydrostatically measured S.G.'s of 1.11.
[g] Spectral groups as discussed in text; individual spectra shown in figures 11 and 12. "None" means that the sample was too fluorescent to get a Raman spectrum with the 514.5 nm argon laser source.
[h] Plus two additional Raman peaks.

TABLE 2. Emeralds clarity enhanced for R.I. tests of "presumed natural" and artificial fillers.

Filler	R.I. of filler[a]	Microscopic features of filled fissures in emerald	Fluorescence to longwave UV in emerald	Raman spectrum of filler in emerald
Epo Tek 314 (artificial resin)	1.500	Not notable	Not seen	Weak aliphatic feature, possibly group C
Baker cedarwood oil ("natural" oil)	1.517	Not notable	Very weak yellow-green in fissures	Positive match to Canada balsam or Baker cedarwood oil; group C
Mixture of Epo Tek 314 and Epo Tek 302-3M (artificial resins)	1.517	Not notable	Very weak yellow-green in fissures	Group C
Sigma clove oil ("natural" oil)	1.531	Incomplete filling; white residue	Not seen	Not identifiable as to group
Mixture of Epo Tek 314 and Epo Tek 302-3M (artificial resins)	1.531	Incomplete filling; flow structure	Very weak yellow-green in fissures	Good match to spectra for both components groups A and C
Mixture of Epo Tek 314 and Epo Tek 302-3M (artificial resins)	1.550	Orange and blue flash effects; incomplete filling; iridescence in fissure; light brownish yellow substance in fissure	Very weak yellow-green in fissures	Shows features of both groups A and C, less distinct overall
Mixture of Sigma clove oil and Sigma cinnamon oil ("natural" oils)	1.550	Yellow-orange and blue flash effects (evaporating rapidly); incomplete filling; iridescence in fissure	Very weak yellow-green in fissures	Weak unidentifiable spectrum
Mixture of Epo Tek 314 and Epo Tek 302-3M (artificial resins)	1.570	Yellow-orange and blue flash effects; incomplete filling; iridescence in fissure; white residue	Very weak yellow-green in fissures	Good match to group A reference spectrum
Mixture of Sigma clove oil and Sigma cinnamon oil ("natural" oils)	1.570	Flash effects (disappearing rapidly as filler evaporates); incomplete filling; iridescence in fissure; brownish yellow substance in fissure; white residue	Not seen	Not identifiable as to group

[a]*All the emeralds for this experiment had R.I. values of 1.571 (± 0.002) to 1.577 (± 0.003).*

Refractive Index. The fillers had R.I.'s of 1.449 to 1.589; by comparison, the R.I. values of emerald range from 1.564 to 1.593 (extraordinary ray), and 1.570 to 1.602 (ordinary ray), depending on their source (Webster and Read, 1994). The UV-setting adhesives we studied had low R.I. values relative to emerald, 1.501–1.527; however, the R.I. values increased to 1.529–1.553 as they cured. The R.I. value of Opticon 224 also increased with curing.

For the mixtures of essential oils and those of artificial resins, the R.I. of the mixture could be predicted from the measured volumes and R.I.'s of its components. However, the mixtures of Baker cedarwood oil with Araldite 6010 behaved nonlinearly, so the R.I.'s did not agree with their predicted values (see table 3).

Fluorescence. As indicated in table 1, not all cedarwood oils fluoresce and those that do fluoresce do not all fluoresce alike. Similarly, although most epoxy prepolymers fluoresced very weak yellowish green to short-wave UV, or were inert, Araldite 502 fluoresced strong yellow and Epon 828 fluoresced weak greenish yellow.

All but one of the polymers displayed strong bluish white to blue fluorescence to long-wave UV, and the same fillers fluoresced weak to moderate blue to short-wave UV. The exception, Norland Optical Adhesive type 65, fluoresced moderate blue to long-wave UV and weak green to short-wave UV.

Viscosity. Some essential oils flowed readily (like water); however, the cedarwood oils and Canada balsam were sluggish (like honey). The cedarwood oil from Antonio Negueruela was nearly solid at room temperature (similar to "petroleum jelly"). The "other oils" all flowed easily. The paraffin wax was a soft solid. The epoxy prepolymers flowed sluggishly, and the UV-setting adhesives flowed easily (Norland Optical Adhesives) or sluggishly. All of the hardened polymers were solids.

Specific Gravity. Some essential oils floated in water (cedarwood oils, Canada balsam), whereas others sank (clove oils, cinnamon oils). The other oils we studied floated, as did paraffin wax. All of the epoxy prepolymers and other prepolymers sank, and all of the hardened resins we studied also sank.

Gemological Characterization of Filling Materials in Emeralds. *Effect of Refractive Index on Apparent*

Clarity. Examination of the emeralds filled with the nine substances in table 2 revealed that as the R.I. of the filling material increases toward the R.I.'s of emerald, the fissures become less prominent (see, e.g., figure 2).

Internal Appearance and Flash Effect. Although most of the substances we used for these R.I. tests are not common filling materials, we were able to reproduce features seen in filled emeralds, including brownish yellow filled voids (figure 4), flow structure (figure 5), incomplete filling (figure 6), and natural iridescence in fractures as well as white residues (figure 7). The white residues were seen in three of the stones (one filled with pure clove oil, one with an Epo Tek mixture, and one with a clove oil–cinnamon oil mixture), deep within the fissures at the time of first examination.

None of the five stones filled with a substance that had an R.I. of 1.53 or lower showed a flash effect, whereas all four stones filled with substances that had R.I.'s of 1.55 or higher *did* show a flash effect (table 2 and figure 8). However, the "natural" fillers were quite volatile, so often this effect was gone within hours. We refilled one emerald with the 1.550 R.I. natural oil mixture, and photographed it within minutes of completing the filling process.

Figure 3. These four bottles of Baker cedarwood oil–Araldite 6010 mixtures show the unmixing of intermediate mixtures with 40% to 70% Araldite (left to right). Photo by Maha DeMaggio.

TABLE 3. Properties of emeralds filled with cedarwood oil–Araldite 6010 mixtures for spectroscopy.

Composition of the filler		Properties						
Baker cedarwood oil (%)	Araldite (%)	Color of the loose filler	R.I. of the filler	Predicted R.I. of the filler[a]	Flash effect in stone?[b]	Unmixing of fillers in bottle?	IR result (in emerald)	Raman result (in emerald)
100	0	Yellow	1.517	—	No	No	Cedarwood oil (reference spectrum)	Cedarwood oil (reference spectrum)
90	10	Yellow	1.522	1.522	Weak blue brightfield	No	Cedarwood oil	Cedarwood oil
80	20	Yellow	1.528	1.528	No	No	Cedarwood oil	Features of both
70	30	Yellow	1.533	1.534	No	No	Cedarwood oil	Features of both
60	40	Yellow	1.539	1.539	Weak blue brightfield	Yes	Cedarwood oil	Features of both
50	50	Yellow	1.544	1.544	Very weak orangy brown darkfield	Yes	Features of both	Features of both
40	60	Light yellow	1.545	1.550	Weak brown darkfield	Yes	Features of both	Features of both
30	70	Light yellow	1.547	1.556	Yellow-orange darkfield	Yes	Features of both	Features of both
20	80	Very light yellow	1.559	1.561	Yellow-orange darkfield, blue brightfield	No	Features of both	Features of both
10	90	Very light yellow	1.564	1.566	Yellow-orange darkfield	No	Araldite 6010	Araldite 6010
0	100	Near-colorless	1.572	—	Yes	No	Araldite 6010 (reference spectrum)	Araldite 6010 (reference spectrum)

[a] *R.I. predicted by: R.I. = [(% cedarwood oil) × 1.517 + (% Araldite) × 1.572] / 100. Where the measured R.I. and predicted R.I. differ by more than 0.002, this indicates that the two components are not mixing ideally.*

[b] *The emeralds in this test had the same refractive indices, 1.571–1.578.*

Figure 4. The filler (mixture of Epo Tek resins, R.I. = 1.550) in this 0.70 ct emerald appears brownish yellow. Photomicrograph by John I. Koivula; magnified 25×.

The flash effects disappeared while we watched as the stone was being photographed (figure 9).

Fluorescence of Filled Fissures. If enough of a fluorescent filling material is present, the fluorescence may be visible within the stone (for example, in six of the nine stones in table 2, we saw very weak yellow-green fluorescence to long-wave UV in the fissures; strictly speaking, we might have expected to see this in all nine stones). In those cases where fluorescence can be observed, this property can be especially useful to target specific fissures for Raman analysis (see Chalain et al., 1998).

Figure 5. Flow structure is evident in the filling material (mixture of Epo Tek resins, R.I. = 1.531) in this 0.82 ct emerald. Photomicrograph by John I. Koivula; magnified 20×.

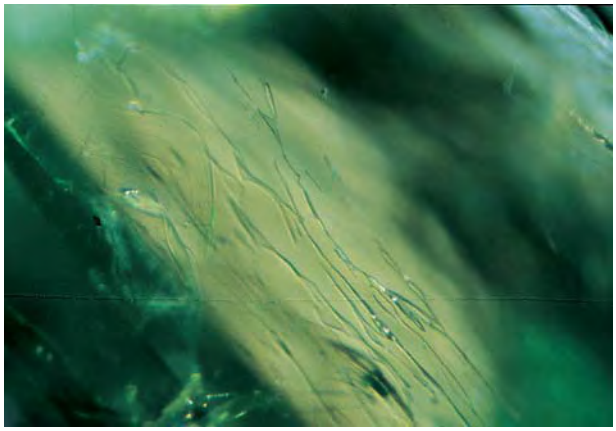

Weight Added. The Epo Tek mixtures added about 0.03%–0.10% to the weight of the stones (i.e., 0.0002–0.0008 ct for a 0.5–1 ct stone). The cinnamon oil mixtures were so volatile that they evaporated before the stones could be reweighed.

FTIR and Raman Spectra. In the infrared region, emerald has a transmission window between about 3200 and 2400 cm^{-1}; therefore, this is the region that we studied for the loose filling substances. The absorption spectra of the glass slides that we used, and of a never-filled Colombian emerald crystal, are shown in figure 10.

The infrared and Raman spectra enabled us to place the loose filler materials into five spectral groups—designated here A, B, C, D, and E—with 17 infrared (figure 11) and 18 Raman (figure 12) subgroups (i.e., each spectrum may represent more than one filler). The five spectral groups are based on assignments of peaks to functional groups (see "Discussion," below), but they can be summarized in terms of the appearance of certain key peaks:

- *Group A* spectra have many peaks, especially at about 2926, 3006 (stronger in the Raman spectrum, and weak in some examples), 3058 (IR) or 3068 (Raman), and—only seen with Raman in emeralds—1609 cm^{-1}. (Recall that peak assignments can vary ± 4 cm^{-1}.) The 2962 cm^{-1} peak is usually, but not always, present. Typical group A IR spectra (see, e.g., figure 11c) show a pattern of three strong peaks decreasing in height from 2962 to 2926 to 2872 cm^{-1}. Typical group A Raman spectra (figure 12c) have a distinctive pattern of five strong peaks in the region between 2870 and 3070 cm^{-1}.
- *Group B* spectra also have many peaks, including those at 2853 (2848 cm^{-1} for paraffin wax), 2882 (Raman only), 2926 (±5), and 2954 cm^{-1} (IR only); there may be Raman peaks at 3010 and 1655 cm^{-1}. The IR spectra of the liquids show a pattern of two peaks, each with shoulders at a higher wavenumber (figures 11f, g); and the Raman spectra show plateaus centered at about 2890 cm^{-1} (figures 12f, g). In contrast, the IR spectrum of the paraffin wax has a broad central feature (figure 11h), while the Raman spectrum is sharp (figure 12h).
- *Group C* spectra exhibit peaks at 2870 (±5), 2929 (ranging to 2942 cm^{-1} in figure 12i), usually 2958, and 1442 (Raman only) cm^{-1}. Sometimes Raman peaks are seen at 1725 (figures 12j, m, and p) or

1643 cm^{-1} (figures 12j, n, and p). Typical IR (figure 11n) and Raman (figure 12l) spectra have an overall "triangular" appearance in the 2800–3050 cm^{-1} region.

- *Group D* spectra exhibit features resembling those of group A *and* group B or C, with six or more peaks in the 2800–3100 cm^{-1} region (see, e.g., figures 11p and 12q).
- The *Group E* Raman spectrum is notable for the low intensity of the 2800–3100 cm^{-1} region (only one peak at 3064 cm^{-1}: figure 12r), compared to three strong peaks at 1598, 1626, and 1674 cm^{-1}.

Additional details were used to place these spectra into subgroups. Although many of these details are unlikely to be discernible in a filled emerald, they may be important in some cases. For example, Raman microspectrometry can distinguish Baker cedarwood oil and Canada balsam from other cedarwood oils, but not from each other (compare figures 12n and o); these IR spectra are identical (figure 11n). In addition, the IR and Raman spectra of "Permasafe" and "Super Tres" (figures 11e and 12e) are slightly different from those of cured Opticon (figures 11d and 12d), although these distinctions (e.g., a peak at 1000 cm^{-1} in the Raman spectrum) might not be obvious in a filled emerald. Last, the Norland Optical Adhesives show a distinctive Raman peak at 2575 cm^{-1} (figure 12j); this peak diminishes significantly on curing (figure 12k).

The IR and Raman spectra of the cedarwood oil–Araldite 6010 mixtures as loose fillers are shown in figure 13. These spectra contain no new features; detection limits based on these results are discussed below.

As noted earlier, the spectra of the fillers in emeralds taken with reflectance IR spectroscopy were almost identical to the IR spectra of the corresponding loose fillers (compare, e.g., figure 10 inset with figure 11n). Consequently, we will refer to the IR spectra of the loose fillers and mixtures throughout the discussion.

DISCUSSION

Separating Filler Materials on the Basis of Their Optical and Physical Characteristics. The following optical and physical characteristics of loose filler materials may be useful in distinguishing among filling substances within emeralds: color, refractive index (and flash effect), fluorescence, viscosity, and distinctive microscopic features.

Figure 6. Note the incomplete filling by clove oil (R.I. = 1.531) in the fissures of this 0.94 ct emerald. Photomicrograph by John I. Koivula; magnified 15×.

Color. Dyed filler materials are distinctly colored (e.g., green Opticon and Joban oil; see table 1). However, other features can be mistaken for dye, including the green polishing compound chromic oxide (Ringsrud, 1983; Hänni, 1988) and green internal reflections. If dye is suspected, the observer should examine the distribution of color within the stone using diffuse transmitted light; another technique is to check whether the fissures are green from all angles and to look for color concentrations along fractures. The yellow color of other materials listed in table 1 is unlikely to be seen in an emerald unless the filler is present in broad fissures or cavities (Koivula, 1999).

Refractive Index (and Flash Effect). As the refractive index of the filling material increases toward the R.I.'s of emerald, the filled fissures become less prominent (again, see figure 2). For the emeralds we studied, which had R.I. values between 1.569 and 1.580, we saw flash effects for all fillers with R.I. values of 1.54 or above. Of the fillers in this study, only those in spectral groups A, D, and E (epoxy prepolymers and polymers, and some essential oils) have R.I.'s above 1.54. Only fillers in spectral group B (other oils) and C (the prepolymer Liquid Resin) have R.I.'s below 1.50, and these are much less effective at disguising fissures in emerald. Mixtures gave intermediate R.I.'s.

An indication of a filler's R.I. value can be provided by the prominence of the filled fissures and

Figure 7. A white residue was seen deep within a fissure in this 0.47 ct emerald, which had been filled with a mixture of clove and cinnamon oils (R.I.= 1.570). Natural iridescence is also visible in this fissure (top of the image). Photomicrograph by John I. Koivula; magnified 20×.

the presence of a flash effect. Because most materials that show flash effects in emeralds are artificial resins, and the high-refractive-index essential oils we examined are extremely volatile, it is likely that an emerald showing this effect contains an artificial resin. However, there are many artificial resins with lower R.I. values, so the *absence* of a flash effect does not mean that the substance should be considered natural. For instance, the early formulation of Arthur Groom–Gematrat had a lower R.I. value than other commonly used artificial resins, as evidenced by the greater prominence of the filled fissures and the lack of a flash effect (see, e.g., Johnson et al., 1997).

Fluorescence. Most of the fillers we studied were inert, or fluoresced very weak or weak yellow-to-green to long-wave UV. However, two of the five cedarwood oils fluoresced moderate white or strong yellowish white, and most of the cured (hardened) polymers fluoresced strong white to blue, so *strong* fluorescence in fissures may be useful for distinguishing cured and surface-hardened fillers from liquid fillers. (Of course, one risks hardening the UV-setting adhesives by exposing them to UV radiation.) Recent formulations of Arthur Groom–Gematrat are said to contain a fluorescent tracer (Weldon, 1998a). We were not able to study the Arthur Groom–Gematrat filler as an isolated material; however, all five polymer samples we examined fluoresced blue to bluish white to long-wave UV, and all but the cured Norland Optical Adhesive 65 fluoresced blue to short-wave UV (again, see table 1).

Viscosity. All filling materials are liquid when they are emplaced in emeralds, but some are hardened once in the fissures (e.g., UV-setting adhesives), others are frequently surface hardened (Opticon: Kammerling et al., 1991), and others slowly solidify over time (e.g., Canada balsam: Kammerling et al., 1991). It is also possible that certain internal characteristics—such as gas bubbles, flow structures, and incomplete filling of fractures—are related to the viscosity of a filling material, but we have not tested this hypothesis.

Before the viscosity of a filler in an emerald can be inferred, its presence must be established. Johnson et al. (1998a), among others, have described procedures for finding evidence of clarity enhancement in emeralds. Using a microscope at low magnification with reflected light will reveal the trace of the fissure on the surface; switching to darkfield illumination will show the extent of the fissure inside the stone. Higher magnification is then used

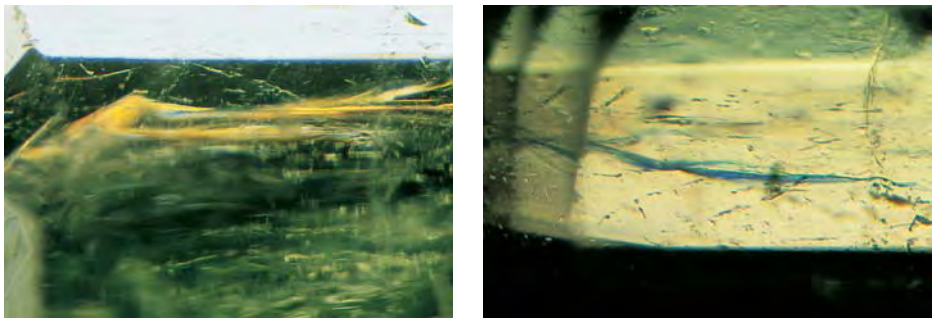

Figure 8. This 0.59 ct emerald filled with a mixture of epoxies (R.I. = 1.570) shows orangy yellow (darkfield, left) and blue (brightfield, right) flash effects. Photomicrographs by John I. Koivula; magnified 15×.

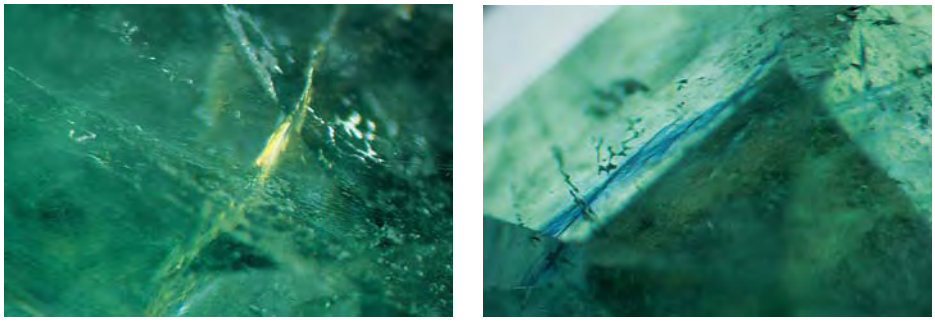

Figure 9. This emerald, filled with a mixture of the natural essential oils clove oil and cinnamon oil (R.I. =1.550), also shows yellow-orange (darkfield) and blue (bright-field) flash effects. Photomicrographs by John I. Koivula; magnified 15×.

to reveal features indicative of a filled fissure: flow structure, gas bubbles (which may be flattened or round), incomplete filling, or yellowish voids (sometimes shaped like crystal inclusions).

Once the presence of a filler has been established, there are at least two ways to see whether the filler is fluid: (1) Watch the emerald as it warms with exposure to the microscope lamp, and see if there is any movement of the filler within the stone; and (2) while observing carefully with the microscope, bring a heated sharp point near—but not touching—the surface of the emerald, and watch for movement of the filler (it may even form droplets on the surface of the stone). In either case, use extreme care to avoid damaging the emerald by extending fissures. A liquid filler may show motion with these techniques, but the absence of a reaction does not guarantee that the filler is solid, because surface-hardened fillers might act the same (Johnson et al., 1998a).

Distinctive White Cloudy Inclusions. Although this internal feature is commonly attributed to "palma" (see, e.g., Ringsrud, 1998), we did see such inclusions in emeralds filled with "natural" essential oils (clove and cinnamon), and with a mixture of epoxy prepolymers (Epo Tek 314 and Epo Tek 302-3M). We suspect that they result from some sort of emulsification, which can be demonstrated—but not proved—by the following test: Place nearly equal amounts of filling material (here, Araldite 6010) and water in a bottle, then close and shake the bottle (figure 14). The white cloudy mixture that forms is an emulsion of small droplets of one substance in the other substance; the droplets are prevented from coalescing by the coating of the other substance. Perhaps in the case of our experimentally filled emeralds, this emulsion formed deep within the filled fissures, where not all the water had been removed from the emeralds before filling. (This could also happen with other substances.)

Another possible source of fine, white surface contamination seen in the trade is quartz dust, which contaminates some polishing compounds used in Bogotá (R. Giraldo, pers. comm., 1999). As volatile filling material evaporates from the surface of an emerald, the 1.54-R.I. quartz dust left behind would gradually become visible.

Figure 10. For reference purposes, we recorded the FTIR spectra of (a) the glass slides we used as "windows" for obtaining the spectra of filling materials, and (b) a 5.01 ct natural (unfilled) emerald crystal. The inset shows a detail of the emerald spectrum in the region where filler peaks are seen, together with the spectrum of an emerald that had been filled with Baker cedarwood oil (in red); note that this area of the spectrum also contains small emerald features..

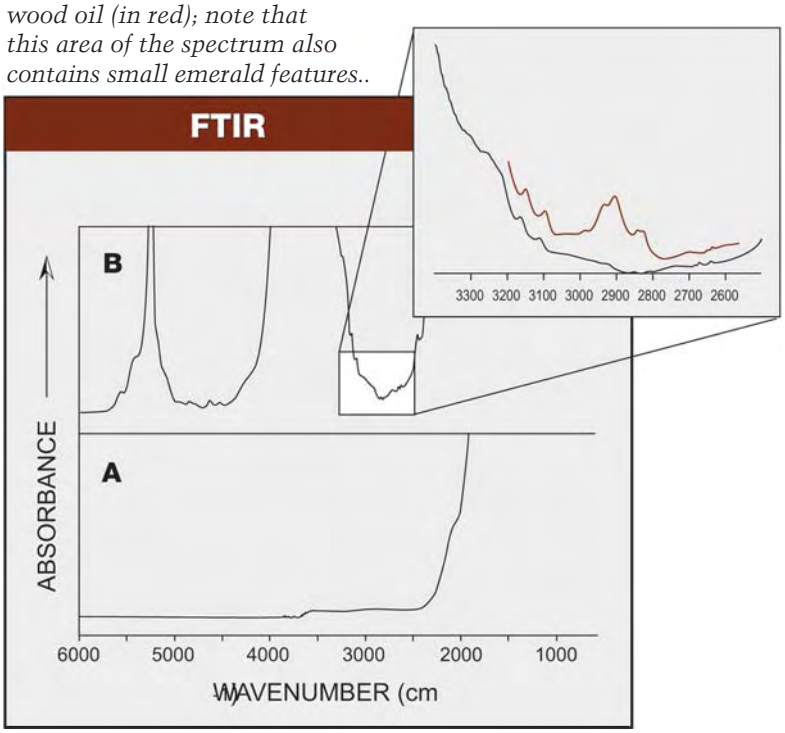

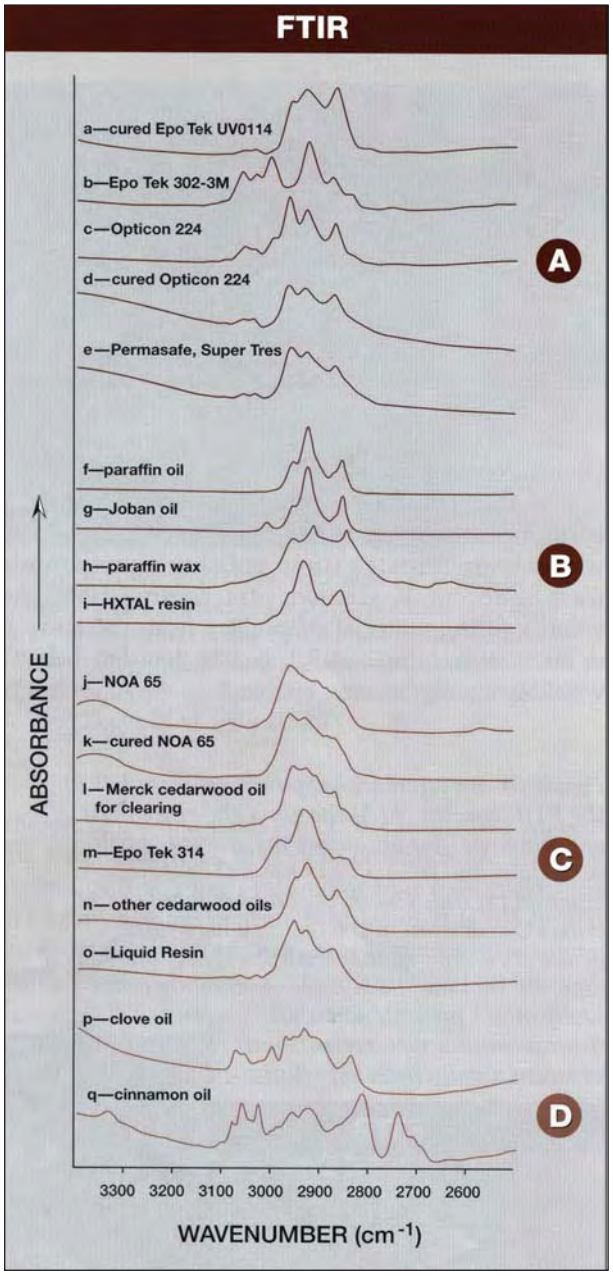

Figure 11. On the basis of their spectra, the filling substances examined were placed in four infrared groups (A–D) and 17 subgroups (a–q). Representative spectra for each subgroup are illustrated here. The appropriate group and spectrum for each of the fillers studied are listed in table 1. NOA = Norland Optical Adhesive.

FTIR and Raman Spectrometry: Complementary Techniques, Similar Information. Peaks in infrared and Raman spectra have the same cause: The radiation excites vibrations between atoms. In crystalline substances, IR and Raman spectra of the same material may look quite different, because the two techniques often excite different vibrations, depending on the symmetry of the material and on quantum mechanical "selection rules" (Harris and Bertolucci, 1978). However, liquids and polymers are less "ordered" than crystalline solids (i.e., they have less overall structural order and greater variability in bond lengths and angles, etc.), so the IR and Raman spectra of a particular liquid or polymer look quite similar in general, with a few differences in peak position and (especially) in relative intensity.

When it comes to examining spectral information of fillers within emeralds, FTIR and Raman often provide similar information from distinct regions within the emerald. With the reflected-beam geometry, FTIR spectroscopy gathers spectral information from much of the interior of the emerald, and it is not necessary to find the filled fissures prior to analysis. In contrast, the Renishaw Raman microspectrometer must be focused at or near the surface of the stone, and the fissures to be examined must first be located with the microscope. Because the spectral information only comes from the near-surface area, other filler substances deeper in the stone would not be detected.

In addition, the emerald host has a different effect on the results obtained with each technique. With FTIR, only the limited spectral region between 3200 and 2400 cm^{-1} is visible in the emerald (again, see figure 10). Fortunately, this region includes one of the two diagnostic spectral regions for polymers. With Raman, the emerald (and some fillers) may luminesce to the 514 nm laser beam that induces the Raman effect; this luminescence causes a large interfering background signal in the spectrum that generally begins at wavenumbers above 3000 cm^{-1} or so (but can be a problem in some emeralds even at 2000 cm^{-1}). With both techniques, the distinctive filler peaks are very small compared to the features of the emerald host.

Reference infrared spectra for many of the materials we tested are available in atlases such as Pouchert (1985) and Julian et al. (1991), software such as the *Omnic Interpretation Guide* (Nicolet, 1992), and references such as those cited by the *ChemFinder* Web site. The Raman peaks (especially for liquids) can be interpreted as if they were infrared peaks. However, the interpretation of both types of spectra requires the terminology of organic chemistry. *Functional groups* are the pieces of a molecule's structure that produce distinctive spectral features. Certain peak

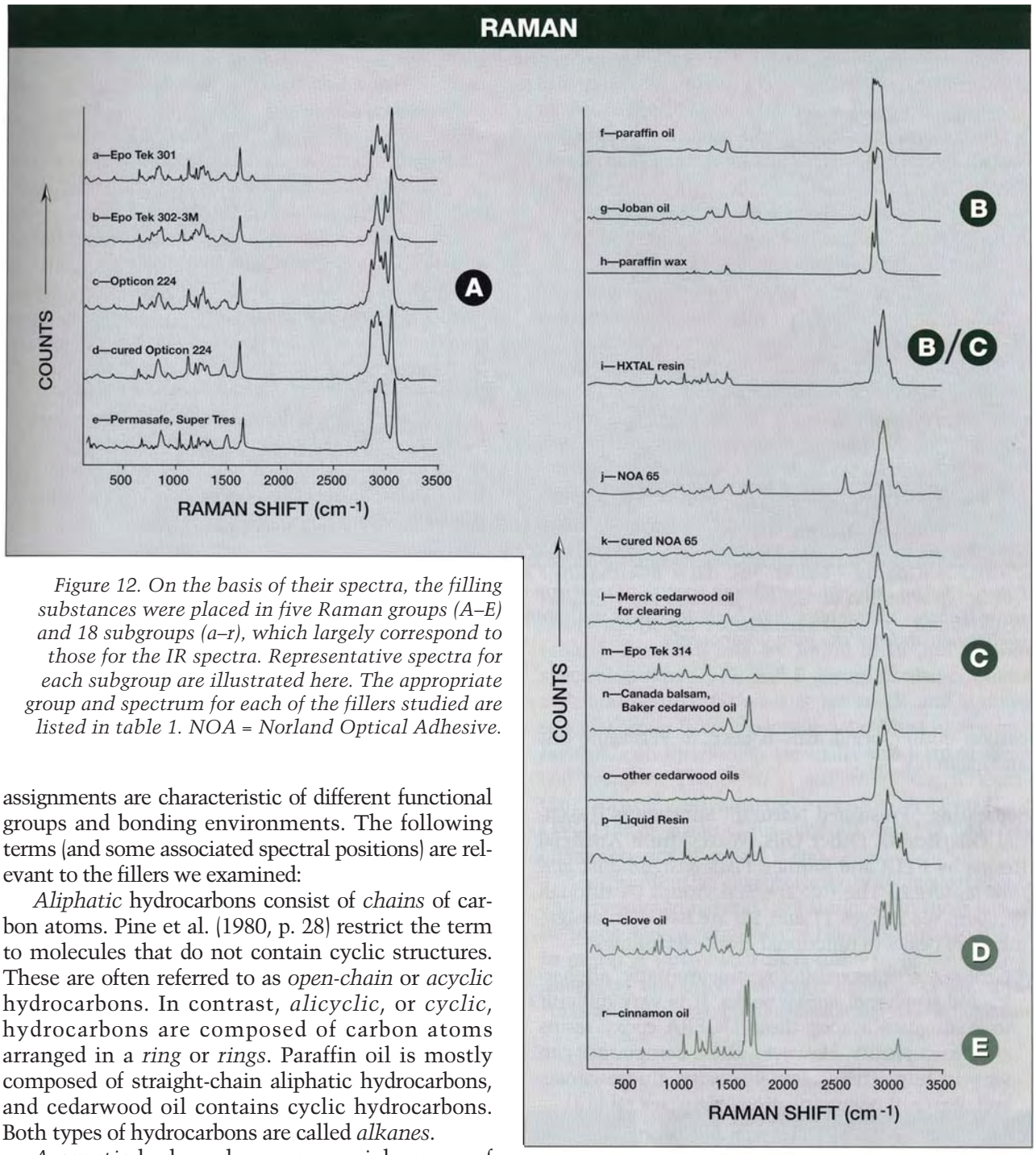

Figure 12. On the basis of their spectra, the filling substances were placed in five Raman groups (A–E) and 18 subgroups (a–r), which largely correspond to those for the IR spectra. Representative spectra for each subgroup are illustrated here. The appropriate group and spectrum for each of the fillers studied are listed in table 1. NOA = Norland Optical Adhesive.

assignments are characteristic of different functional groups and bonding environments. The following terms (and some associated spectral positions) are relevant to the fillers we examined:

Aliphatic hydrocarbons consist of *chains* of carbon atoms. Pine et al. (1980, p. 28) restrict the term to molecules that do not contain cyclic structures. These are often referred to as *open-chain* or *acyclic* hydrocarbons. In contrast, *alicyclic*, or *cyclic*, hydrocarbons are composed of carbon atoms arranged in a *ring* or *rings*. Paraffin oil is mostly composed of straight-chain aliphatic hydrocarbons, and cedarwood oil contains cyclic hydrocarbons. Both types of hydrocarbons are called *alkanes*.

Aromatic hydrocarbons are special groups of cyclic compounds that usually have six-member rings that may be visualized as having alternate single and double bonds (i.e., benzene rings). Cinnamon oil contains benzene rings. When an OH (hydroxyl) group is connected to a carbon atom of a benzene ring, the compound is known as a *phenol* (Pine at al., 1980, pp. 28, 47). DGEBA resins (see Box A) contain phenol groups that are connected together in pairs (*bisphenol* groups). These artificial resins are rich in aromatic bonds (e.g., a large peak at 3066 cm^{-1} is seen in the Raman spectrum of Opticon 224).

Hydrocarbons that have one or more carbon-carbon double bonds are called *alkenes* or *olefins* (Pine at al., 1980, p. 37). For instance, a peak in the 3000–3020 cm^{-1} region is associated with a hydrogen atom attached to one of the carbons in a carbon-

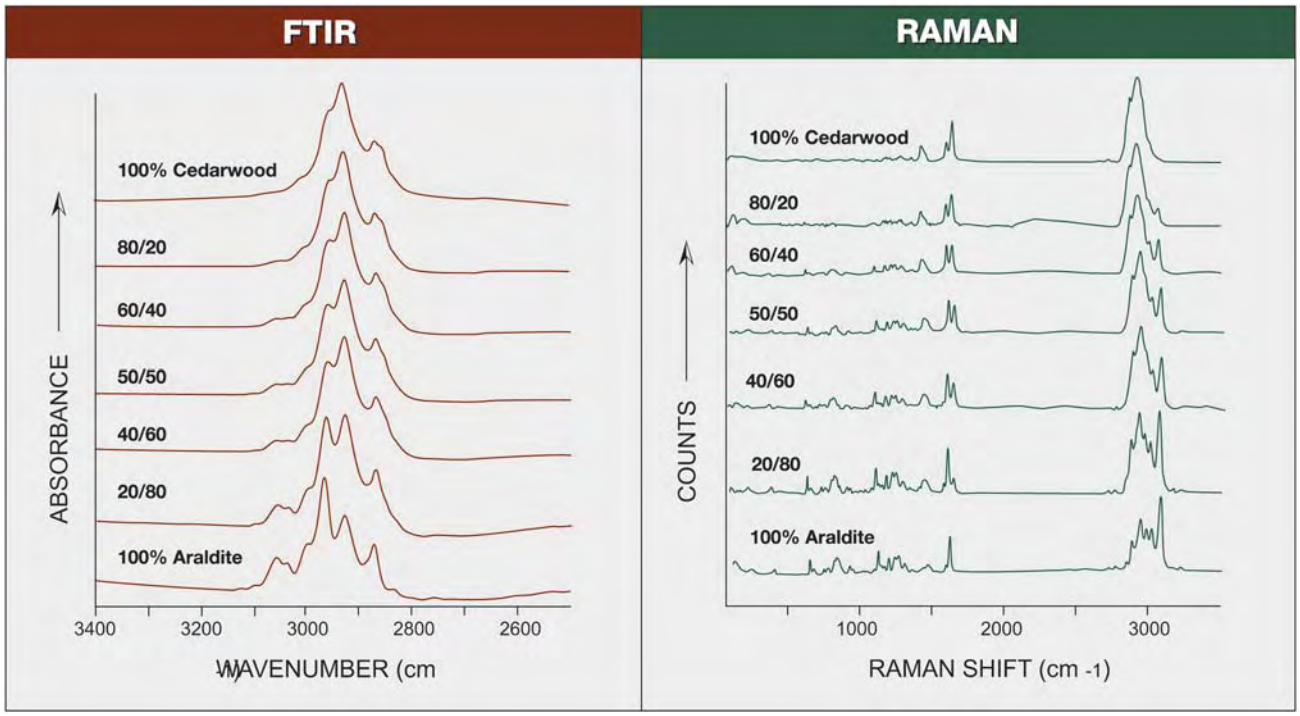

Figure 13. The infrared and Raman spectra of mixtures of (Baker) cedarwood oil and Araldite 6010 show features characteristic of both; mixtures with much more of one filler than the other are hard to distinguish from the pure compounds.

carbon double bond; this is seen in vegetable oils and Joban oil.

Separating "Presumed Natural" Substances (Essential Oils/Resins, Other Oils, Waxes) from Artificial Resins by FTIR and Raman. *Peak assignments and Interpretation.* The five spectral groups (A through E; again, see figures 11 and 12) are based on assignments of peaks to functional groups as follows:

- *Group A* spectra exhibit strong aromatic, aliphatic, and bisphenol epoxy peaks. It is very difficult to distinguish among these DGEBA epoxy resins spectroscopically. However, these compounds can vary in refractive index, viscosity, fluorescence, and degree of polymerization (again, see table 1).
- *Group B* spectra exhibit multiple strong aliphatic peaks, generally producing several distinct peaks in the 2925–2850 cm^{-1} region of the IR spectrum (or a broad overall peak in the Raman spectrum); some spectra also exhibit traces of alkene (olefin). The artificial resin HXTAL has a group B infrared spectrum (figure 11i), and affinities to both groups B and C in its Raman spectrum (figure 12i).
- *Group C* spectra exhibit less-distinct multiple IR peaks, but a single dominant aliphatic Raman peak, with small aromatic features seen in some compounds.
- *Group D* spectra exhibit both aromatic and aliphatic features.
- The *Group E* spectrum is a Raman spectrum only. The substance (cinnamon oil) that has this spectrum is unusual in that it exhibits both aliphatic and aromatic IR features (so its IR spectrum is in group D), but mostly aromatic Raman features. We observed no Raman spectrum for the other (cassia) cinnamon oil due to its strong fluorescence.

Spectra versus "Flash Effect" as a Detection Technique for Mixtures. Looking again at our experimental mixtures of Baker cedarwood oil and Araldite 6010, we found that mixtures with up to 20% Araldite (for Raman) or 40% Araldite (for IR) could not be distinguished from pure cedarwood oil on the basis of their spectra. Similarly, the spectra of the mixture with 90% Araldite–10% cedarwood oil could not be distinguished from those of pure Araldite 6010 with either technique (again, see figure 13 and table 3).

The fractures in stones filled with these mix-

tures became less apparent as the filler increased in refractive index. Although a weak flash was noted in the stone filled with the 1.522 R.I. mixture (90% cedarwood oil–10% Araldite), in general the flash effect became noticeable (as a weak blue flash) in the 1.539 R.I. mixture (60% cedarwood–40% Araldite), growing stronger as the R.I. increased. We concluded that, in this case, the variation in relative peak heights in the IR and Raman spectra was about as sensitive as flash effect for determining the presence of the high-R.I. artificial resin in the cedarwood oil mixtures.

Comparison with Previous Published Work. In general, there is good agreement between the Raman spectra published by Hänni et al. (1996a) and this study. Our results are similar to Hänni's for Permasafe ("New type of epoxy resin," 1998), but we saw an additional peak at 2928 cm^{-1}. According to Hänni et al. (1996b), artificial resins can be distinguished from "presumed natural" substances by the 1250, 1606, 3008, and 3069 cm^{-1} peaks in the Raman spectra of the former. In our filling substances, however, we could see (generally small) examples of each of these peaks in the spectra of certain cedarwood oils, other essential oils, or other vegetable oils. Hänni et al. (1996b) also saw features for cedarwood oil at 1440–1457 cm^{-1}, which we observed in some prepolymers as well.

Chalain et al. (1998) examined several UV-setting materials with lower R.I. values than the ones we studied; they also mentioned natural hydrocarbons in emerald, which we have not seen. They did not report the spectra for any of these, however.

Zecchini and Maitrallet (1998) looked at the IR spectra of several emerald fillers and related substances, including cedarwood oil, methyl methacrylate polymer, olive oil, "Israeli" (paraffin?) oil, Opticon 224, "palm oil," Indian Joban oil, red-colored Indian oil, and the Arthur Groom–Gematrat treatment, as well as the oil from human fingerprints. Our results agree with most, but not all, of theirs, in the cases where we studied the same materials. However, they interpreted the 3009 cm^{-1} peak in Joban and red oil as a dye band, whereas we saw this olefin band in all the vegetable oils we examined.

Sometimes, complete characterization cannot be done using FTIR or Raman, and only the type of chemical class can be identified (Julian et al., 1991). This is especially true for DGEBA epoxies, and neither FTIR nor Raman is likely to be useful in distinguishing prepolymers from hardened polymers in emeralds (but see the discussion of fluorescence, above, for another test).

Comparison with Substance Categories. Unfortunately, our spectral groups do not correspond precisely to the six substance categories indicated in table 1. *Essential oils* are found in IR and Raman spectral groups C, D, and E (group C also contains artificial resins). *Other oils* are in IR and Raman spectral group B; so is paraffin *wax*. Most *epoxy prepolymers* and *polymers* are in IR and Raman spectral group A. The *other prepolymers* (e.g., UV-setting adhesives) can be in group A (Epo Tek UVO114) or group C (in general), and HXTAL has characteristics of groups B and C.

Consequently, distinctions between artificial and "presumed natural" substances can most easily be made spectroscopically if the substance found is in group A (artificial resins only) or group D or E (essential oils only; but even in these cases, mixtures and multiple compounds must also be consid-

Figure 14. When water-insoluble filling substances (here, Araldite 6010) are mixed with water, they form a white cloudy emulsion. Left: Araldite 6010 and water before mixing; right: the substances shaken together. Photos by Maha DeMaggio.

ered). Distinctions between artificial and "presumed natural" substances are more problematic if the substance shows a group B or C spectrum. The distinctions within a spectral group may not be evident in filled emeralds, although this remains to be tested. The distinctions among groups C, D, and E can also be difficult to discern in a filled stone.

As another complication, the presence of spectral features indicating one particular compound does not preclude the existence of some other substance. As mentioned above, there can be almost 40% Araldite 6010 ("palma") in cedarwood oil—and the IR spectrum will still look like cedarwood oil, and not a mixture (although the Raman spectrum of the 20% Araldite mixture shows a DGEBA peak at 3068 cm^{-1}). Similarly, there can be about 10% cedarwood oil in Araldite before its presence is detected.

Combining the Approaches. That different gemological laboratories already determine the nature of filling materials is evident from auction records and other publications. Auction records (cited below) indicate that the identification of clarity enhancement substances by category or type has been performed by at least two laboratories: the SSEF in Basel, Switzerland, and the American Gemological Laboratory (AGL) in New York City.

SSEF provides identification reports, or "treatment slips," which state the category of filling material present (or the categories of fillers that are *not* present). This information is based on gemological examination as well as on Raman microspectrometry and FTIR spectroscopy (see, e.g., SSEF Swiss Gemmological Institute, 1998). The categories of fillers mentioned in SSEF treatment slips, as quoted in auction catalogs, include: oil, "natural oil," "natural resin," "artificial resin," and wax (Christie's, 1997b, 1997c, 1998a). According to Dr. Hänni (pers. comm., 1999), the categories currently in use are "oil," "Canada balsam," and "artificial resin."

As reported in auction catalogs, the AGL categories for "types" of filling materials include: "oil type," "Opticon/oil type," and "unidentified type" (Sotheby's 1997; Christie's 1998b). As of July 1997, AGL did not have Raman microspectrometry, and relied on the "flash effect" to identify the "vast majority" of fillers in emeralds examined there (Edry, 1997).

Our research has shown that the best results come from a combination of all the testing methods we have described. For instance, the conclusion that a material showing a flash effect is probably an artificial resin (DGEBA-based epoxy) is reasonable but not perfect; and the Raman and IR spectra of the common epoxy fillers are easily distinguished from those of available cedarwood oils. Raman and IR are more effective than gemological observation for distinguishing low-R.I. artificial resins from commonly used essential oils (all of which have no flash effect), and high-R.I. essential oils from DGEBA epoxies (all of which show a flash effect). However, the artificial resins in spectral group C all have low R.I.'s (and no flash effect) and may not be distinguishable from cedarwood oils.

CONCLUSIONS

Filler Terminology. On the basis of the findings presented here, and the discussion in Box A, we recommend the following terminology:

- The term *natural* should be avoided in discussions of emerald fillers, as "natural" substances are not currently distinguishable from their chemical equivalents synthesized in the laboratory (with the nondestructive tests we have available). Instead, substances such as essential oils, other oils, natural resins, and waxes should be referred to as "presumed natural."
- A distinction should be made between essential oils and other oils, as essential oils have different properties (e.g., they must be volatile) and a broader range of chemical structures (e.g., they can contain aromatic compounds). This difference may also be relevant to durability concerns.
- The term *synthetic* should be avoided, as it does not have the same meaning in chemistry that it has in gemology. Instead, manufactured prepolymers and polymers should be referred to as "artificial resins," as they have no natural equivalent.
- Prepolymers and polymers should be distinguished wherever possible, as their different mechanical properties are probably significant (e.g., liquid versus solid states), and may affect their durability in an emerald.
- Artificial resins should not be called "epoxies" unless they contain epoxide groups—if still liquid—or were joined into polymers with these groups (if solid; again, see Box A).
- Artificial resins should not be called "Opticon" or "Opticon type" unless they are known to be the

specific resin Opticon 224 (manufactured by Hughes Associates).

- Because a large quantity of one filler may make small amounts of another undetectable, we recommend restricting comments to the filler identified, and making no assurances that any others are absent.

Separating Fillers by Categories: Possible? Of the thousands of possible filling materials—about 3,500 essential oils and natural resins, many other oils, and several thousand commercially available polymers and prepolymers—we studied fewer than 40. None of the microscopic features (e.g., flash effect, fluorescence of the filled fractures) fully differentiates between the various categories of substances (again, see table 1), although such features may provide important clues.

Using Raman and FTIR spectroscopy, we found that the 39 isolated materials could be categorized into five spectral groups. The two groups that contain the most important "natural" fillers—cedarwood oil, Canada balsam, and vegetable oils—also contain materials that are not natural (Epo Tek 314 resin, UV-setting adhesives, Isocut fluid). Hence, identification of the spectral group alone is not sufficient to prove that a filling material is "natural." (However, the most commonly used artificial resins—Opticon 224, Araldite 6010, Epon 828—do occur in a spectral group that is easily distinguished from those in which the "presumed natural" fillers occur.)

Most of the isolated fillers we tested were "loose," that is, not in an emerald. A number of factors may limit the effectiveness of spectroscopic testing of substances after their emplacement in an emerald. In particular, transmission IR techniques are complicated by the fact that emerald is opaque in one diagnostic region (below 2000 cm^{-1}). Raman microspectrometry only samples near-surface areas of fissures, and fluorescence in the 3000 cm^{-1} region may interfere with the strongest Raman peaks. For both techniques, the filler peaks are generally much less prominent than the emerald spectral features.

On the basis of our results, we believe that the artificial resins most commonly used as emerald fillers can, *as pure substances*, be distinguished from cedarwood oils by a combination of gemological and spectroscopic properties, but other artificial resins also used in the trade cannot be so separated. The UV-setting adhesives are particularly problematic. At this time, we recommend the following procedure to identify individual fillers (or at least a substance category or spectral group): first, estimate the filler's refractive index (based on the presence or absence of a "flash effect"), and then obtain IR and/or Raman data. Other properties, such as fluorescence, also may be useful.

New filling materials and mixtures will continue to be discovered or adapted from other branches of science and technology. Competing factors make it unlikely that one best filler exists, and filler development continues. Kammerling et al. concluded their 1991 article with the comment: "It would, therefore, seem both inappropriate and misleading, in describing a filled fracture, to use wording that implies that the filling substance has been conclusively identified if in fact it has not." We must keep these uncertainties in mind as we try to identify specific substances.

However, the issue of filler identification is not the only one that must be addressed to understand fully the use of fillers in general, or of a specific filler in a particular emerald. Key questions remain: What is the effect of the degree of enhancement on an emerald's appearance? How does the enhancement change with time, normal wear, and other typical events in the life of a piece of jewelry? Given these questions, we are focusing on two main topics as we continue our research: (1) determination of the extent to which any particular emerald has been clarity enhanced; and (2) durability testing of several common emerald treatments.

Acknowledgments: The authors thank the following individuals for sharing their knowledge of emerald enhancements: Ricardo Alvarez Pinzon, Luis Ernesto Vermudez, and others at Treatment World Emerald, Gemológico Universal, Bogotá, Colombia; Dr. Rodrigo Giraldo, Centro Gemológico para la Investigación de la Esmeralda, Bogotá; Carlos Osorio, Mineralco, Bogotá; Jaime Rotlewicz, C. I. Gemtec, Bogotá; the staff of Alagecol (Asociación de Laboratorios Gemológicos), Bogotá; Ray Zajicek, Equatorian Imports, Dallas, Texas; Darrold Allen, Gemological Laboratory of Los Angeles, California; Kenneth Scarratt, AGTA Gemological Testing Center, New York City; Amnan Gad, Amgad Inc., New York City; Michael and Ari Gad, Gad International Ltd., New York City; Arthur Groom and associates, Arthur Groom–Gematrat, New York City; Morty Kostetsky, Arigad Gems, New York City; Dr. Kumar Shah, Real Gems Inc., New York City;

I. Z. Eliezri, Colgem Ltd., Ramat Gan, Israel; Ron Ringsrud, Constellation Colombian Emeralds, Saratoga, California; and Jess Williams and Andy Rendle, EmeraldStone Inc., Vancouver, BC.

Dr. Henry Hänni, Dr. Lore Kiefert, and J.-P. Chalain, SSEF Swiss Gemmological Institute, Basel, provided hospitality and information about the identification techniques used in their laboratory. MLJ also thanks the organizers of the First World Emerald Congress in Bogotá for their warm hospitality, and Mark Parisi for his support. Dr. George Rossman, of the California Institute of Technology in Pasadena, California, supplied much useful chemical information and advice.

Many GIA colleagues provided support for this project, including: Shane McClure, Maha DeMaggio, John Koivula, and Dino DeGhionno, GIA Gem Trade Laboratory (GTL), Carlsbad, California, and curator Jo Ellen Cole, GIA Carlsbad, who determined gemological properties; Margot McLaren of GIA's Richard T. Liddicoat Gemological Library and Information Center, Carlsbad, who located auction records; and GIA and GIA GTL colleagues Dr. James Shigley, Tom Moses, Dr. Ilene Reinitz, and Phil York, who gave suggestions that improved this manuscript.

GIA thanks Jewelers' Circular-Keystone, Radnor, Pennsylvania, and Kyocera Corp., Kyoto, Japan, for financial support of this research project. Michael Scott generously donated a Renishaw Raman microspectrometer to GIA, which was used in this research.

REFERENCES

Alger M.S.M. (1989) *Polymer Science Dictionary*. Elsevier Applied Science, London.

Benson L. (1960) Highlights at the Gem Trade Lab in Los Angeles. *Gems & Gemology*, Vol. 10, No. 1, pp. 3–6, 30–31.

Bleumink E., Mitchell J.C., Nater J.P. (1973). Allergic contact dermatitis from cedar wood (Thuja plicata). *British Journal of Dermatology*, Vol. 88, No. 5, pp. 499–504.

Bower D.I., Maddams W.F. (1989) *The Vibrational Spectroscopy of Polymers*. Cambridge University Press, Cambridge, England, 326 pp.

Brady G.S., Clauser H.R. (1986) *Materials Handbook: An Encyclopedia for Managers, Technical Professionals, Purchasing and Production Managers, Technicians, Supervisors, and Foremen*, 12th ed. McGraw-Hill Book Co., New York, 1038 pp.

Chalain J.-P., Hänni H.A., Kiefert L. (1998) Détermination des substances de remplissage dans les émeraudes. In D. Giard, Ed., *L'émeraude: Connaisances Actuelles et Prospectives*. Association Française de Gemmologie, Paris, pp. 107–115. (Translations where cited are by Mary Johnson.)

Christie's (1993) *Magnificent Jewels*. Auction catalog for Christie's Geneva, November 16 and 18, 1993.

Christie's (1997a) *Magnificent Jewels*. Auction catalog (in two parts) for Christie's New York, October 27–28, 1997.

Christie's (1997b) *Magnificent Jewels*. Auction catalog for Christie's Geneva, November 20, 1997.

Christie's (1997c) *Important Jewellery*. Auction catalog for Christie's London, December 16, 1997.

Christie's (1998a) *Important Jewels*. Auction catalog for Christie's St. Moritz, February 20–21, 1998.

Christie's (1998b) *Magnificent Jewels*. Auction catalog (in two parts) for Christie's New York, April 6–7, 1998.

Congress votes yes to promotion, no to codes (1995). *ICA Gazette*, August 1995, p. 9.

Crowningshield, G.R. (1958) Ascertaining the nature and extent of damage or inherent flaws in gemstones. *Gems & Gemology*, Vol. 9, No. 5, pp. 131–133, 159.

Crowningshield, G.R. (1960–1961) Developments and highlights at the Gem Trade Lab in New York. *Gems & Gemology*, Vol. 10, No. 4, pp. 114–123.

Edry S.G. (1997) Emerald filling: More research sought. *National Jeweler*, Vol. 41, No. 13, pp. 1, 64, 65.

Elias H.-G. (1993) *An Introduction to Plastics*. Weinheim, New York.

Federman D. (1997) Beyond buyer beware. *Modern Jeweler*, Vol. 96, No. 3, pp. 50, 51, 53–55.

Federman D. (1998a) *Modern Jeweler's Consumer Guide to Emeralds*. Supplement to *Modern Jeweler*, Vol. 97, No. 1, 7 pp.

Federman D. (1998b) Fair play. *Modern Jeweler*, Vol. 97, No. 2, p. 108.

Fryer C., Crowningshield R.C., Hurwit K., Kane R.E. (1984) Gem trade lab notes: Emerald, oiled. *Gems & Gemology*, Vol. 20, No. 1, pp. 46–47.

Genis R. (1997) The emerald controversy. *Rapaport Diamond Report*, Vol. 20, No. 38, pp. 69, 72–73.

Hänni H.A. (1988) An oil well in your garden. *Swiss Jewellery Journal*, No. 3, pp. 461–464.

Hänni H.A. (1998) Fracture filling in emeralds and its detection with laboratory methods. *ICA Gazette*, July/August 1998, pp. 5–7.

Hänni H.A., Kiefert L., Chalain J.-P., Wilcock I.C. (1996a) Ein Renishaw Raman Mikroscop im gemmologischen Labor: Erste Erhfarhrungen bei der Anwendung. *Zeitschrift der Deutschen Gemmologischen Gesellschaft*, Vol. 45, No. 2, pp. 55–70.

Hänni H.A., Kiefert L., Chalain J.P. (1996b) How to identify fillings in emeralds using Raman spectroscopy. *Jewellery News Asia*, No. 145, pp. 154, 156.

Hänni H.A., Kiefert L., Chalain J.P. (1997) Renishaw Raman nothing new. *Rapaport Diamond Report*, Vol. 20, No. 40, p. 11.

Harris D.C., Bertolucci M.D. (1978) *Symmetry and Spectroscopy: An Introduction to Vibrational and Electronic Spectroscopy*. Oxford University Press, Oxford, England, 550 pp.

Herout V. (1982) Sesquiterpene alcohols. In E.T. Theimer, Ed., *Fragrance Chemistry: The Science of Smell*. Academic Press, New York, pp. 222–263.

Hurwit K. (1989) Gem trade lab notes: Emerald, with plastic-like filling. *Gems & Gemology*, Vol. 25, No. 2, p. 104.

Johnson M.L., Koivula J.I. (1997) Gem news: A new emerald filler. *Gems & Gemology*, Vol. 33, No. 2, pp. 148–149.

Johnson M., McClure S., Koivula J., Moses T. (1998a) How to detect clarity enhancement in emeralds. *Modern Jeweler*, Vol. 97, No. 1, pp. 58–61.

Johnson M.L., Koivula J.I. (1998b) Gem news: A preliminary report from the First World Emerald Congress. *Gems & Gemology*, Vol. 34, No. 1, pp. 56–57.

Julian J.M., Anderson D.G., Brandau A.H., McGinn J.R., Million A.M., Brezinski D.R. (1991). *An Infrared Spectroscopy Atlas*

for the Coatings Industry, 4th ed., Vol. 1. Federation of Societies for Coatings Technology, Blue Bell, PA.
Kammerling R.C., Koivula J.I., Kane R.E., Maddison P., Shigley J.E., Fritsch E. (1991) Fracture filling of emeralds: Opticon and traditional "oils." *Gems & Gemology*, Vol. 27, No. 2, pp. 70–85.
Kammerling R.C. (1993) Gem trade lab notes: Emerald, with large filled etch channels. *Gems & Gemology*, Vol. 29, No. 4, p. 280.
Kammerling R.C., McClure S.F., Johnson M.L., Koivula J.I., Moses T.M., Fritsch E., Shigley J.E. (1994) An update on filled diamonds: Identification and durability. *Gems & Gemology*, Vol. 30, No. 3, pp. 142–177.
Kammerling R.C., Maddison P., Johnson M.L. (1995) Gem trade lab notes: Emerald, with unusual flash-effect colors. *Gems & Gemology*, Vol. 31, No. 1, p. 54.
Kane R.E. (1990) Gem trade lab notes: Emerald, with filled fractures. *Gems & Gemology*, Vol. 26, No. 1, pp. 95–96
Kennedy H.F. (1998) Brazilian emeralds: Oiling at the source. *National Jeweler*, Vol. 42, No. 10, pp. 36–52 passim.
Koivula J.I. (1999) Gem trade lab notes: Emerald, the case of the invisible filler. *Gems & Gemology*, Vol. 35, No. 1, pp. 43–44.
Lee H., Neville K. (1967) *Handbook of Epoxy Resins*. McGraw-Hill Book Co., New York.
Liddicoat R.T. Jr.(1962) *Handbook of Gem Identification*, 6th ed. Gemological Institute of America, Los Angeles, 396 pp.
Lincoln W.A. (1986) *World Woods in Color*. Linden Publishing, Fresno, CA, 320 pp.
Mutton, D.B. (1982) Wood resins. In W.E. Hillis, Ed., *Wood Extractives and Their Significance to the Pulp and Paper Industries*. Academic Press, New York, pp. 331–365.
Nassau K. (1994) *Gemstone Enhancement: History, Science, and State of the Art*, 2nd ed. Butterworth-Heinemann, Oxford, England, 252 pp.
New type of epoxy resin. (1998) *Jewellery News Asia*, No. 172, p. 60.
Nicolet (1992) *Omnic Interpretation Guide: Infrared Spectroscopy*, Version 1.0, Nicolet Instrument Corp., Madison, Wisconsin.
Ottaway T.L., Wicks F.J., Bryndzia L.T., Kyser T.K., Spooner E.T.C. (1994) Formation of the Muzo hydrothermal emerald deposit in Colombia. *Nature*, Vol. 369, pp. 552–554.
Pine S.H., Hendrickson J.B., Cram D.J., Hammond G.S. (1980) *Organic Chemistry*, 4th International Student Edition. McGraw-Hill International, Tokyo, 1039 pp.
Pouchert, C.J. (1985). *The Aldrich Library of FT-IR Spectra*, Vol. 1. The Aldrich Chemical Co., Milwaukee, WI.
Review on ruby promotion. (1997) *Jewellery News Asia*, No. 158, p. 58.
Ringsrud R. (1983) The oil treatment of emeralds in Bogotá, Colombia. *Gems & Gemology*, Vol. 19, No. 3, pp. 149–156.
Ringsrud (1998) Stick with cedarwood. *Modern Jeweler*, Vol. 97, No. 3, p. 10.
Sinkankas J. (1981) *Emeralds and Other Beryls*. Chilton Book Co., Radnor, PA, 665 pp.
Sivry B. (1985) Colles et adhédifs. *Encyclopaedia Universalis*, Corpus 5, pp. 74–78. (Translations where cited are by Mary Johnson.)
Sotheby's (1992a) *Magnificent Jewels*. Auction catalog for Sotheby's Geneva, November 18, 1992.
Sotheby's (1992b) *Jewels*. Auction catalog for Sotheby's London (Colonnade), November 26, 1992.
Sotheby's (1993) *Magnificent Jewelry*. Auction catalog for Sotheby's New York, October 20–21, 1993.
Sotheby's (1997) *Magnificent Jewels*. Auction catalog for Sotheby's New York, October 29–30, 1997
SSEF Swiss Gemmological Institute (1998) *Standards and Applications for Diamond Report, Gemstone Report, Test Report*. SSEF, Basel, Switzerland, 118 pp.
Stecher P.G., Windholz M., Leahy D.S., Bolton D.M., Eaton L.G. (1968) *The Merck Index*, 8th ed. Merck & Co., Rahway, NJ.
Survey: Emerald treatments (1997). *The Guide Quarterly Report*, Vol. 16, No. 2, p. 15.
Webster R., Read P.G. (1994) *Gems: Their Sources, Descriptions, and Identifications*, 5th ed. Butterworth-Heinemann, Oxford, 1026 pp.
Webster's Ninth New Collegiate Dictionary (1987) Merriam-Webster Inc., Springfield, MA, 1,563 pp.
Weldon R. (1998a) Treatment tracer. *Professional Jeweler*, Vol. 1, No. 3, p. 50.
Weldon R. (1998b) Filling a need. *Professional Jeweler*, Vol. 1, No. 5, pp. 80, 82, 84.
Zecchini P., Maitrallet P. (1998) Que peut apporter la spectrographie infrarouge dans l'étude des émeraudes? In D. Giard, Ed., *L'émeraude: Connaisances Actuelles et Prospectives*. Association Française de Gemmologie, Paris, pp. 81–96.

SAPPHIRE AND GARNET FROM KALALANI, TANGA PROVINCE, TANZANIA

By Antonin V. Seifert and Jaroslav Hyrsl

Located just 3 km south of the famous Umba locality, the geologically similar Kalalani area hosts deposits of gem-quality sapphire (reddish orange, yellow-brown, and other colors), pyrope-almandine, and tsavorite. The gems are mined principally from primary and eluvial sources associated with a serpentinite body and surrounding metacalcareous rocks. The gemological properties of sapphires from Kalalani are very similar or identical to those from Umba. The garnets, however, are different: Tsavorite is not known from the Umba area, and the dark red to brownish red pyrope-almandine from Kalalani is distinct from the pink-purple rhodolite more commonly found at Umba.

ABOUT THE AUTHORS

Dr. Seifert (seifert@cgu.cz) is a senior officer at the Czech Geological Survey, Klarov 3, Prague 1, Czech Republic. Dr. Hyrsl is a consulting mineralogist-gemologist based in Prague, and a former staff member of the Faculty of Natural Sciences at Charles University in Prague.

Please see acknowledgments at the end of the article.

Gems & Gemology, *Vol. 35, No. 2, pp. 108–120*

The Kalalani area in northeastern Tanzania hosts several primary deposits of sapphire and the largest primary deposit of pyrope-almandine in that country. In 1989–1990, two significant discoveries of reddish orange ("Umba padparadscha"; see figure 1) and yellow-brown sapphires were made in desilicated pegmatites that cross-cut a small serpentinite massif. In 1994, a primary deposit of tsavorite was discovered in the surrounding graphitic gneisses, and two pieces of gem-quality tanzanite were found in alluvial sediments adjacent to the Kalalani serpentinite massif.

This article is based on field research by the senior author, who acted as a consultant in the exploration and mining of the sapphire deposits in 1989–1990, and also mined the large pyrope-almandine deposit in 1994. The second author visited the Kalalani area in 1993, and provided the laboratory data on the samples.

LOCATION AND ACCESS

The Kalalani gem deposits are located approximately 100 km northwest of the town of Tanga, and 6 km (or 14 km by dirt road) south of the Umba camp, at coordinates 4° 34′ S, 38° 44′ E (figure 2). This flat terrain is characterized by red-brown lateritic soil that is covered by thick bush vegetation and grasslands. The mining area, called "Vipigoni" by locals, lies about 5 km northwest of Kalalani village, from where it can be accessed by a rough dirt road. During the rainy season (December–March), access to the area may be difficult.

GEOLOGY

Regional Geology. The gem-bearing districts of both the Umba River and Kalalani areas are hosted by rocks of the Usagaran System, a part of the Mozambique Belt. These rocks underwent several episodes of metamorphism, plutonism, thrusting, and folding during the Late Proterozoic to Early Paleozoic Pan-African orogenic event (Malisa and

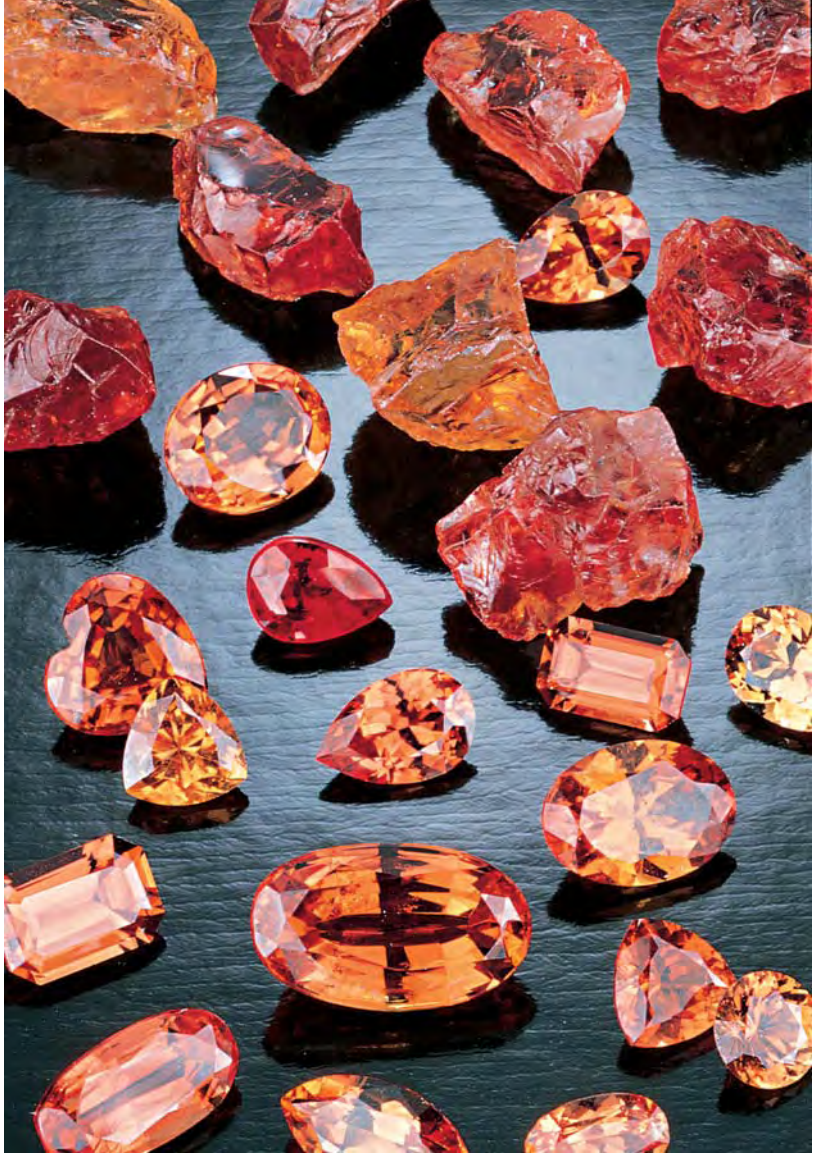

Figure 1. Most of the sapphires from the Kalalani area, which are typically fancy colors, have been mined from primary deposits. These reddish orange sapphires are from the Cham-Shama claim. The faceted stones range from 0.22 to 0.91 ct. Courtesy of Varujan Arslanyan, Arslan Jewelers, New York; photo © GIA and Tino Hammid.

Muhongo, 1990). The area was geologically surveyed by Hartley and Moore (1965) as part of the *Quarter Degree Sheet 91 and 110, Daluni* (scale 1:125,000). The rocks consist of high-grade banded gneisses of the granulite facies, gneisses of the amphibolite facies, graphitic gneisses, metacalcareous rocks, quartzites, crystalline limestones, and meta-amphibolites. These rocks surround two isolated bodies of serpentinite (i.e., the Umba and Kalalani serpentinite massifs; see figures 2 and 3). The geologic setting, mineral assemblages, and presence of gem-corundum-bearing pegmatites at both localities suggest that these massifs have a similar geologic history.

Local Geology. *Corundum Deposits.* Gem-quality sapphire and ruby are confined to desilicated pegmatites that cross-cut the serpentinite (figure 3). They generally form lenticular (lens-like) bodies that are oriented vertically, and measure about 5–10 m long and up to 2–3 m wide. The dimensions are quite variable, since the pegmatites commonly pinch and swell (see, e.g., figure 4). Like those at Umba (see Solesbury, 1967), the Kalalani pegmatites are generally coarse grained (up to 5 cm), and contain calcic plagioclase (andesine-labradorite) but no quartz. Other major constituents include amphibole, vermiculite, chlorite, biotite, spinel, corundum, and kyanite (see, e.g., figure 5).

The mineralized zones of the two pegmatites that yielded reddish orange and yellow-brown sapphires measured approximately 6 m long and 2 m wide. Although these pegmatites were only about 50 m apart, they showed distinct differences. The reddish orange sapphire was mostly concentrated in patches of clay minerals within "golden" yellow vermiculite and was accompanied by pink spinel (of low cabochon quality) as an important indicator. However, the yellow-brown sapphire was found within bluish green vermiculite, in the absence of clay, and the tracer mineral was spinel-pleonaste.

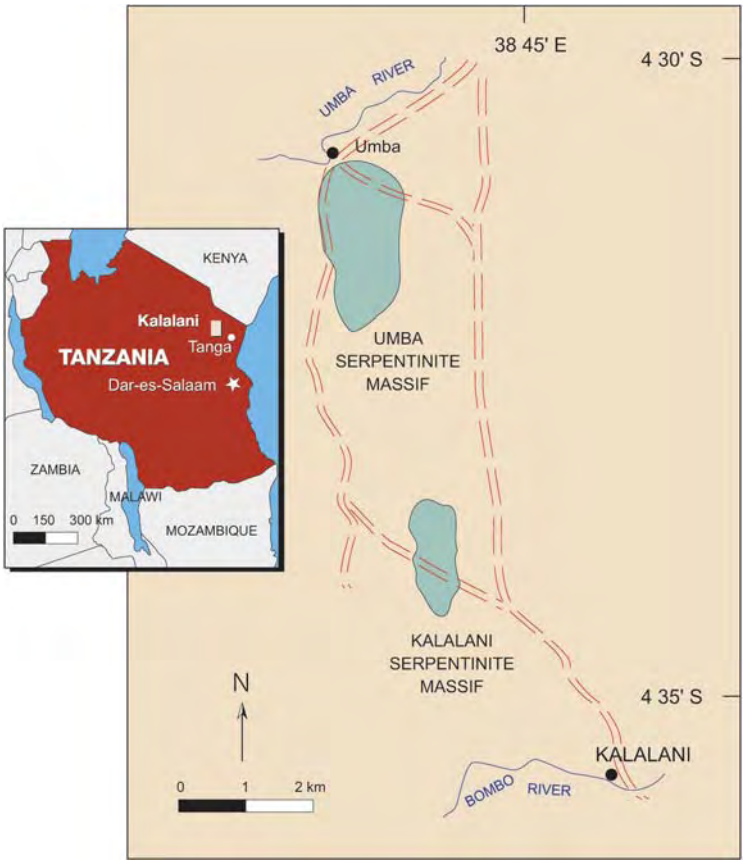

Figure 2. The Kalalani gem deposits are associated with the Kalalani serpentinite massif in northeastern Tanzania (inset), a few kilometers south of the Umba area. Dirt tracks (shown here in brown) traverse both sides of the two serpentinite massifs between the villages of Umba and Kalalani.

Ruby has been found at only two locations in Kalalani. At one of these, the senior author noted that tabular ruby was randomly distributed within biotite in a desilicated pegmatite, and was accompanied by crystals of color-change sapphire.

Pyrope-Almandine Deposits. Along the eastern periphery of the Kalalani serpentinite are two areas

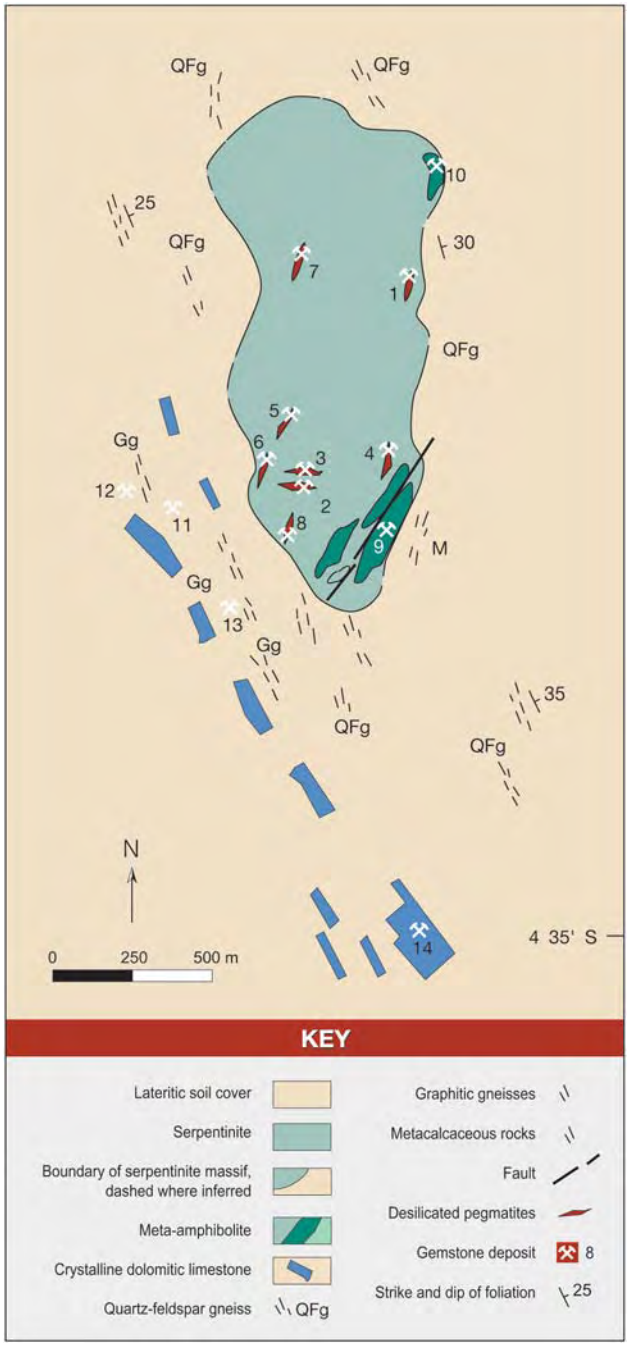

Figure 3. The Kalalani serpentinite is cross-cut by desilicated pegmatites that locally contain gem corundum. Pyrope-almandine is mined from metaamphibolites near the boundary of the serpentinite, and tsavorite deposits are hosted by graphitic gneisses southwest of the serpentinite. The deposits are designated here according to the name of their claim block: 1 = original "Papas" pit, reopened by Ruvu Gem Ltd. (color-change sapphire, ruby); 2 = Cham-Shama (reddish orange sapphire); 3 = Cham-Shama (yellow-brown sapphire); 4 = Peter A. (an old "Papas" pit; light blue and pink sapphires, ruby); 5 = Sumai (yellow-brown sapphire); 6 = old "Papas" pit, reopened by Africa-Asia Precious Stones and Mining Co. (light blue and yellow sapphires); 7 = Peter A. (pink sapphire); 8 = Cham-Shama (pink sapphire); 9 = Peter A. (pyrope-almandine/rhodolite); 10 = Salehe J. (pyrope-almandine) 11 = Abdalah (tsavorite, main pit); 12 = Ruvu Gem Ltd. (tsavorite); 13 = Maluki C. (tsavorite); and 14 = Kwendo N. (alluvial garnet, sapphire, and rare tanzanite). Mapped by A.V. Seifert, 1994.

that contain meta-amphibolites (see figure 3). The southern amphibolite body hosted an economic deposit of pyrope-almandine (Peter A. claim), along the faulted and sheared contact with serpentinite (figure 6). The mineralized zone measures 100 m long, varies from 6 to 12 m wide, and dips 45° northwest. The pyrope-almandine occurred in nodules averaging 10 cm in diameter. The nodules were typically fractured masses that contained flattened pieces of pyrope-almandine embedded in a fine-grained yellowish dolomite (figure 7). The best-quality stones were recovered from the northeastern part of the deposit; the material from the southwestern part was more fractured and was heavily included.

Tsavorite Deposits. Graphitic gneisses near the southwestern part of the serpentinite body are interbedded with quartz lenses that are accompanied by accumulations of pure graphite, where tsavorite has formed locally. These lenses crop out locally over a distance of about 1.7 km, and each is elongated up to 25 m in a southeasterly direction; they vary in width from a few centimeters up to 2 m. At least four parallel zones showing surface signs of tsavorite mineralization were traced in this area.

Figure 4. This geologic map (top) and cross-section (bottom) of the Cham-Shama reddish orange sapphire deposit show the sapphire-bearing desilicated pegmatite and associated veins. Abbreviations: a = desilicated pegmatite containing patches of clay minerals (white) with sapphire; b = blue-green vermiculite vein; c = golden yellow vermiculite vein; d = pyroxenite vein. Mapped by A.V. Seifert, 1990.

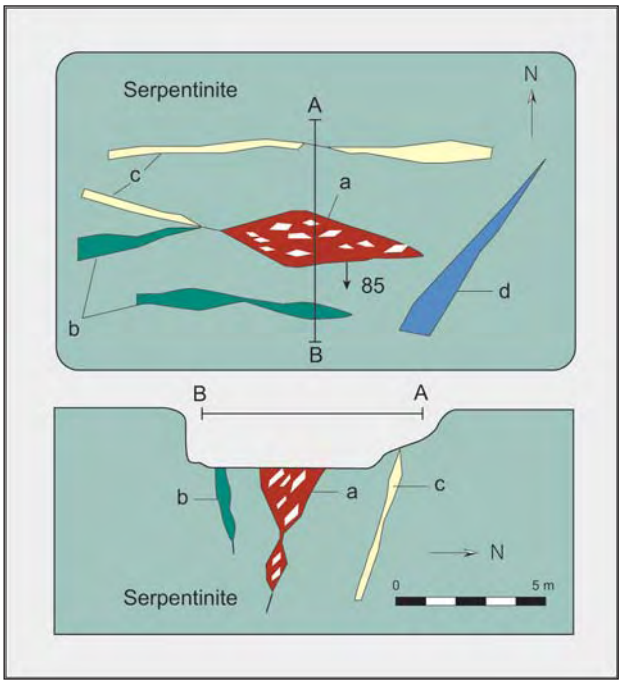

Figure 5. At the Cham-Shama claim, reddish orange sapphire crystals were recovered from desilicated pegmatites composed mainly of vermiculite (brown flakes), calcic plagioclase (white), and amphibole and chlorite (dark green). The prismatic sapphire crystal in the center of the photo is about 4 cm long. Photo by Varujan Arslanyan.

Figure 6. This geologic cross-section shows the northeastern part of the Peter A. pyrope-almandine deposit. The garnet is found as fractured nodules within altered lenses of meta-amphibolite. The mineralized meta-amphibolites have been faulted and sheared within the serpentinite. Mapped by A.V. Seifert, 1994.

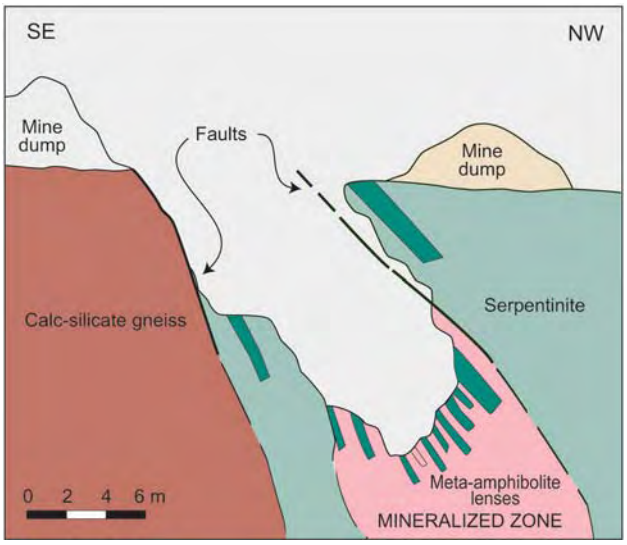

Figure 7. This nodule of pyrope-almandine (4 cm across) from the Peter A. deposit contains gem-quality fragments that are embedded in fine-grained dolomite. The rhodolite nodule is attached to its meta-amphibolite matrix. Photo by J. Hyrsl.

Alluvial Deposits. About 1 km south of the Kalalani serpentinite, gem-bearing alluvial sediments have been deposited among outcrops of the crystalline dolomitic limestones. Irregularities on the surface of the limestones have trapped the gems at about 2–5 m below the surface. These stones (sapphire, garnet, and—very rarely—tanzanite) have been derived from the Kalalani serpentinite and its surroundings. The gems generally show a slightly worn surface, which is consistent with what we believe to be a relatively short transport distance.

HISTORY, MINING, AND PRODUCTION

The history of the Kalalani area is closely associated with the nearby Umba River area, which has been described by Solesbury (1967), Dirlam et al. (1992), and Keller (1992). Although there are no official data on gem production from the Kalalani area, the senior author estimates that to date, the total production of fancy-color sapphire from the area is about 400 kg. Thus far, less than 1% of this production has been facet grade.

Sapphire and Ruby. The first organized mining of sapphire in the Kalalani area was by Umba Ventures Ltd., owned by George "Papas" Papaeliopoulos, who developed three shallow open pits to explore the pegmatites in the 1960s. Since then, the Kalalani area has been worked continuously by local miners who hand sieve the eluvial soil cover in search of fancy-color sapphires and ruby. Organized mining of primary deposits virtually ceased from the 1970s into the early 1980s, when the original "Papas" pit, situated on the eastern border of the serpentinite (figure 3, location 1), was reopened by Ruvu Gem Ltd. At 40 m, this is now the deepest mine in the Kalalani area. The serpentinite rock is very soft, and mining was carried out only by pick and shovel. A modified block mining method was used in the open pit; that is, individual blocks measuring about 5 m were excavated along the pegmatite dike, leaving vertical walls in the surrounding serpentinite (figure 8). When the dike pinched off, the miners dug a haulage level at another 5 m depth, and the process was repeated. The

Figure 8. The deepest pit in the Kalalani area (40 m) was excavated for sapphire and ruby by Ruvu Gem Ltd., using a modified block mining method. Mining ceased here in 1994. Photo by A. V. Seifert.

material from the pit was shoveled or winched to the surface, where it was sieved and examined by hand.

During the time of greatest activity, in the mid-1980s, about 30 people were involved in mining. Some cabochon-grade color-change sapphire was recovered, but transparent material was rare and the faceted stones seldom exceeded 1 ct. Cabochon-grade ruby (typically up to only 0.5 ct) accompanied the sapphire in places. Although Ruvu Gem ceased mining there in 1994, collector-quality sapphire crystals can still be found in the mine dump.

In August 1989, an important discovery of reddish orange sapphire was found in a pegmatite dike at the Cham-Shama claim (figure 3, location 2; see also figure 4). The rights to develop this locality, as well as to explore the remaining part of the claim, were secured by V. Arslanyan of New York and H. D. Patel of Dar es Salaam. Systematic trenching of this claim led to the discovery of yellow-brown sapphire in another pegmatite dike (figure 3, location 3) in March 1990.

Prior to mining the pegmatites, the overlying eluvium was removed by a backhoe and sieved for loose sapphire crystals. The exposed pegmatites were then worked by pick and shovel (figure 9), or with a backhoe after drilling and blasting. The sapphires were removed from the soft vermiculite by hand. The mining of both deposits ceased at about 5–7 m depth in July 1990, and there has been no further organized activity since then.

The transparent pieces of reddish orange sapphire seldom exceeded 3–5 ct, although some cabochon-grade rough reached over 100 grams. Of the approximately 80 kg of reddish orange sapphire produced, about 1.5% was of excellent gem quality. A few of the stones were red enough to be considered ruby (figure 10). The yellow-brown sapphire rough ranged up to 4–6 ct, but clean, transparent rough reached only 2 ct. About 100 kg of yellow-brown sapphire were recovered, with less than 1% of gem quality. These were the only commercially significant sapphire finds in Kalalani over the past 30 years.

In December 1989, the team briefly concentrated on developing an old "Papas" pegmatite dike for ruby and sapphire at the Peter A. claim (figure 3, location 4). Gemmy tabular crystals of ruby up to 1 ct reportedly were found there in the early 1980s (Peter Alfred, pers. comm., 1989). However, the 1989 effort saw no production and the locality was abandoned. Nevertheless, small-scale mining by primitive methods continues, to a present depth of about 30 m, and light blue and pink sapphires are occasionally recovered in sizes ranging up to 1 ct.

Figure 9. Miners work the desilicated pegmatite at the Cham-Shama claim from which reddish orange sapphire was recovered. The pegmatite is visible here as patches of white and greenish blue beneath the horizon of red lateritic soil. The hose to the left carried compressed air for removing the excavated material and cleaning the bottom of the pit. Photo by A. V. Seifert.

During 1991–1994, the Sumai claims (figure 3, location 5) were worked by the American venture Down to Earth Co. More than 10 pegmatites were mined to an average depth of 5 m, but none proved economic. About 20 people were involved in the drilling, blasting, and excavating. The pegmatitic material was processed in a nearby crushing and

Figure 10. In addition to reddish orange sapphire (upper left, 5.07 ct), the Cham-Shama claim has produced a few rubies (here, 0.61–1.31 ct). Courtesy of Varujan Arslanyan; photo by Maha DeMaggio.

sieving apparatus (figure 11). Tens of kilograms of yellow-brown sapphire were recovered from the main pit. However, only a small percentage of this was cabochon grade, and rare small (<1 ct rough) pieces were facetable.

In 1994, an old "Papas" pit near the western boundary of the serpentinite (figure 3, location 6) was reopened briefly and mined to a depth of 25 m. About 10 people were involved in the mining, including Africa-Asia Precious Stones and Mining Co. of Bangkok. Light blue and yellow sapphires were recovered, but the facet-grade rough rarely exceeded 1 ct.

Sapphires have also been found by locals at many other localities in the Kalalani serpentinite massif. Open pits for pink sapphire at the Peter A. claim (figure 3, location 7) and at the Cham-Shama claim (figure 3, location 8) were worked to a depth of approximately 5 m before being abandoned. About six claims are presently being worked in the Kalalani area by small groups of up to about five local miners, with a foreman appointed by the claim owners. Currently there is little gem production from the area.

Pyrope-Almandine. The Peter A. "rhodolite" claim (figure 3, location 9) has been mined since the early 1980s, and until 1989 it produced stones mostly from the topsoil. The senior author's team began mining the primary deposit in late 1989, using a backhoe to strip the overburden. In 1990 about 40 workers selectively mined the mineralized zone with drilling and blasting. The upper part of the mineralized zone, to 6 m depth, was extremely rich, and approximately 30 kg of garnet were recovered per day.

Figure 11. Simple crushing and sieving equipment was used to recover sapphires at the Sumai claims by Down to Earth Co. Photo by A. V. Seifert.

From 1991 to 1994, the deposit was worked by local miners using only hammers and chisels. The mineralized zone (approximately 9 m wide) was followed to 10 m depth. The best rough—some weighing over 10 grams—was found in a tunnel that followed the productive zone to a depth of 20 m.

In 1994–1995, the local venture Skyline Enterprises Ltd. worked the deposit. They removed the dangerous hanging wall, and built an access road to the bottom of the pit. The waste rock was removed from the open pit with the help of a backhoe, two trucks, and a bulldozer. The gem-bearing ore was crushed and sieved at a nearby treatment plant. The treatment plant, which had a daily capacity of about 25 tons, yielded about 50 kg of garnet per day. Since many larger stones were cracked or broken during the crushing procedure, nodules that would yield the largest, best-quality stones were recovered directly after blasting and carefully hand cobbed. The best stones were sold in Idar-Oberstein, Germany, with the remainder sold in Dar es Salaam or Bangkok.

The mine was worked to a depth of 12 m; for six months, it produced approximately one ton of pyrope-almandine per month. About 5% of this was eye-clean, and 1% was microscopically clean. The color was typically dark red to brownish red, although some purplish red rhodolite (figure 12) was recovered from the northeastern part of the deposit. Gem-quality fragments averaging 1–2 grams were common, with some gem pieces exceeding 10 grams. Generally, the faceted stones ranged from 2 to 10 ct, with some over 20 ct. Mechanized mining ceased in mid-1995, and the mine recently closed completely.

Another pyrope-almandine deposit associated with meta-amphibolites was briefly mined on the northeastern margin of the Kalalani serpentinite in 1991 (figure 3, location 10). The garnet was dark red-brown and mostly translucent, but it contained abundant black inclusions, so the pit was closed at a depth of only 3 m.

Tsavorite. In 1994, tsavorite was discovered at the Abdalah claim, about 200 m southwest of the Kalalani serpentinite. About 60 people were

Figure 12. Pyrope-almandine from the Peter A. deposit is typically dark red to brownish red (here, 2.22–7.05 ct). Some, however, was the purplish red variety, rhodolite (inset, 3.17–11.85 ct). Courtesy of Varujan Arslanyan; photo © GIA and Tino Hammid.

involved in drilling, blasting, and operating a backhoe. The main pit (figure 3, location 11) measured 100 m × 50 m × 20 m, and followed a mineralized zone that was concordant with the graphitic gneisses. A single lens found at 15 m depth produced about 6 kg of predominantly light green tsavorite. About 1% was gem quality (see, e.g., figure 13); the remainder showed abundant white oval inclusions and dark impurities. The faceted stones rarely exceeded 2 ct. Official production figures are confidential, but local miners indicated that a total of about 20 kg of tsavorite were recovered from the Abdalah claim in 1994. The mine closed in 1995, and we know of no further mining activity.

Following the discovery of tsavorite at Abdalah, exploration was launched at the adjacent Ruvu Gem and Maluki C. claims (figure 3, locations 12 and 13, respectively) with the help of a bulldozer and backhoe. Many signs of primary tsavorite mineralization were detected, but none of these was of economic interest.

Tanzanite. Miners recovered two pieces of gem-quality tanzanite in 1994, while searching for garnet and sapphire in the alluvium at the Kwendo N. claims, about 1 km south of the Kalalani serpentinite (figure 3, location 14). The larger tanzanite was deep blue as found, and weighed over 10 ct; it was cut into two pieces and sold in Dar es Salaam. News of the discovery brought hundreds of local villagers into the area. The soil covering the naturally pitted bedrock was loosened by picks, commonly to depths of 2–5 m, and shoveled into sieve boxes at the surface. Limited mining of the alluvial deposits has continued, but no more tanzanite has been recorded.

MATERIALS AND METHODS

The gem material studied was collected by the authors at the mines, and consisted of rough, polished rough, cabochons, and faceted samples of sapphire and garnet. The sapphires studied were: three polished flattened crystals of reddish orange sapphire (0.46, 0.91, and 1.16 ct) from the Cham-Shama claim; 10 cabochons (up to 10 ct each) and about 800 grams of rough yellow-brown sapphire from the main pit of the Sumai claim; and four color-change sapphire crystals (up to 5 cm long) in matrix from the Ruvu Gem claim. About 1 kg of rough pyrope-almandine and 12 faceted stones (up to 5 ct) from

Figure 13. Tsavorite from the Kalalani area is typically light green, although material showing a range of tone and saturation has been produced (shown here, 1.19–3.94 ct). The tsavorite in the platinum and diamond ring weighs 3.44 ct. Courtesy of Varujan Arslanyan; photo © GIA and Tino Hammid.

the Peter A. claim were available for the investigation. A parcel of rough containing seven polished pieces of tsavorite (up to 1 gram each) from the Abdalah claim was obtained later from P. Pongtrakul of Dar es Salaam for examination.

Gemological testing was performed on all polished samples, except for five cabochons of yellow-brown sapphire which were not tested for R.I. and S.G. Refractive indices were measured with a German "Schneider" refractometer with a near-monochromatic light source. Specific gravity was determined hydrostatically (an average of three sets of measurements). Fluorescence to ultraviolet radiation was observed in a darkened room using a short- and long-wave UV lamp. A polariscope was used to observe the polarization behavior. Internal features were examined using an immersion microscope and a standard gemological microscope in conjunction with brightfield, darkfield, and oblique fiber-optic illumination, as well as polarizing filters.

The visible spectra of one reddish orange sapphire, one yellow-brown sapphire, and two pyrope-almandine garnets were recorded using a Perkin-Elmer "Lambda 9" spectrophotometer, in a range from 350 nm to 800 nm. The chemical composition of two polished reddish orange sapphires and three faceted pyrope-almandines (five measurements each) was determined quantitatively using a CAMEBAX electron microprobe at Charles University of Prague.

TABLE 1. Properties of sapphire and garnet from Kalalani.

Property	Sapphire		Garnet	
	Reddish orange[a]	Yellow-brown	Brownish red (pyrope-almandine)	Green (tsavorite)
Refractive index	1.768–1.777	1.76–1.77 (spot)	1.763–1.770	1.737–1.740
Birefringence	0.009	Not determined	None	None
Specific gravity	3.98	4.00–4.05	3.86–3.90	3.63–3.65
Pleochroism	Distinct reddish orange to yellow	Weak yellow-brown to yellow	None	None
UV luminescence	None	None	None	None
Absorption spectrum	Lines at 700, 693, 557, and 490 nm; bands at 450, 388, and 376 nm	Lines at 550, 453, and 421 nm	Bands at 571, 523, 508, 460, 425, and 366 nm	Not determined
Inclusions	Isotropic irregular plates oriented parallel to the basal plane	Fractures, red-brown and yellow-brown flakes, rutile needles, zircon crystals, rare two-phase "fingerprints"	Apatite, rutile, "fingerprints"	Anisotropic white particles and negative crystallites in rows, two- and multi-phase inclusions, black plates, rounded colorless crystals

[a]*Electron microprobe analyses of two samples showed 0.9 wt.% Fe_2O_3 and 0.15 wt.% Cr_2O_3; other trace elements were below the detection limit.*

The mineralogical identification of some surface-reaching inclusions was made using an X-ray diffractometer (DRON II) at Charles University.

RESULTS

The properties of the sapphires and garnets are reported in table 1. None of the sapphires showed evidence of heat treatment.

Corundum. The reddish orange Cham-Shama sapphire that we studied formed tabular crystals with no pyramidal faces; only prism and basal pinacoid faces were present. The dichroism was reddish orange (parallel to the c-axis) and bright yellow. The greatest range in the R.I. values was 1.768 and 1.777, yielding a birefringence of 0.009. The average S.G. of the three samples was 3.98. Electron microprobe analyses showed the presence of 0.9 wt.% Fe_2O_3 and 0.15 wt.% Cr_2O_3; other trace elements were below the detection limit. The absorption spectrum showed lines at 700, 693, and 557 nm; bands at 450, 388, and 376 nm; and a fine line at 490 nm. The samples did not exhibit any fluorescence. Microscopic observation revealed inclusions of very small (up to 0.05 mm), pale, isotropic irregular plates, oriented parallel to the basal plane {0001}. Their R.I. was higher than that of corundum, as verified by the Becke line. Some of these plates had an incomplete hexagonal outline, and some had twin lines.

The yellow-brown sapphire crystals were opaque to translucent, and tabular to rhombohedral. They showed weak pleochroism, with a notable orange tint seen parallel to the c-axis and yellow perpendicular to the c-axis. The R.I. values were 1.76–1.77 (spot method), and the S.G. varied from 4.00 to 4.05. No fluorescence to UV radiation was observed. The absorption spectrum showed two major lines at 550 and 453 nm, and a minor line at 421 nm. The samples contained many cracks and dark inclusions. The most common inclusions were very thin red-brown and yellow-brown flakes (figure 14) oriented parallel to the basal plane, which produced a schiller effect in the samples. These flakes are probably hematite, as seen by Hänni (1987) in Umba sapphire. Similar-appearing inclusions in some samples were identified as vermiculite by X-ray diffraction analysis. Some stones showed a network of rutile needles oriented at 120° to one another. Also noted were tiny zircon crystals and very rare "fingerprints" consisting of two-phase inclusions (liquid and gas).

The samples of color-change sapphire were only slightly translucent. They consisted of a hexagonal prism $\{11\bar{2}0\}$ that was terminated by a basal plane {0001} or rhombohedron $\{10\bar{1}1\}$. The samples showed a distinct change of color from blue or grayish blue in daylight to purple in incandescent light. The sapphire fluoresced weak red to long-wave UV and was inert to short-wave UV.

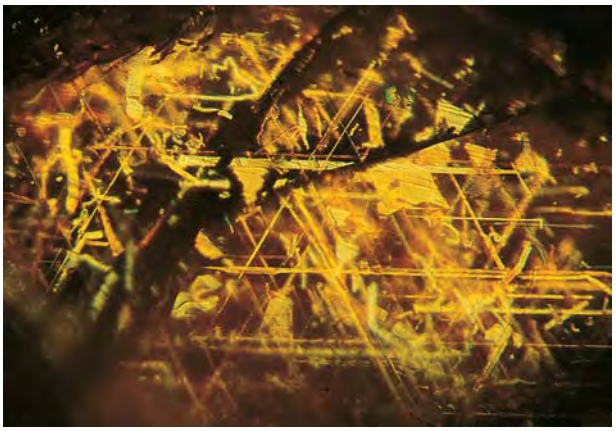

Figure 14. The thin flakes in this yellow-brown sapphire cabochon are probably hematite; vermiculite might also be present. Photomicrograph by J. Hyrsl; oblique illumination, magnified 6×.

Pyrope-Almandine. The pyrope-almandine samples were brownish red. R.I. ranged from 1.763 to 1.770, and S.G. from 3.86 to 3.90. They showed moderate anomalous double refraction in the polariscope. The absorption spectra had three characteristic bands centered at 571, 523, and 508 nm, and other bands at 460, 425, and 366 nm. The most common inclusions were anisotropic rounded crystals of apatite and needle-like rutile (figure 15). Also prominent were partially healed fractures (figure 16) that appeared similar to the "fingerprints" commonly

Figure 15. Rounded apatite crystals and needle-like rutile crystals were commonly seen in pyrope-almandine from the Peter A. claim. Photomicrograph by J. Hyrsl; brightfield illumination, magnified 15×.

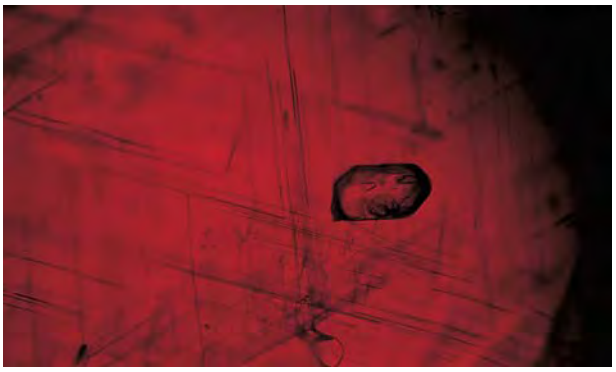

Figure 16. Some of the pyrope-almandine samples had "fingerprints"—actually, partially healed fractures—that formed attractive patterns. Photomicrograph by J. Hyrsl; brightfield illumination, magnified 15×.

seen in sapphire or spessartine, as illustrated by Gübelin and Koivula (1986, p. 293). The substance (gas or liquid) within the fingerprints is mostly isotropic, but some portions are anisotropic, with an R.I. lower than that of the host garnet (as seen with the Becke line). The electron microprobe data showed that each sample was chemically homogeneous (see standard deviations in table 2). As expected, those samples with greater iron content had higher R.I. and S.G. values (table 2). Mineralogically, the garnet is referred to as an iron-rich pyrope; gemologically, it is pyrope-almandine or, if there is a purple component, rhodolite (Stockton and Manson, 1985).

TABLE 2. Physical and chemical properties of pyrope-almandine from the Peter A. claim.

	Sample		
Property	1.64 ct	1.28 ct	0.76 ct
Refractive index	1.763	1.767	1.770
Specific gravity	3.86	3.87	3.90
Oxides (wt.%)[a]			
SiO_2	39.63 ± 0.72	39.23 ± 0.99	38.12 ± 1.36
TiO_2	na[b]	0.06 ± 0.01	na
Al_2O_3	23.53 ± 0.27	22.20 ± 0.55	22.73 ± 0.40
FeO	19.05 ± 0.24	21.66 ± 0.37	23.90 ± 0.18
MnO	0.81 ± 0.08	0.80 ± 0.02	0.64 ± 0.05
Total	101.03	100.12	99.74

[a]*For each sample, the average of five analyses (by electron microprobe) is provided together with the standard deviation.*

[b]*na = not analyzed.*

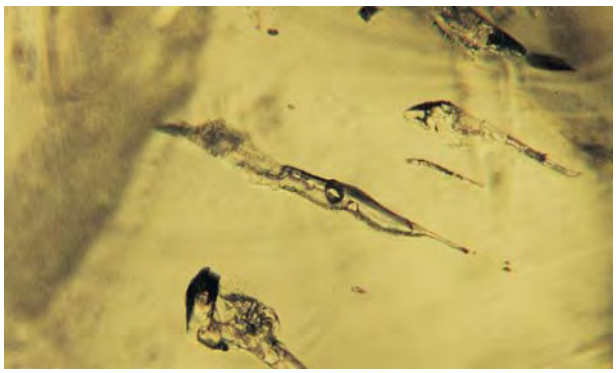

Figure 17. The central elongate inclusion (0.35 mm long) in this tsavorite is partially filled with a fluid that contains a single bubble and three isotropic daughter minerals. Such multiphase inclusions are rare in tsavorite. Photomicrograph by J. Hyrsl; brightfield illumination.

Tsavorite. The tsavorite samples revealed R.I. values of 1.737–1.740, and S.G.'s of 3.63–3.65. Moderate anomalous double refraction was seen with the polariscope. The samples were inert to UV radiation and appeared pink with the Chelsea filter. Microscopic observation revealed planes of irregular anisotropic white inclusions and negative crystallites, often in parallel rows. Several inclusions consisted of a flaky anisotropic substance together with a small bubble. One sample contained an unusual multiphase inclusion that was mostly filled by a fluid in which floated a small bubble and three isotropic crystals (cubes?); all of these were attached

Figure 18. Rarely, opaque black plates were observed as inclusions in the Kalalani tsavorite; they were probably graphite. This crystal measures 0.5 mm in diameter, and appears light colored due to reflections off its shiny surface. Photomicrograph by J. Hyrsl; oblique brightfield illumination.

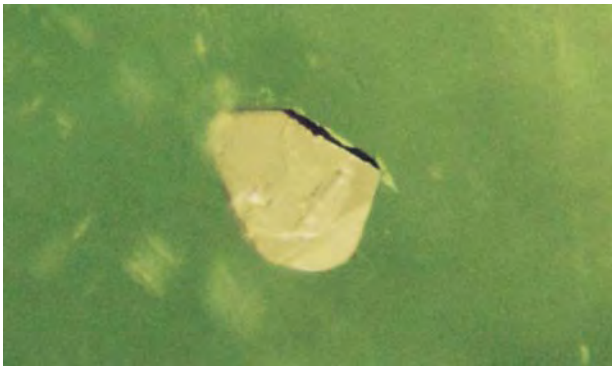

to an anisotropic material (figure 17). Rare, opaque black plates were probably graphite (figure 18). Small rounded colorless crystals with a high relief (probably apatite) were common in some samples. All of the anisotropic inclusions described above have a lower R.I. than tsavorite, as determined by Becke line observations.

Four multiphase inclusions in tsavorite from Kalalani were studied by Petra Neumanova of Charles University at Prague. They were interpreted as primary fluid inclusions because of their large size, relative isolation, and similar phase composition and phase ratios. The mineral phase within the fluid inclusions was anisotropic, and these crystals apparently were daughter minerals.

DISCUSSION

Gemstones from Kalalani are similar to those from Umba, which is well known for the production of sapphires in an unusually broad range of fancy colors—particularly the color-change and "Umba padparadscha" sapphires—as well as for light blue sapphire and ruby. The garnet group at Umba is represented by pink-purple rhodolite, "malaia" garnet (called also "Umbalite"), color-change garnet, and pale pink grossular. Cr-tourmaline, spinel, scapolite, apatite, zircon, Cr-diopside, kyanite, and turquoise have also been reported from the Umba area (Dirlam et al., 1992). The second author recently identified a mineral new to Umba, gemmy brown enstatite. While most Umba gems have been recovered from alluvium, gems at Kalalani are mined almost entirely from primary deposits.

The color range and characteristic inclusions of reddish orange sapphires from Kalalani (figure 19) are very similar to those from Umba, as well as to orange sapphires from the Tunduru region in southern Tanzania (Henn and Milisenda, 1997) and to orange sapphires from Malawi (Henn et al., 1990). Although the traditional padparadscha sapphire from Sri Lanka shows more pink and less orange, some reddish orange sapphires from Kalalani have a prominent pinkish tint. The visible absorption spectrum of the reddish orange sapphire from Kalalani is identical that of similar material from Umba (as recorded by Hänni, 1987), and confirms the presence of Fe^{3+} and Cr^{3+} as the main coloring agents. On the basis of the studies of similar sapphires from Umba (e.g., Schmetzer et al., 1982), the reddish orange sapphires from Kalalani probably do not respond favorably to heat treatment, because color centers apparently are not present.

Figure 19. The Kalalani area has yielded sapphires in colors similar to those seen in sapphires from Umba and Tunduru. These yellow to reddish orange sapphires from the Cham-Shama claim range from 1.53 to 2.29 ct. Courtesy of Varujan Arslanyan; photo © GIA and Tino Hammid.

The Kalalani garnets differ from their Umba counterparts. "Malaia" garnet, color-change garnet, and pale pink grossular are not known from Kalalani, and tsavorite has not been found at Umba. The Kalalani pyrope-almandine is typically dark red to brownish red, whereas that from Umba is pink-purple (i.e., rhodolite). Tsavorite from Kalalani has the same R.I. and S.G. as most tsavorite from Kenya or Tanzania (see, e.g., Keller, 1992). Tsavorite from the Merelani Hills in Tanzania (see Kane et al., 1990) can be distinguished easily from Kalalani tsavorite due to its negative reaction to the Chelsea filter. Green grossular from Mali, which has a similar pink to red response to the Chelsea filter, shows a higher R.I. than Kalalani tsavorite.

Curiously, the parcel of rough tsavorite from Kalalani that we obtained for study was also found to contain minor amounts of green to dark green Cr-tourmaline and light green kornerupine, as confirmed by X-ray diffraction analyses. These gem minerals can be easily distinguished from tsavorite by their anisotropy, pleochroism, and particularly their fluorescence to UV radiation. Chrome tourmaline fluoresces light yellow to short-wave, and is inert to long-wave, UV radiation; whereas kornerupine shows strong yellow fluorescence to both short- and long-wave UV. When viewed with a Chelsea filter, Cr-tourmaline appears pink to red and kornerupine remains green.

FUTURE POTENTIAL

The Kalalani area has never been systematically prospected, but there is some evidence that additional sapphire-rich pegmatites exist. Except for the old "Papas" pits, mining generally has extended to an average depth of only 5–7 m. Below this depth, there is a high potential for the discovery of additional sapphires, and efforts should be made to reach the deeper zones of abandoned deposits that were formerly productive.

The remaining reserves of pyrope-almandine ore at the Peter A. deposit may be roughly estimated at up to 100 tons, to a depth of 25 m. Also, the abundant surface signs of primary tsavorite mineralization southwest of the Kalalani serpentinite should be explored more thoroughly. In both cases, a large initial investment in prospecting and mining would be necessary. Although a source of tanzanite has not been found in the Kalalani area, favorable geologic potential is indicated by the presence of crystalline dolomitic limestones and graphitic gneisses with quartz veins and pure graphite, together with widespread hydrothermal alteration.

The Kalalani area also has potential for other gem materials. The senior author has found green tourmaline in small pegmatite lenses hosted by quartz-feldspar gneisses southwest of the Kalalani massif. Also, small crystals of transparent green diopside have been recovered from fissures inside the Kalalani massif.

Acknowledgments: The principal author appreciates the friendship and assistance of J. P. Giordano of New York, who was part of the Kalalani team in 1989–1990. H. D. Patel of Dar es Salaam and V. Arslanyan of New York are thanked for their friendship and generous support during the fieldwork. Mr. Arslanyan also kindly provided additional information, mining photos, and gem material for photography. We thank Dr. C. Milisenda of the Gemmological Institute of Idar-Oberstein for providing spectrophotometric analyses, Dr. J. Hovorka of Charles University for the electron microprobe analyses of pyrope-almandine, and E. Zitova of the Geological Survey in Prague for drafting the maps. Rough samples of tsavorite, as well as recent locality and production information, were kindly provided by P. Pongtrakul of Dar es Salaam.

REFERENCES

Dirlam D.M., Misiorowski E.B., Tozer R., Stark K.B., Basset A.M. (1992) Gem wealth of Tanzania. *Gems & Gemology*, Vol. 28, No. 2, pp. 80–102.

Gübelin E.J., Koivula J. (1986) *Photoatlas of Inclusions in Gemstones*. ABC Edition, Zurich, Switzerland.

Hänni H.A. (1987) On corundum from Umba Valley, Tanzania. *Journal of Gemmology*, Vol. 20, No. 5, pp. 278–284.

Hartley E.W., Moore W.R. (1965) *Quarter Degree Sheet 91 and 110, Daluni* (scale 1:125,000), Geological Survey of Tanzania, Dodoma.

Henn U., Bank H., Bank F.H. (1990) Red and orange corundum (ruby and padparadscha) from Malawi. *Journal of Gemmology*, Vol. 22, No. 2, pp. 83–89.

Henn U., Milisenda C.C. (1997) Neue Edelsteinvorkommen in Tansania: Die Region Tunduru–Songea. *Zeitschrift der Deutschen Gemmologischen Gesellschaft*, Vol. 46, No. 1, pp. 29–43.

Kane R.E., Kampf A.R., Krupp H. (1990) Well-formed tsavorite gem crystals from Tanzania. *Gems & Gemology*, Vol. 26, No. 2, pp. 142–148.

Keller P.C. (1992) *Gemstones of East Africa*, Geoscience Press, Tucson, AZ, pp. 32–41.

Malisa E., Muhongo S. (1990) Tectonic setting of gemstone mineralization in the Proterozoic metamorphic terrane of the Mozambique Belt in Tanzania. *Precambrian Research*, Vol. 46, Nos. 1–2, pp. 167–176.

Schmetzer K., Bosshart G., Hänni H. (1982) Naturfarbene und behandelte gelbe und orange-braune Sapphire. *Zeitschrift der Deutschen Gemmologischen Gesellschaft*, Vol. 31, No. 4, pp. 265–279.

Solesbury F.W. (1967) Gem corundum pegmatites in NE Tanganyika. *Economic Geology*, Vol. 62, No. 7, pp. 983–991.

Stockton C.M., Manson D.V. (1985) A proposed new classification for gem-quality garnets. *Gems & Gemology*, Vol. 21, No. 4, pp. 205–218.

RUSSIAN SYNTHETIC AMETRINE

By Vladimir S. Balitsky, Taijin Lu, George R. Rossman, Irina B. Makhina, Anatolii A. Mar'in, James E. Shigley, Shane Elen, and Boris A. Dorogovin

Gem-quality synthetic ametrine has been produced commercially in Russia since 1994, by hydrothermal growth from alkaline solutions. Faceted synthetic ametrine has many similarities to its natural counterpart from Bolivia. For the most part, however, the synthetic ametrine obtained for this study could be identified by a combination of characteristics, including growth features such as twinning and color zoning. EDXRF chemical analyses revealed higher concentrations of K, Mn, Fe, and Zn than in natural ametrine. IR spectra of the synthetic citrine portions showed more intense absorption in the 3700–2500 cm^{-1} range compared to natural ametrine; the synthetic amethyst zones showed a weak diagnostic peak at 3543 cm^{-1}.

ABOUT THE AUTHORS

Dr. Balitsky (balvlad@iem.ac.ru) is head of the Laboratory of Synthesis and Modification of Minerals at the Institute of Experimental Mineralogy, Russian Academy of Science (IEM RAS), in Chernogolovka, Moscow District, Russia. Dr. Lu is a research scientist, Dr. Shigley is director, and Mr. Elen is a research gemologist at GIA Research, Carlsbad, California. Dr. Rossman is professor of mineralogy at the California Institute of Technology (Caltech) in Pasadena, California. Dr. Makhina is project leader, Dr. Mar'in is head of the Department for Experimental Mineralogy, and Dr. Dorogovin is a director at the Russian Research Institute for Material Synthesis (VNIISIMS) in Alexandrov, Vladimir District, Russia.

Please see acknowledgments at the end of the article.

Gems & Gemology, *Vol. 35, No. 2, pp. 122–134*

Amethyst is one of the most popular colored gemstones because of its color, availability, and affordability. Citrine is less often encountered in nature, although large quantities are produced by the heat treatment of amethyst. In the 1970s a spectacular combination of amethyst and citrine, commonly referred to as ametrine, became available (Hehar, 1980; Koivula, 1980; Vargas and Vargas, 1980). Although there was early speculation (stimulated in part by observations of Nassau, 1981) that such ametrine was synthetic or the effect was produced by treatment, the source of natural, untreated ametrine was eventually revealed to be the Anahí mine in Bolivia (Jones, 1993; Vasconcelos et al., 1994). In fact, efforts were underway in Russia in 1977 to understand the fundamental mechanisms of synthesizing ametrine (Balitsky and Balitskaya, 1986). By 1994, the growth technology was successfully established, and the first commercial batch (on the order of 100 kg) of synthetic ametrine crystals was produced.

Currently, a few kilograms per month of synthetic ametrine crystals and polished slabs are being sold. Faceted synthetic ametrine is also available (see, e.g., figure 1). Batch capacity has now grown to more than 300 kg. If necessary to meet demand, several tons of synthetic ametrine a year could be produced by a single laboratory (the Russian Research Institute for Material Synthesis [VNIISIMS] of the Ministry of Geology of the Russian Federation, in Alexandrov, Vladimir District). Most of the synthetic ametrine is sold in Russia. Recently, however, synthetic ametrine (of unknown origin) has appeared in the Bolivian market (Rivero, 1999).

Although at least three morphological types of synthetic ametrine crystals can be grown, this article reports on the most abundant commercial type. The cause of color, growth conditions, crystal morphology, gemological properties, internal features, spectra, and chemical composition are described, and key tests to separate this synthetic ametrine from its natural counterpart are summarized.

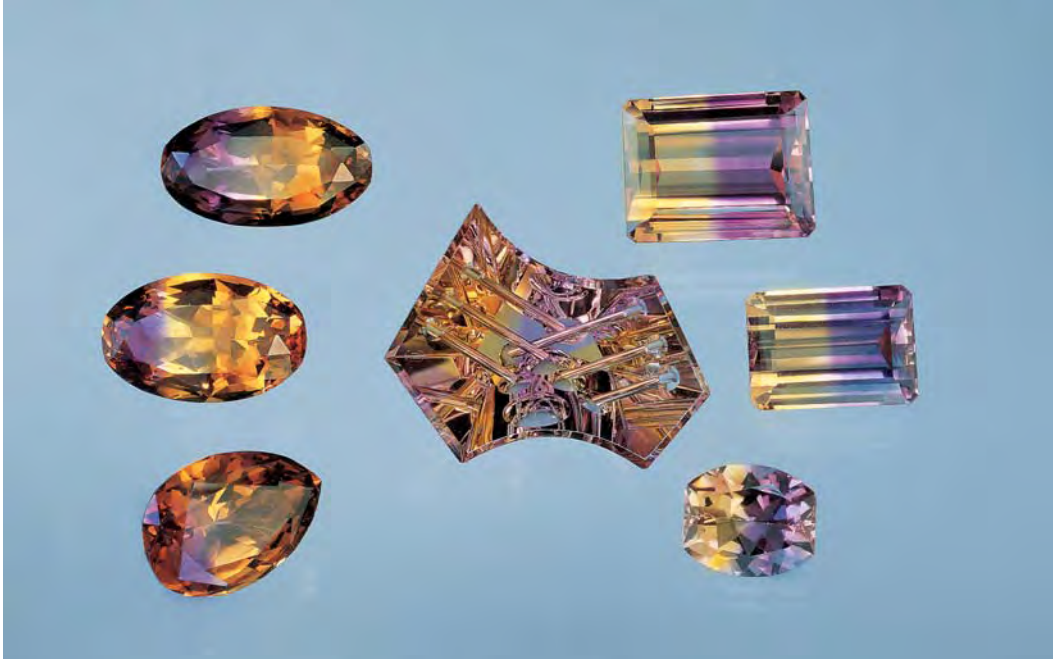

Figure 1. Synthetic ametrine hydrothermally grown in Russia became commercially available in the mid-1990s. Here, faceted synthetic ametrine (the three samples on the left, 11.30–13.38 ct) is shown together with natural ametrine from the Anahí mine in Bolivia. The carving of natural ametrine in the center weighs 35.15 ct and was executed by Michael Dyber; the faceted stones on the right weigh 4.71–22.31 ct. Photo © Harold & Erica Van Pelt.

HISTORICAL BACKGROUND

Synthetic quartz with the distinctive amethyst-citrine bi-coloration was first mentioned in the Russian scientific literature in the late 1950s and early 1960s. In particular, Tsinober and Chentsova (1959) reported that, after X-ray irradiation, certain crystals of brown synthetic quartz developed purple (amethyst) coloring in the rhombohedral growth sectors. This treatment phenomenon was revisited in the course of research into synthetic brown quartz and synthetic amethyst (e.g., Balakirev et al., 1979; Balitsky, 1980; Balitsky and Lisitsina, 1981; Nassau, 1981).

The first investigations aimed at producing synthetic ametrine on a commercial scale began in 1982 at the Institute of Experimental Mineralogy of the Russian Academy of Science (IEM RAS) in Chernogolovka, Moscow District. These experiments investigated how physical, chemical, and growth factors affected the capture and distribution of color-causing iron impurities during the growth of synthetic ametrine (as well as other iron-bearing varieties of quartz; see Balitsky and Balitskaya, 1986). In 1993–1994, the research was transferred to VNIISIMS, also near Moscow, although colleagues at both institutions continued to collaborate. Later, VNIISIMS organized a special company named "Аметрин" (Ametrine) to market synthetic ametrine. Today, almost all synthetic ametrine is produced at VNIISIMS.

SCIENTIFIC FOUNDATIONS FOR THE GROWTH OF SYNTHETIC AMETRINE

Iron Impurities in Colored Quartz. As previously established by several researchers (e.g., Hutton, 1964; Zaitov et al., 1974; Lehmann, 1975; Balakirev et al., 1979; Balitsky, 1980; and Rossman, 1994), the various colors of iron-bearing quartz (e.g., amethyst, citrine, green, and brown quartz) are related to different forms of iron (Fe) in the crystal structure. Only a small quantity of iron (e.g., about 0.01–0.05 wt.% Fe for amethyst) is needed to produce coloration in quartz. Even though the element iron and the mineral quartz are both common in nature, the occurrence of ametrine is quite rare. This is due to the specific physical, chemical, and geological conditions necessary for ametrine formation (Balitsky and Balitskaya, 1986; Vasconcelos et al., 1994).

The basic unit of the quartz structure is a tetrahedron consisting of a silicon (Si) atom and four oxygen (O) atoms. Trivalent iron (Fe^{3+}) can substitute for Si^{4+} in a tetrahedral site, or it can fill interstitial sites (as extra atoms in voids) between neighboring tetrahedra. At least two different interstitial positions exist in the quartz structure (Rossman, 1994, p. 434).

The amethyst coloration develops in a two-step process. First, the substitution of Si^{4+} by Fe^{3+} during growth produces a precursor center (Fe^{3+} substitutional center, $[FeO_4]^-$). The resulting deficiency of positive charge is compensated by the introduction of alkali metal ions (such as Li^+ or Na^+) or protons (H^+) into the quartz. This precursor center absorbs so little light that the material is almost colorless. The purple color develops only when the precursor center is converted to the amethyst color center ($[FeO_4]^0$) by exposure to ionizing radiation. For synthetic amethyst, a dose of 5–6 Mrads of cobalt-60 gamma-ray radiation is commonly used, although electron irradiation is employed occasionally.

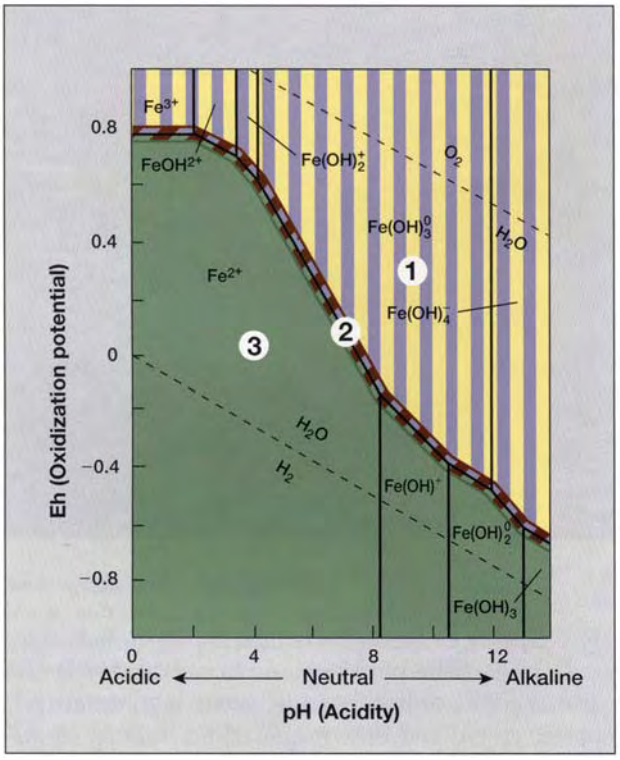

Figure 2. This diagram relates the Eh (oxidation potential) and pH (acidity) of iron (Fe)-containing aqueous solutions to the chemical form in which the iron exists in the solution. The regions corresponding to the various color varieties of iron-containing quartz are indicated by purple (amethyst), yellow (citrine), brown (brown quartz), and green (green quartz). 1 = region of amethyst, citrine, and ametrine (purple-and-yellow striped) formation; 2 = narrow region of brown quartz formation (along line), with adjacent green-and-brown quartz and amethyst-and-brown quartz regions; and 3 = region of green quartz formation. After Melnik et al. (1974).

Citrine coloration in synthetic quartz is also related to Fe^{3+}. However, in contrast to the color mechanism for amethyst, the iron does not enter the crystal structure. Rather, it is captured on growth faces of the quartz crystal—possibly as a small aggregate of a hydrated iron hydroxide—in the form of a so-called "nonstructural" impurity. Various colors can result, depending on the oxidation state (valence) of the nonstructural iron: Green coloration is caused by the presence of Fe^{2+} impurities, and the simultaneous capture of both Fe^{2+} and Fe^{3+} gives rise to brown quartz.

Because the color of iron-bearing quartz depends on the valence state of the iron, the Russian researchers first had to determine the conditions under which the desired form of iron ions would exist in the quartz-forming hydrothermal solutions. They did this with the help of a calculated diagram (known as an Eh-pH diagram—see e.g., Garrels and Christ, 1965; figure 2), which shows the stability of ionic and molecular forms of iron in aqueous solution as a function of the oxidation potential (Eh) and the acidity (pH). From this diagram, it can be seen that there is a limited regime under which all the iron will be in the trivalent state (i.e., region 1 in figure 2). This observation was fundamental to the development of technologies for growing both synthetic amethyst and ametrine (Balitsky et al., 1970; Balitsky, 1980). The diagram further shows that there are conditions under which synthetic amethyst, citrine, or ametrine—as well as bi-colored amethyst-brown quartz and amethyst-green quartz—can be grown in acidic, neutral, or alkaline solutions.

Growth Rate and Coloration. The incorporation of iron impurities—and thus the development of the specific ametrine coloration—is dependent on the growth rate and surface structure of the different growth sectors (as explained by Balitsky and Balitskaya, 1986; see figure 3). The growth conditions must be closely regulated so that the amethyst- and citrine-forming iron impurities are captured simultaneously by different growth sectors in a crystal.

Commercial Growth and Irradiation Processes. The technology for synthesizing ametrine is similar to that for synthetic amethyst and synthetic citrine. The crystals are grown hydrothermally in concentrated alkaline (K_2CO_3) solutions at temperatures of 330°–370°C and pressures in the range of 1,200 to 1,500 atmospheres, in autoclaves ranging from 1,000 to 1,500 liters in volume (for photos of the factory, visit the Web site http://minerals.gps.caltech.edu/ametrine). The crushed silica used to grow the synthetic quartz is derived from natural or synthetic quartz with a very low aluminum content (10–100 ppm). To facilitate the incorporation of Fe^{3+} into the growing crystal structure, manganese nitrate, $Mn(NO_3)_2$, is used as an oxidizer.

The synthetic ametrine crystals are grown on seeds, prepared from colorless synthetic quartz crystals, that have a specified crystallographic orientation, shape, and size. Two types of seeds are used to produce the tabular synthetic ametrine crystals: (1) seeds cut parallel to the positive and negative rhombohedra; and, more commonly, (2) seeds cut parallel to the basal pinacoid. In both cases, the crystals are

grown at rates slightly below the critical rates (see figure 3) to produce the optimum distribution and intensity of color. The basal surfaces of crystals grown on seeds cut parallel to the basal pinacoid grow at about 0.8–1.0 mm/day. Rhombohedral faces, however, grow much slower (0.3–0.4 mm/day for the negative rhombohedral face, and 0.08–0.1 mm/day for the positive rhombohedral face). The rhombohedral *r* and *z* sectors are colorless or pale yellow as grown; subsequent gamma-ray irradiation, as described below, produces the purple color in these sectors (figure 4). The pinacoidal *c* sectors are yellow to orange as grown. Their primary citrine color is unaffected by the irradiation, although in a small proportion of crystals these sectors turn brownish orange due to the presence of a minor amethyst component.

Figure 3. The growth rate of synthetic ametrine strongly influences the coloration of the r *and* z *sectors (see figure 4 for an example of the coloration of the* r, z, *and* c *growth sectors). This schematic diagram shows the effect of growth rate on the capture and distribution of amethyst- and citrine-forming impurities in these two sectors. The color intensity is directly related to the quantity of captured iron impurities.* V^r_{cr} *and* V^z_{cr} *are the critical growth rates for the* r *and* z *faces, respectively (i.e., the growth rate at which the maximum color intensity will be produced). Above these critical values, the color intensity decreases, and the* r *and* z *sectors begin to capture citrine-forming impurities. In the diagram, the color of each line indicates the particular color-forming impurities that are incorporated into the* r *and* z *sectors at various growth rates. At higher growth rates, the* r *and* z *faces incorporate only citrine-forming impurities (i.e., in regions III, IV, and V for* r *and region V for* z*). To grow synthetic ametrine crystals with* r *and* z *sectors that will show an intense purple with irradiation, the growth is carefully maintained at just below the critical rate. The* c *faces capture only the citrine-forming impurities, regardless of the growth rate.*

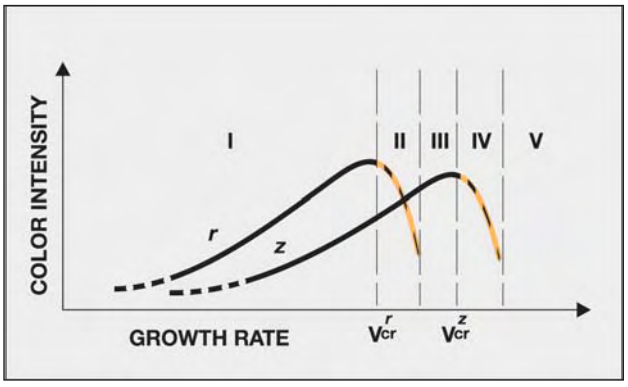

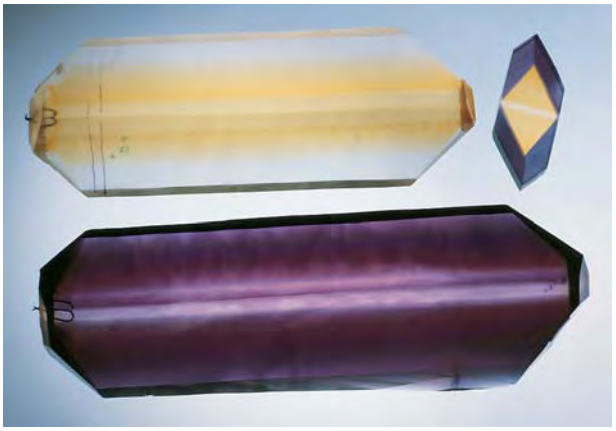

Figure 4. Commercially important synthetic ametrine is produced using rectangular seeds cut parallel to the basal pinacoid. The crystal on the upper left is shown before—and the crystal on the bottom (1.1 kg) after—gamma-ray irradiation. The slice on the upper right is a cross-section of an irradiated crystal; about 20 such slabs can be cut from a typical crystal. Within the slice, the colorless band is the seed plate, the yellow regions on either side of the seed are the c *sectors, and the dark purple zones are the* r *and* z *sectors (the* r *sectors are darker purple). Photo by Maha DeMaggio.*

By changing the shape, size, and orientation of the seed, and using other proprietary techniques, it is possible to grow synthetic ametrine crystals showing various habits, from tabular to prismatic (both symmetric and asymmetric), with a complex distribution of amethyst- and citrine-colored internal growth sectors. Most commercial production employs rectangular seed plates that are cut parallel to the basal pinacoid and elongated in the trigonal prism *x* [$11\bar{2}0$] direction (known as the ZX-cut). All of the synthetic ametrine samples examined for this study were grown using these seeds, which are typically 200–300 mm long, 20–50 mm wide, and 1.5–2.0 mm thick. Their use results in tabular crystals with the best color contrast between the different growth sectors. Very small quantities of crystals have been grown with the rectangular basal pinacoid seeds elongated in the hexagonal prism *m* [$10\bar{1}0$] direction (the ZY-cut), to get a more varied distribution of color.

To study the influence of seed orientation on the development of the synthetic amethyst and citrine portions, the Russian researchers are growing some crystals on seeds oriented at 15°–30° to the basal pinacoid face. Synthetic ametrine crystals with a

Figure 5. Each slab of synthetic ametrine typically yields 8–10 faceted samples. The largest faceted synthetic ametrine shown here weighs 20 ct. Photo by Maha DeMaggio.

prismatic morphology are also grown; they require special seeds and a proprietary morphology-controlling technique. Currently, these crystals are being produced for commercial use at a rate of only 2–3 kg per month. A detailed gemological study of this material is underway by the current authors.

The largest synthetic ametrine crystal grown thus far by the Russian authors weighed 4.5 kg. Crystals typically range from 0.45 to 1.2 kg, and measure 20 × 6 × 2 cm to 21 × 8 × 4 cm. For maximum amethyst color saturation, the crystals are irradiated with a cobalt-60 gamma-ray source for about three hours, resulting in a dose of about 5 Mrads. To fulfill customer requests, occasionally the crystals are heat treated (at 330°–350°C for one hour) to reduce the color intensity of the synthetic citrine portions.

Figure 6. These faceted synthetic ametrines (7.53–46.44 ct) represent some of the samples examined for this study. Photo by Maha DeMaggio.

CUTTING

The elongate, tabular crystals of synthetic ametrine are first cut perpendicular to their length into several slabs (see, e.g., figures 4 and 5). A 200-mm-long tabular crystal typically yields 20 slabs. The slabs contain both amethyst- and citrine-colored portions, except for those cut from near the ends of the crystals. Each slab yields about 8–10 faceted gems with an average weight of 10–15 ct (see, e.g., figure 5), although gems exceeding 50 ct can be cut. Some of the faceted gems will be almost entirely purple or yellow, depending on the portion of the slab from which they were cut. Rectangular, cushion, and oval shapes are most common.

Approximately 180 faceted stones are obtained from a typical rough crystal, for an overall yield of about 50%. No noticeable differences in physical properties, such as brittleness and hardness, have been reported for synthetic and natural ametrine during cutting and polishing.

MATERIALS AND METHODS

All of the synthetic ametrine samples included in this study were grown on tabular ZX-cut seeds. About 300 synthetic ametrine crystals (80 × 20 × 10 mm to 250 × 80 × 50 mm) and 150 faceted gems (1–40 ct) were examined by the Russian authors and their staff. The GIA and Caltech authors studied seven crystals, six polished crystal fragments, and 10 faceted samples of synthetic ametrine. The largest crystal studied at GIA measured 207.1 × 64.5 × 30.2 mm and weighed 1.1 kg. The faceted samples examined at GIA were cut in oval and various fancy shapes, and ranged from 7.53 ct to 46.44 ct (figure 6). To explore the dependence of physical and gemological properties on crystallographic orientation, we had 12 rough samples cut and polished in specific orientations (e.g., parallel and perpendicular to the optic axis). The resulting slabs weighed 10.30–65.80 ct and were studied by authors from all three institutions.

In addition, the GIA and Caltech researchers documented the gemological properties of the following samples of natural ametrine from the Anahí mine: seven crystals (50–56 grams), three slabs cut parallel to the optic axis (25.88–48.55 ct), three slabs

cut perpendicular to the optic axis (26.00–168.90 ct), and 30 faceted samples (3.90 ct–140.39 ct; see, e.g., figure 7) in various shapes.

Standard gem-testing equipment and methods were used to characterize all 40 of the faceted samples examined at GIA. The equipment included: a GIA GEM Duplex II refractometer with a near-monochromatic, sodium-equivalent light source; a polariscope, a calcite dichroscope, a Chelsea color filter, a GIA GEM combination long- and short-wave ultraviolet lamp unit (4 watts), a Beck desk-model prism spectroscope mounted on an illumination base, and a binocular gemological microscope. Twinning was observed with an immersion cell and cross-polarized light, at 7×–45× magnification. Specific gravity values were hydrostatically determined for three synthetic and five natural samples using a Mettler AM100 electronic balance.

Absorption spectra in the ultraviolet-visible-near infrared (UV-Vis-NIR) were obtained at GIA with two instruments (a Hitachi U-4001 and a Pye-Unicam 8800) for some of the natural ametrine (two crystals, three slabs, and 15 faceted stones) and synthetic ametrine (five crystals, three slabs, and 10 faceted samples). UV-Vis-NIR absorption spectra were also collected at Caltech, with a diode array microspectrometer. Four slabs and one cube of natural ametrine, and four slabs of synthetic ametrine, were chosen for detailed study on this system. Infrared spectra were recorded at GIA (on the same samples as for UV-Vis-NIR spectroscopy) with a Nicolet Magna-550 spectrophotometer, and at Caltech (four slabs each of natural and synthetic ametrine) with a Nicolet 860 instrument. Additional data for 20 crystals, 30 slabs, and 20 faceted synthetic ametrine samples were collected by the Russian authors using a SPECORD M40 spectrometer (visible range) and a Perkin-Elmer 983 spectrophotometer (infrared range). Equivalent instruments at the three locations gave comparable results.

Qualitative chemical analyses of 15 natural and 15 synthetic ametrine samples were obtained at GIA by energy-dispersive X-ray fluorescence (EDXRF) spectrometry, using a Tracor-Northern Spectrace TN 5000 instrument. Semi-quantitative chemical analyses of five natural (two slabs, three faceted) and four synthetic (two slabs, two faceted) ametrine samples were also performed at Caltech, using a Kevex-IXRF 7000 system in conjunction with the Fundamental Parameters program (supplied with the instrument's software) and silica-metal oxide mixtures as confirmatory standards.

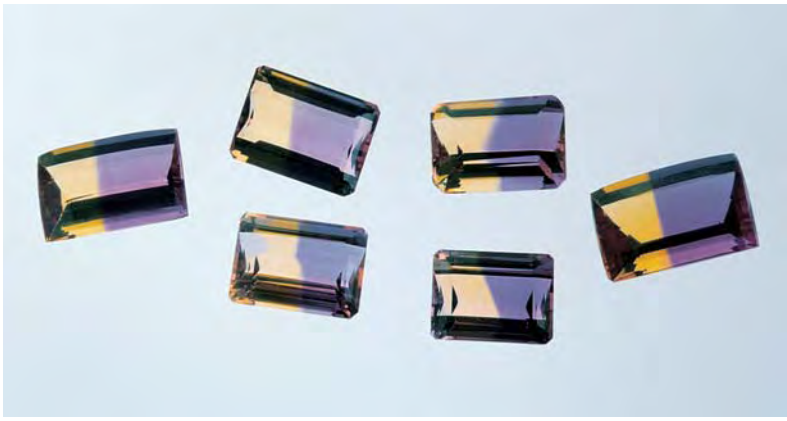

Figure 7. Natural ametrine was obtained for comparison with the synthetic material. The largest faceted ametrine shown here weighs 21.93 ct. Photo by Maha DeMaggio.

Raman spectra were collected using a Renishaw 2000 laser Raman microspectrometer at GIA on 10 natural and 10 synthetic faceted samples. Each was analyzed in both the citrine and amethyst regions without any change in the orientation of the sample. In addition, Raman spectra of doubly polished slabs of both natural and synthetic ametrine were obtained at Caltech using a Kaiser Optics Holoprobe instrument with an EIC probe head. Because the initial results obtained by both instruments suggested that Raman spectra were not particularly useful for identification purposes, a comprehensive Raman study was not undertaken.

To evaluate the color stability of the synthetic ametrine, the Russian authors heated 30 rough crystals, 20 slabs, and 50 crystal fragments in air, at temperatures up to 700°C. After the amethyst color faded in a particular temperature range, the faded samples were re-irradiated with gamma rays to investigate color restoration.

RESULTS AND DISCUSSION

Morphology of Natural and Synthetic Ametrine. As seen in most natural amethyst, natural ametrine crystals typically have a prismatic habit, elongated parallel to the optic axis (c-axis), and are terminated by the rhombohedral faces *r* $\{10\bar{1}1\}$ and *z* $\{01\bar{1}1\}$ (figure 8). In some crystals, both of these rhombohedra are equally developed, so that the terminations resemble hexagonal pyramids; a small, rough *c* (0001) face is occasionally present (Vasconcelos et al., 1994). Prism faces *m* $\{10\bar{1}0\}$ are commonly developed, and are striated at right angles to the c-axis. Rarely, other faces are developed, such as the trigonal prism *x* $\{11\bar{2}0\}$ and trigonal dipyramid *s* $\{11\bar{2}1\}$; if present, they are very small.

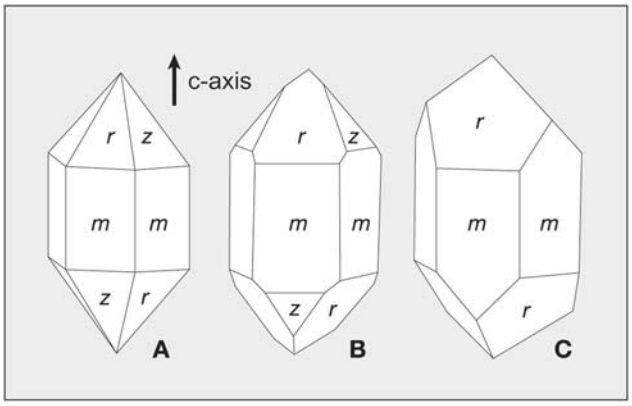

*Figure 8. Natural quartz crystals commonly show a simple arrangement of prism (*m*) and rhombohedral (*r *and* z*) faces. Ametrine crystals are typically prismatic, and are terminated by* r *and* z *faces of variable size. In natural ametrine crystal A, the rhombohedral faces are equally developed, so that the terminations resemble hexagonal pyramids. In most ametrine crystals, however, the terminations resemble those shown by B and C.*

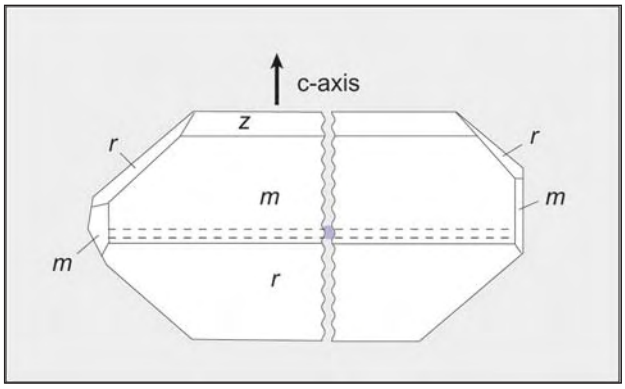

Figure 9. This schematic diagram illustrates a synthetic ametrine crystal that has been grown on a ZX-cut seed. The crystal is elongated along the seed (indicated here by dashed lines), and is bounded by r, z, m, *and* +x *faces. The* +x *faces are not visible in this diagram, because they are located on the back of the crystal, behind the* m *faces.*

Unlike natural ametrine, synthetic ametrine crystals are usually tabular, because a seed plate is used to start the growth. As noted earlier, the crystal morphology varies depending on the characteristics of the seed plate and the growth conditions. The crystals we examined for this study, all grown on ZX-cut seeds, were bounded mainly by *m* and *r* faces (figure 9); *z* faces were smaller, and the *+x* and *–x* faces were seldom present. A short steel wire—used to suspend the seed plate in the autoclave—was usually present at one end of the crystals.

Color and Color Distribution. The color distribution and internal features of the synthetic ametrine crystals are best seen when the they are sliced parallel to the *x* and *m* faces (figure 10). As noted earlier, the *c* sectors are synthetic citrine (orangy yellow to moderate orange), and the *r* and *z* sectors are synthetic amethyst (moderate to strong purple). The purple coloration is somewhat more intense in the *r* sectors than the *z* sectors. The samples exhibited moderate dichroism (violet purple to violet) in the amethyst-colored portion, and very weak to weak dichroism (orangy yellow to orange) in the citrine-colored portion.

In the synthetic ametrine samples we examined, the synthetic citrine portions were often more intensely colored than those in natural ametrine of similar thickness (see, e.g., figure 1). In general, we observed that the synthetic amethyst portions in

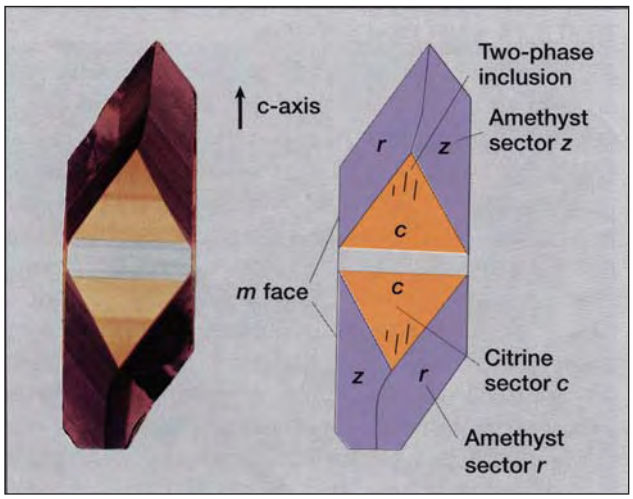

Figure 10. Several internal features in synthetic ametrine grown on tabular ZX-cut seeds are visible in this slab (6.0 cm long) and the corresponding schematic diagram. The slab was sliced parallel to the x *faces; it shows amethyst coloration in the* r *and* z *sectors, and citrine coloration in the c sectors. Color zoning is present in both the synthetic citrine and amethyst regions, and faint streaks consisting of liquid-gas inclusions are elongated parallel to the optic axis in the citrine region. The citrine color zoning is oriented parallel to the colorless seed (and perpendicular to the optic axis), and the amethyst color zoning is oriented parallel to the rhombohedral crystal faces. Photo by Maha DeMaggio.*

our samples were also more intensely colored than their natural amethyst counterparts.

The amethyst-citrine color boundary in synthetic ametrine (i.e., the boundary between the *c* sectors and the adjacent *r* and/or *z* sectors) is oriented roughly parallel to the rhombohedral faces, or at about 51° to the optic axis for *r* sector amethyst and 23° to the optic axis for *z* sector amethyst. In contrast, the color boundary in natural ametrine (i.e., the boundary between the amethyst *r* sectors and the citrine *z* sectors) is oriented roughly parallel to the optic axis.

In addition, to obtain maximum cutting yield from the slabs, some synthetic stones may show a sharp bend or angle in the amethyst-citrine color boundary (see, e.g., figure 5). This angle varied from 22°–48° in the synthetic slabs and faceted samples examined at GIA. When natural ametrine is faceted to show the maximum color contrast between amethyst and citrine, the color boundary is usually straight (see, e.g., figure 7).

Color Stability. The citrine color in the synthetic ametrine remained stable during heating (at temperatures up to 700°C). The amethyst color was stable below 400°C. In the temperature range of 400°–450°C, the purple faded completely within two hours of exposure, but it was fully restored by subsequent gamma-ray irradiation. However, when the synthetic ametrine samples were heated to higher temperatures, especially above the α–β phase transformation of quartz at 573°C, the amethyst color centers in nearly all samples were destroyed irreversibly (i.e., the purple could not be restored with gamma-ray irradiation), and a milky turbidity obscured the color and transparency of both the amethyst and citrine zones. As the temperature was increased from 550° to 700°C, in particular, the intensity of milkiness increased, cracks appeared, and the orange component of the citrine color decreased.

Microscopic Characteristics. Amethyst and citrine color zoning, stream-like structures, polysynthetic Brazil-law twinning, and two-phase (liquid-gas) inclusions were the principal microscopic features seen in the synthetic ametrine. The slab in figure 10 shows most of these features, and the corresponding schematic diagram illustrates their interrelationships and their orientation relative to the optic axis.

The citrine portions (*c* sectors) of the faceted synthetic ametrine commonly showed color zoning, oriented perpendicular to the optic axis. In the amethyst portion (*r* and *z* sectors), color zoning was generally observed, and was always oriented parallel to either the *r* or the *z* crystal faces, or at about 50° to the optic axis. Rarely, stream-like structures were observed in the synthetic citrine portions. With oblique lighting, these appeared as wavy stripes of color (figure 11) that were subparallel to the optic axis. They result from surface irregularities caused by growth hillocks on the basal pinacoid as the crystal grew.

Figure 11. Stream-like structures are visible in the citrine portion of this 4.25 ct faceted synthetic ametrine. Photo by Taijin Lu.

No twinning was observed in the citrine portion of the faceted synthetic ametrine. Brazil twins (see, e.g., figure 12, left) were observed by the Russian authors in the synthetic amethyst *r* sectors of only a few of the 150 faceted samples. As observed with crossed polarizers, Brazil twins in the synthetic amethyst portions formed a distinctive polysynthetic twinning pattern: a group of straight, thin, parallel lamellae showing various interference colors. In contrast, the amethyst sectors in all of the natural ametrine studied showed Brazil twinning. Brazil twin boundaries in natural amethyst show distinctive curved or mottled patterns that are sometimes accompanied by linear areas of extinction called Brewster fringes (Brewster, 1823; Crowningshield et al., 1986; Lu and Sunagawa, 1990; Vasconcelos et al., 1994; see figure 12, center and right). Brewster fringes were not observed in the synthetic ametrine.

Two-phase (liquid-gas) inclusions were observed only rarely in the synthetic citrine portions (figure 13), and very rarely in the synthetic amethyst portions. These inclusions were oval or needle shaped, and were elongated parallel to the optic axis and the stream-like structures; in a few instances, they were visible to the unaided eye with strong light.

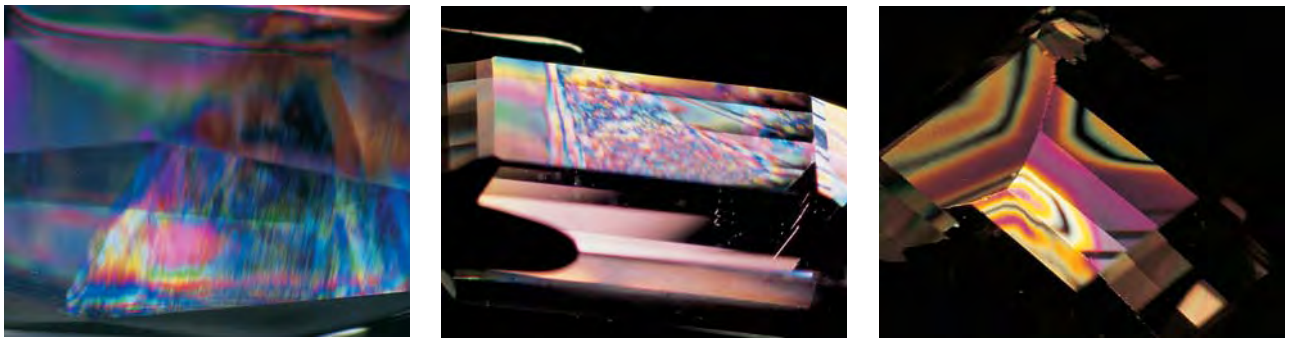

Figure 12. Brazil twins were observed only rarely in the amethyst portion of the faceted synthetic ametrines. They were composed of polysynthetic twin lamellae (thin, straight parallel lamellae showing various interference colors), as shown in the 12.42 ct faceted synthetic amethyst on the left (photomicrograph by John I. Koivula, magnified 15×). In contrast, the Brazil twins in the amethyst portion of the 11.47 ct natural ametrine in the center (photomicrograph by Taijin Lu) form complex curved patterns; the citrine portion is demarcated by the untwinned area on the far left side of the stone. Although the twinning in these two examples appears somewhat similar, the striated appearance of the twinning in the synthetic sample is diagnostic. Some natural samples show distinctive curved "classic" Brazil twins that may be accompanied by the darker Brewster fringes, as shown by the amethyst on the far right (photomicrograph by Shane McClure).

Occasionally, small dark brown-to-black particles were seen, sometimes with a needle-like morphology, along the interface between the seed plate and the citrine portions of the synthetic ametrine. Although they were not identified, the growth conditions suggest that they could be hydrous Fe-oxides or Mn-oxides.

According to J. Koivula (pers. comm., 1999), other primary fluid inclusions showing a flattened morphology are occasionally observed along the synthetic amethyst-citrine color boundaries. Such inclusions have also been noted along the length of the seed plate interface, and near the location of the wire used to suspend the crystals during growth. Both the synthetic amethyst and citrine portions also may have partially healed fractures composed of numerous tiny voids containing both liquid and gas phases. Unlike some of the primary fluid inclusions described above, these secondary fingerprint-like fluid inclusions are not oriented in any specific direction.

Figure 13. Needle-like two phase (liquid-gas) inclusions were seen only rarely in the citrine portion of the synthetic ametrines. The inclusions are elongated parallel to the optic axis. Photo by Taijin Lu; magnified 10×.

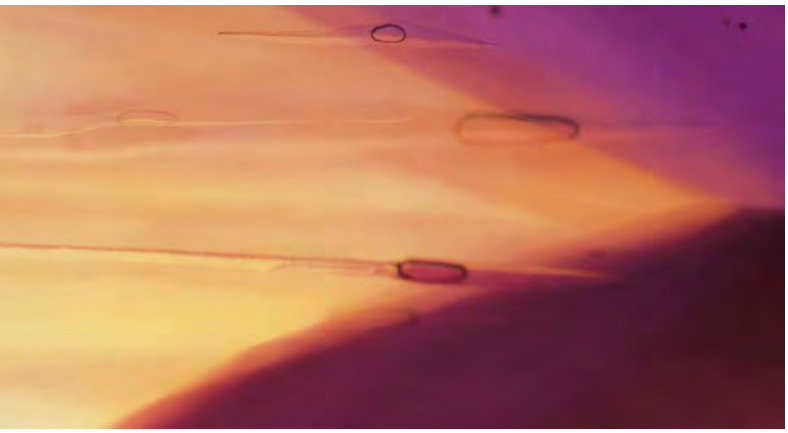

Spectroscopic Features. The absorption spectra in the UV-Vis-NIR regions were identical for natural and synthetic ametrine. In the amethyst portions of both types of ametrine, we saw characteristic absorption bands at 270, 350, 540, and 930 nm. In the citrine portions, an absorption edge rose abruptly in the 400–500 nm range, and showed weak bands superimposed at 540 and 930 nm.

Although the infrared spectra of the natural and synthetic ametrines were similar, we noted some distinctive differences. The synthetic citrine portions showed a broad, strong region of absorption from about 3700 to 2500 cm^{-1} (figure 14A), which is due to water. A similar broad band occurs in the citrine portion of natural ametrine (Vasconcelos et al., 1994), but it is much weaker. Weak OH^- peaks are superimposed on the broad band in the 3700–3500 cm^{-1} region of both materials, but the natural citrine has a weak peak at 3595 cm^{-1}, which is not seen in the synthetic material (figure 14B). In addition, one dark sample of synthetic ametrine showed weak peaks at 3555 and 3528 cm^{-1} in the citrine portion.

The infrared spectra of the amethyst zones in both the synthetic and natural ametrine show more

intense OH^- peaks, superimposed on a broad absorption band at 3435 cm^{-1} (figure 14C). The main distinction between the synthetic and natural amethyst portions is a weak band in most of the synthetic amethyst at 3543 cm^{-1} (figure 14D). Other differences, such as a weak band at 3595 cm^{-1} in the natural material, are probably too subtle to use for identification purposes.

The Raman spectra of synthetic ametrine are typical for quartz. When a comparison of the spectra of oriented samples was made for the different color zones in natural and synthetic ametrine, there was only a very slight difference: A weak 1046 cm^{-1} peak observed in both natural and synthetic ametrine was somewhat weaker in the natural ametrine.

Chemical Analyses. Qualitative EDXRF spectra of the synthetic ametrine showed the presence of iron (Fe, all 15 samples) potassium (K, 12 samples), manganese (Mn, 12 samples), and zinc (Zn, 11 samples) as trace elements. In general, higher concentrations of these elements were present in the citrine zones than in the amethyst zones. Traces of nickel (Ni) and chromium (Cr) were also observed in the citrine and amethyst portions, respectively, of single synthetic samples. We were not surprised to find these elements, since Fe is the chromophore, K and Mn are used in the growth process, and Ni, Cr, and Zn are components of the steel used in the autoclaves.

Semi-quantitative EDXRF analyses of two slabs of synthetic ametrine revealed large variations in

Figure 14. Some differences were noted in the mid-infrared spectra of the natural and synthetic ametrine. Compared to natural material, the synthetic citrine zones exhibit a more intense, broad absorption band in the 3700–2500 cm^{-1} region (A); weak peaks at 3555 and 3528 cm^{-1} were diagnostic features in one darker synthetic citrine section (B). The spectra of the amethyst zones in both synthetic and natural ametrine are similar (C), but a weak 3543 cm^{-1} peak is usually seen in the synthetic material (D). The spectra are presented normalized to 1.0 mm thickness.

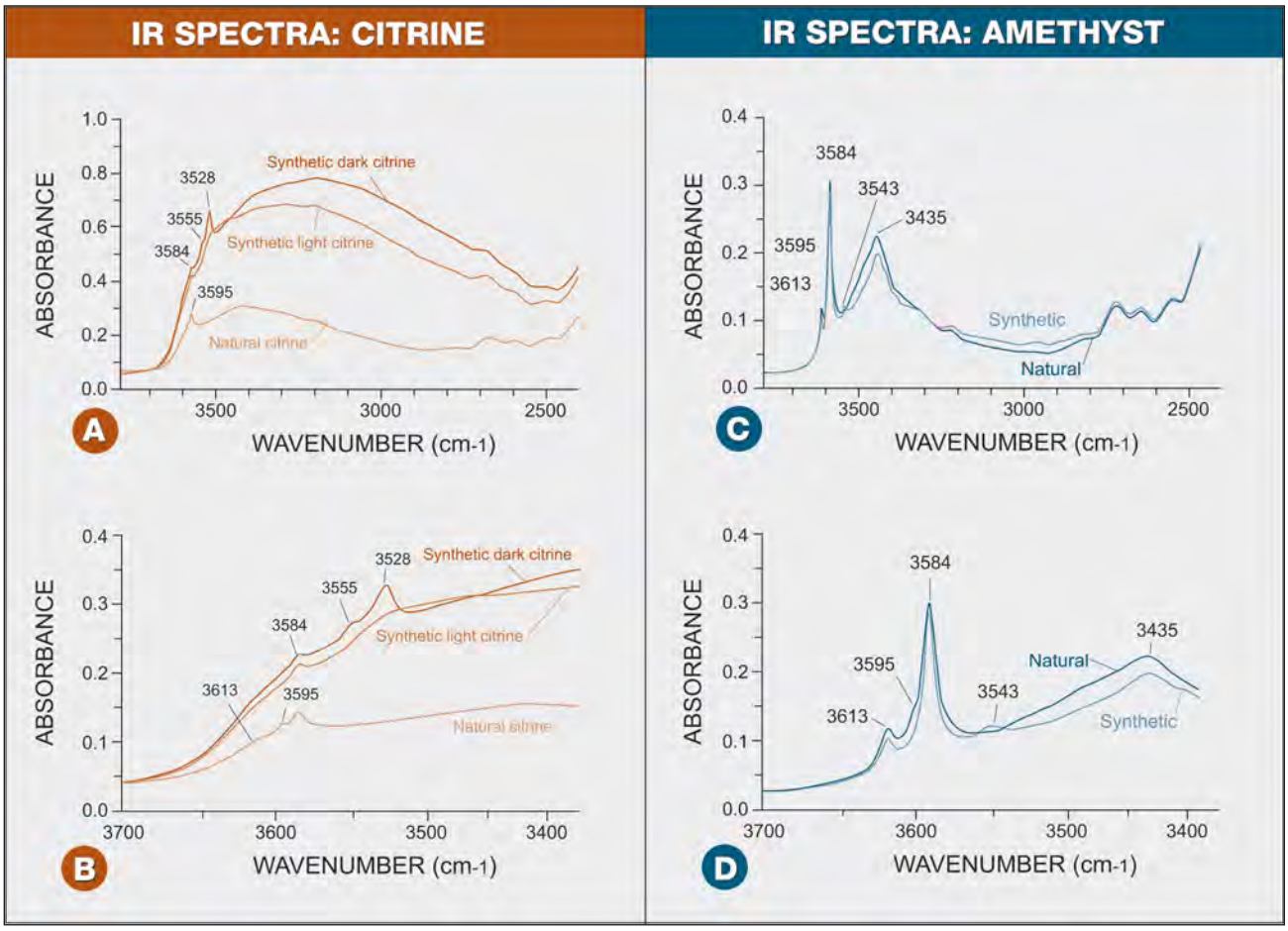

the concentrations of the above-mentioned trace elements which could be correlated to the amount of inclusions present. The two faceted samples analyzed, which were eye-clean, had lower impurity contents and showed less-pronounced chemical variations.

The quantitative (electron microprobe) analyses of natural ametrine reported by Vasconcelos et al. (1994) showed higher concentrations of iron (68–125 ppm) in the citrine zones than in the amethyst zones (19–40 ppm); data for other trace elements were not reported. In our samples of natural ametrine, we detected traces of Fe, Zn, K, Mn, and Al. The semi-quantitative data we obtained provided only relative amounts of the elements detected, so we compared the concentrations of K, Mn, Fe, and Zn in both natural and synthetic ametrine by normalizing the raw data to 1000 silicon counts per second. We found that the synthetic ametrine had higher contents of Zn (×2), Fe (×2 to ×3), Mn (×4 to ×6), and K (×4) than the natural ametrine; aluminum was present at similar (low) levels in both materials. It appears that a combination of higher K, Mn, Fe, and Zn is a distinctive feature of synthetic ametrine.

SEPARATING NATURAL FROM SYNTHETIC AMETRINE

Table 1 compares some distinguishing properties of natural ametrine and the Russian synthetic ametrine grown on tabular ZX-cut seeds. Note that R.I., birefringence, S.G., UV fluorescence, and UV-Vis-NIR absorption spectra were identical in the natural and synthetic samples.

Separating the crystals is straightforward, since their morphology is distinctive. Natural ametrine usually forms as prismatic crystals with well-developed rhombohedral faces, whereas the commercially important synthetic ametrine crystals display a tabular habit bounded mainly by *m* and *r* faces. The synthetic crystals also commonly contain a short steel wire at one of the end.

Faceted stones are more difficult to distinguish, but a number of properties provide indications:

1. The citrine color in synthetic ametrine may span a wide range, from pale yellow to moderate orange. In the synthetic samples we studied, the citrine portions were often more intensely colored than those in natural ametrine of similar thickness (again, see figure 1). The amethyst portions of our samples were also more intensely colored than those in natural ametrine of similar thickness.
2. Faceted natural ametrine commonly displays a sharp, straight boundary between the citrine and amethyst portions. Synthetic ametrine, especially when cut in fancy shapes, sometimes displays a sharp bend in the color boundary (angles of 22°–48° were measured in the GIA samples). While the amethyst-citrine color boundary in the synthetic ametrine examined for this study is oriented roughly parallel to the rhombohedral faces (or at about 51° to the optic axis for *r* sector amethyst and 23° to the optic axis for *z* sector amethyst), in natural ametrine it is oriented roughly parallel to the optic axis.
3. The crystallographic orientations of the color zones and the rare stream-like structures in the synthetic citrine portions are distinctive. The color zones are oriented perpendicular to the optic axis, and the stream-like structures are oriented parallel to the optic axis. We recommend using cross-polarized light to locate the optic axis in faceted samples, in order to provide a reference for checking the orientation of color zones and stream-like structures. In natural ametrine, the color zoning in both the amethyst and citrine portions is oriented parallel to the rhombohedral faces, and the bands usually are spaced irregularly.
4. In the amethyst portions of natural ametrine, Brazil-law twinning is almost always present, and Brewster fringes are often observed. However, Brazil twinning was seen only rarely in the amethyst portions of synthetic ametrine, in the form of subtle parallel twin lamellae. Due to the variety in forms and patterns displayed by Brazil twinning in both natural and synthetic amethyst (see, e.g., Koivula and Fritsch, 1989), this feature should not be used alone to identify a stone as synthetic. However, if a sample does show the "ideal" curved Brazil twins with Brewster fringes (again, see figure 12, right), it can be identified as natural.
5. Irregular planes of two-phase (liquid-gas) inclusions are commonly observed in both color portions of natural ametrine (Vasconcelos et al., 1994). In synthetic ametrine, elongate two-phase (liquid-gas) inclusions were seen only rarely. However, these inclusions would be diagnostic

only for those who are very experienced with quartz inclusions.

6. Natural and synthetic ametrine can usually be separated by their infrared spectra. The synthetic citrine portion has more intense absorption in the 3700–2500 cm^{-1} range of the infrared spectrum, and weak peaks at 3555 and 3528 cm^{-1} in dark material may be diagnostic. The synthetic amethyst showed a weak band at 3543 cm^{-1} that has not been observed in the natural amethyst portions.
7. As determined by EDXRF chemical analysis, synthetic ametrine will typically show higher contents of K, Mn, Fe, and Zn than occur in natural ametrine.

Even with advanced testing, the identification of natural and synthetic ametrine should rely on multiple criteria, since some of the distinguishing characteristics may be absent, and some features overlap. Positive identification may not be possible in all cases.

CONCLUSIONS

By 1994, the technology was available to produce synthetic ametrine commercially. To date, several hundred kilograms of this material have been grown and are being distributed in the jewelry marketplace.

Although there are many similarities between natural ametrine and the hydrothermal synthetic ametrine grown in Russia that was examined for this study, most faceted samples can be separated by a combination of standard gemological methods, especially by observation of internal features such as color zoning and twinning. Advanced techniques

TABLE 1. Distinguishing properties of natural ametrine and the Russian synthetic ametrine obtained for this study.[a]

Property	Synthetic	Natural
Crystal morphology	Tabular habit, normally elongated in the trigonal prism *x* direction. Prism *m* and rhombohedral *r* faces are the best developed. Seed plate is oriented perpendicular to the c-axis.	Prismatic habit consisting of rhombohedral faces *r* and *z*, and prism faces *m*.
Color	*Amethyst portion:* moderate to strong purple in the *r* and *z* sectors. *Citrine portion:* orangy yellow to orange in the *c* sectors. Typically more intensely colored than natural ametrine in both portions.	*Amethyst portion:* pale purple to intense violet-purple in *r* sectors. *Citrine portion:* light yellow to orange-yellow in *z* sectors.
Color boundary	Usually a sharp straight boundary, oriented at 51° or 23° to the optic axis for the *r* and *z* sectors, respectively; may show a sharp bend.	Usually a sharp straight boundary, oriented parallel to the optic axis.
Growth and color zoning	*Amethyst portion:* color zoning oriented parallel to the *r* or *z* crystal faces, or at about 50° to the optic axis. *Citrine portion:* color zoning oriented parallel parallel to the seed plate, or perpendicular to the optic axis; rarely, stream-like structures observed subparallel to the optic axis.	Color zoning in both the amethyst and citrine portions oriented parallel to the rhombohedral faces.
Twinning	Polysynthetic Brazil twins are observed very rarely in the amethyst portion. No twins in the citrine portion.	Brazil twins (sometimes with Brewster fringes) in the amethyst portion, typically with distinctive curved or mottled patterns. No twins in the citrine portion.
Inclusions	Rare two-phase (liquid-gas) inclusions in the citrine portion, elongated parallel to the optic axis.	Irregular planes of two-phase inclusions often observed along cracks in both portions.
IR absorption spectrum	*Amethyst portion:* usually a weak peak at 3543 cm^{-1}. *Citrine portion:* a more intense, broad absorption in the 3700–2500 cm^{-1} region; weak peaks at 3555 and 3528 cm^{-1} present in one darker sample.	*Amethyst portion:* no peak at 3543 cm^{-1}. *Citrine portion:* weaker broad absorption in the 3700–2500 cm^{-1} region; no 3528 cm^{-1} peak.
Trace elements detected by EDXRF	K, Mn, Fe, and Zn significantly higher than in natural samples; also traces of Al detected.	Fe and Zn; K, Mn, and Al detected in some samples at low concentrations.

[a]*Both materials share the following properties: R.I.—nw=1.540–1.541, ne=1.550; birefringence—0.009–0.010; S.G.—2.65; UV fluorescence—Inert to both short- and long-wave UV; UV-Vis-NIR absorption spectrum—amethyst portion: bands at 270, 350, 540,and 930 nm; citrine portion: very strong absorption at 400–500 nm and weak lines at 540 and 930 nm.*

(infrared spectroscopy and EDXRF analysis) can provide further useful data for the separation of these two materials. Note, however, that the diagnostic features presented here are specific to ametrine and are not necessarily applicable to either amethyst or citrine in general.

It must also be noted that the technology of synthetic crystal growth is constantly evolving. Prismatic synthetic ametrine crystals are now being commercially produced, and these are very similar in crystal morphology and color distribution to natural ametrine. It is, therefore, especially important that the gemologist continue to use a multitude of tests to make a conclusive identification.

Acknowledgments: The authors thank Dr. Ilene Reinitz, John Koivula, Shane McClure, and Dr. Mary Johnson of the GIA Gem Trade Laboratory for their useful comments on the manuscript, and Julia Goreva of Caltech for her assistance with the translation of technical articles from Russian to English. Funding for research at Caltech was provided by the White Rose Foundation. Funding for research in Russia was provided by the Russian Basic Research Foundation (grant # 97-05-64805).

REFERENCES

Balakirev V.G., Keivlenko E.Y., Nikolskaya L.V., Samoilovich M.I., Khadzhi V.E., Tsinober L.I. (1979) *Mineralogy and Crystal Physics of Gem Varieties of Silica*. Nedra Publishers, Moscow. [in Russian].

Balitsky V.S. (1980) Synthetic amethyst: Its history, methods of growing, morphology and peculiar features. *Zeitschrift der Deutschen Gemmologischen Gesellschaft*, Vol. 29, No. 1, pp. 5–16.

Balitsky V.S., Khetchikov L.N., Dorogovin B.A. (1970) Some specific geochemical conditions of amethyst formation. In V.P. Butusov, Ed., *Trudy VNIISIMS, Synthesis and Experimental Investigation*, Vol. 13, Nedra Publishers, Moscow, pp. 75–82 [in Russian].

Balitsky V.S., Lisitsina E.E. (1981) *Synthetic Analogues and Imitations of Natural Gemstones*. Nedra Publishers, Moscow [in Russian].

Balitsky V.S., Balitskaya O.V. (1986) The amethyst-citrine dichromatism in quartz and its origin. *Physics and Chemistry of Minerals*, Vol. 13, pp. 415–421.

Brewster D. (1823) On circular polarization, as exhibited in the optical structure of the amethyst, with remarks on the distribution of the coloring matter in that mineral. *Transactions of the Royal Society of Edinburgh*, Vol. 9, pp. 139–152.

Crowningshield R., Hurlbut C., Fryer C.W. (1986) A simple procedure to separate natural from synthetic amethyst on the basis of twinning. *Gems & Gemology*, Vol. 22, No. 3, pp. 130–139.

Garrels R.M., Christ C.L. (1965) *Solutions, Minerals and Equilibria*. Freeman, Cooper & Co., San Francisco, CA, 450 pp.

Hehar W.C. (1980) The discovery of golden amethyst. *Lapidary Journal*, Vol. 34, pp. 582–583.

Hutton D.R. (1964) Paramagnetic resonance of Fe^{3+} in amethyst and citrine quartz. *Physics Letters*, Vol. 4, pp. 310–311.

Jones B. (1993) Is ametrine for real? *Rock & Gem*, Vol. 23, No. 9, pp. 46–52.

Koivula J.I. (1980) Citrine-amethyst quartz. *Gems & Gemology*, Vol. 16, No. 9, pp. 290–293.

Koivula J.I., Fritsch E. (1989) The growth of Brazil-twinned synthetic quartz and the potential for synthetic amethyst twinned on the Brazil law. *Gems & Gemology*, Vol. 25, No. 3, pp. 159–164.

Lehmann G. (1975) On the color centers of iron in amethyst and synthetic quartz: A discussion. *American Mineralogist*, Vol. 60, No. 3–4, pp. 335–337.

Lu T., Sunagawa I. (1990) Structure of Brazil twin boundaries in amethyst showing Brewster fringes. *Physics and Chemistry of Minerals*, Vol. 17, pp. 207–211.

Melnik Y.P., Drozdovskaya A.A., Vorobeva K.A. (1974) Physicochemical analysis of the dissolution, migration and deposition of iron in modern volcanic regions. In S. Naboko, Ed., *Modern Volcanic Systems*, Nauka publishers, Novosibirsk, pp. 119-126 [in Russian].

Nassau K. (1981) Artificially induced color in amethyst-citrine quartz. *Gems & Gemology*, Vol. 17, No. 1, pp. 37–39.

Rivero R. (1999) Synthetic ametrine and amethyst infiltrates Bolivian market. *ICA Gazette*, May/June/July issue, p. 15.

Rossman G.R. (1994) The colored varieties of silica. In P.J. Haney, Ed., *Silica, Reviews in Mineralogy*, Vol. 29, Mineralogical Society of America, Washington, DC, pp. 433–468.

Tsinober L.I., Chentsova L.G. (1959) Synthetic quartz with amethyst color. *Kristallografiya*, Vol. 4, pp. 633–635 [in Russian].

Vargas G., Vargas M. (1980) A new quartz gem material. *Lapidary Journal*, Vol. 34, No. 7, pp. 1504–1506.

Vasconcelos P., Wenk H.R., Rossman G.R. (1994) The Anahí ametrine mine, Bolivia. *Gems & Gemology*, Vol. 30, No. 1, pp. 4–23.

Zaitov M.M., Zaripov M.M., Samoilovich M.I. (1974) The Fe^{3+} EPR spectrum in irradiated quartz. *Kristallografiya*, Vol. 19, pp. 1090–1093 [in Russian].

1999 Challenge Winners

Congratulations to the many readers from all over the world who demonstrated their dedication to education by participating in the 1999 *Gems & Gemology* Challenge, which tested their knowledge of articles published in the 1998 volume year. Participants who earned a score of 75% or better will receive a GIA Continuing Education certificate. Those who scored a perfect 100% are also listed below.

◆**UNITED STATES** **Alabama** *Gadsden:* Jerome Denson Thomas **Arizona** *Fountain Hills:* Hank T. wodynski. *Oro Valley:* Geraldine Alex Towns. *Sun city:* Anita R. Wilde. *Tucson:* Luella Dykhuis, David D. Arens **California** *Beverly Hills:* Sina A. Mozafarian. *Carlsbad:* Lori Burdo, Carl Chilstrom. Diane Flora, Brian I. Genstel, William J. Herberts, Mark Johnson, Doug Kennedy, Jan Luree Lombardi, Roxana J. Lucas, Wendi M. Mayaerson, Catherine McIntyre, Jana Miyahaara-Smith, Lynn L. Myers, Duncan L. Pay, Diane H. Saito, Laura Small, Abba R. Steinfeld, Ric Taylor, James Viall, Melissa Watson-Lafond, Philip G. Yourk. *Chino Hills:* Virgilio M. Garcia, Jr. *Huntington Beach:* Barr L. Doty. *Laguna Niguel:* Shawn Anne Shannon. *Los Angeles:* Veronica Clark-Hudson, Margaret Shikibu. *Mill Valley:* Susan F. Bickford. *Oceanside:* Sarah A. Horst, Laverne M. Larson. *Orcutt:* Sabra Rounds. *Pacifica:* Diana L. Gamez. *San Diego:* Tracy Nuzzo, *San Jose:* Wendy L. Bilodeau *Santa Cruz:* Tony Averill, *Walnut Creek:* Ying Ying Chow. *West Hills:* Bradley A. Partington **Colorado** *Colorado Springs:* Molly K. Knox. *Denver:* Kyle Hain, Alan J. Winterscheidt **Connecticut** *Simsbury:* Jeffrey A. Adams. *Westport:* William A. Jeffery **Florida** *Cape Coral:* Harold E. Holzer. *Clearwater:* Timothy D. Schuler. *DeLand:* Sue Angevine Guess. *Miami Beach:* Pinchas Schechter. *Plantation:* Garrett Walker. *Satellite Beach:* Consuelo Schnaderbeck. *Sunny Isles Beach:* Fabio S. Pinto **Idaho** *Victor:* Deborah L. Mock **Illinois** *Genoa:* Dale L. Johnson. *Oaklawn:* Eileen S. Barone. *St. Charles:* Lori M. Mesa **Indiana** *Indianapolis:* Mary Campbell Wright **Iowa** *Iowa City:* Gary R. Dutton. *West Des Moines:* Franklin Herman **Louisiana** *Baton Rouge:* Harold Dupuy. *New Orleans:* Jon Randall Duryee, Duncan Parham **Maryland** *Potomac:* Alfred L. Hirschman **Massachustts** *Adams:* Marc Krutiak. *Braintree:* Alan R. Howarth. *Boxford:* Sharon Kendall Heller. *Brookline:* Martin D. Haske. *Lynnfield:* John A. Caruso. *Uxbridge:* Bernard M. Stachura **Michigan** *Plymouth:* Sarah K. Bukowski **Nevada** *Las Vegas:* Deborah A. Helbling. *Reno:* Terence E. Terras **New Jersey** *Long Valley:* Lorraine Lopezzo **New Mexico** *Corrales:* Susan Gaspar Wilson **New York** *New York:* Joseph V. Mochulski **North Carolina** *Hendersonville:* Robert C. Fisher. *Kernerville:* Jean A. Marr. *Manteo:* Eileen Alexanian **Ohio** *Columbus:* John A. Schwab. *Dayton:* Michael Williams. *Highland Heights:* Michael B. Saxon. *North Royalton:* Christine M. Blankenship. *Steubenville:* Vincent A. Restifo **Oregon** *Beaverton:* Robert H. Burns. *Portland:* Geri Jeter. *Salem:* Donald Lee Toney **Pennsylvania** *Hamburg:* Janet L. Steinmetz. *Yardley:* Peter R. Stadelmeier **Rhode Island** *Providence:* Mark W. Burns **South Carolina** *Sumter:* James S. Markides **Tennessee** *Germantown:* Charles L. Rose **Texas** *Corpus Christi:* Warren A. Rees, Jr. *Flower Mound:* Elizabeth M. Roach. *Houston:* Karen L. Jensen, Christine Sehnaderbeck. *Tomball:* Carroll Joseph Kiefer **Virginia** *Hampton:* Edward A. Goodman **Washington** *Lakebay:* Karen Lynn Geiger. *Lacey:* John H. Vivian **Wisconsin** *Beaver Dam:* Thomas G. Wendt **West Viginia:** *Charleston:* Randall R. Sims ◆**AUSTRALIA** *Coogee,* Western *Australia:* Helen Judith Haddy. *Slacks Creek, Queensland:* Ken Hunter. *Success, Western Australia:* Tereena Tobias. *Sydney, New South Wales:* Barbara Wodecki ◆**AUSTRIA** *Vienna:* Eberhard Layr ◆**BELGIUM** *Diegem:* Guy Lalous. *Diksmuide:* Honoré Loeters. *Hemiksem:* Danial De Maeght. *Ruiselede:* Lucette Nols ◆**BRAZIL** *São Paulo:* Alejandro B. Ferreyra, Maria Amelia Franco, Ana Flavia Pantalena ◆**CANADA** *Bobcaygeon, Ortario:* David R. Lindsay, *Calgary, Alberta:* Diane Koke. *Cowansville, Quebec:* Alain Deschamps, *Montreal, Quebec:* Christiane Beauregard, *Prince George British Columbia:* Gerald E. Cooke. *St. Catharines, Ontario:* Alice J. Christianson. *Vancouver, British Columbia:* Michael J.P. Cavanagh, John Mattinson ◆**CYPRUS** *Nicosia:* George Stephanides ◆**ENGLAND** *Tenterden, Kent:* Linda Anne Bateley ◆**FINLAND** *Kajaani:* Petri Tuovinen ◆**INONESIA** *Ciputat, Jakarta:* Warli Latumena ◆**ITALY** *Agrate:* Zambone Ginafranco, *Caltanissetta, Sicily:* Francesco Natale, *Malnate, Varese:* Gabriele Trali. *Lucca:* Roberto Filippi. *Porto Azzurro:* Diego Giuseppe Trainini. *Rome:* Andrea Damiani. *Valenza:* Rossella Conti ◆**NETHERLANDS** *Rotterdam:* Joop G. Heetman, E. van Velzen. *Wassenaar:* Jane M. Orsak ◆**PHILIPPINES** *Mandaluyong City, Metro Manila:* Mark Alexander B. Velayo ◆**POLAND** *Lublin:* Marek A. Prus ◆**PORTUGAL** *Figueira, Vilado Bispo, Algarve:* Johanne Cardin Jack ◆**RUSSIA** *Chernogolovka, Noginsk, Moscow Province:* Vadim I. Prygov ◆**SCOTLAND** *Edinburgh:* James W. M. Heatlie ◆**SPAIN** *Madrid:* Maria Isabel Cerijo Hierro, Shahrazad Krewi de Urquijo, *Valencia:* Monika Bergel-Becker ◆**SWEDEN** *Jarfalla:* Thomas Larsson ◆**SWITZERLAND** *Basel:* Christina Dahlstroem. *Geneva:* Jean-Marie Duroc-Danner. *Lucerne:* Marisa Zachovay. *Zollikon:* Adrian Meister ◆**VIRGIN ISLANDS** *Christiansted:* Karin Ann Exposito

Answers (See page 61 of the Spring 1999 issue for the questions):
(1) b, (2) a, (3) d, (4) a, (5) c, (6) b, (7) c, (8) c, (9) d, (10) b, (11) c, (12) d, (13) a, (14) c, (15) d, (16) a, (17) d, (18) b, (19) b, (20) a, (21) b, (22) c, (23) c, (24) b, (25) b

GIA GEM TRADE

LAB NOTES

Editors
Thomas Moses, Ilene Reinitz, and Shane F. McClure
GIA Gem Trade Laboratory

Contributing Editors
G. Robert Crowningshield
GIA Gem Trade Laboratory, East Coast
Karin Hurwit, Mary L. Johnson, and Cheryl Y. Wentzell
GIA Gem Trade Laboratory, West Coast

BASTNÄSITE, A Rare Faceted Example

We seldom see rare-earth carbonates fashioned as gems, for several reasons: These minerals typically do not occur in large transparent crystals, they are usually brown, and they have low hardness. Recently, staff members in the West Coast laboratory examined an unusual 19.64 ct orangy brown oval modified brilliant (figure 1), which the client represented as the rare-earth carbonate bastnäsite. The following gemological properties were determined by senior staff gemologist Dino DeGhionno and staff gemologist Phil Owens: diaphaneity—transparent; refractive indices—1.722 and greater than 1.81 (over the limits of our standard refractometer); pleochroism—light and dark orangy brown; optic character—uniaxial positive; specific gravity (measured hydrostatically)—5.16; inert to both long- and short-wave UV radiation. These properties were consistent with those reported for bastnäsite by W. L. Roberts et al. (*Encyclopedia of Minerals*, 2nd ed., Van Nostrand Reinhold, New York, 1990, pp. 73–74).

Figure 1. This 19.64 ct bastnäsite (15.79 × 11.38 × 10.66 mm) is the first faceted example of this mineral that has been seen in the Gem Trade Laboratory.

The handheld spectroscope revealed a "rare earth" spectrum: general absorption below 490 nm, and bands at 500–525, 530, 560–585, 610, 660, and 690 nm. With magnification, we could see negative crystals (e.g., figure 2), "needles" (figure 3), and a partially healed fracture containing fluid inclusions (figure 4). As bastnäsite is quite soft (Roberts et al. list a hardness of 4 to 4$^1/_2$), we would not expect it to be in common use as a gem material.

According to Roberts et al., the formula for bastnäsite is (Ce,La)(CO_3)F; energy-dispersive X-ray fluorescence (EDXRF) analysis revealed rare-earth elements (lanthanum, cerium, and neodymium) and yttrium, but we were not able to measure these quantitatively with our system. Raman spectroscopy revealed peaks at 164, 258, 304, 351, 394, 733, 1095 (strong), 1437, and 1738 cm^{-1}, with a good match to the bastnäsite spectrum in our reference library. An X-ray powder diffraction pattern matched the spectrum in the International Centre

Figure 2. A large negative crystal was present in the bastnäsite shown in figure 1. Magnified 15×.

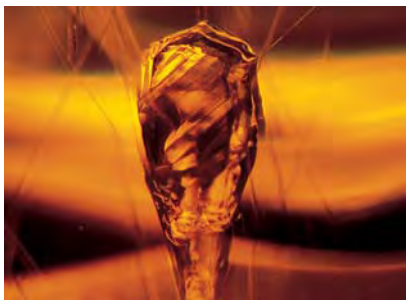

Figure 3. The bastnäsite also contained numerous needle-like inclusions. Note the optical doubling of most of the inclusions. Magnified 40×.

Figure 4. This partially healed fracture, or "feather," in the bastnäsite showed interesting geometric patterns. Magnified 25×.

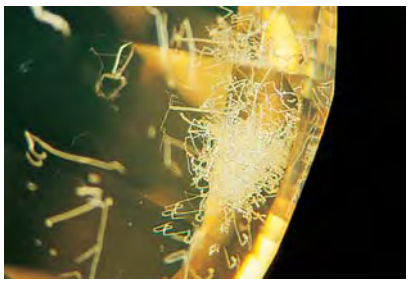

Figure 5. This dense tangle of natural etch channels was typical of the numerous etch features observed in a 25.02 ct brownish yellow round brilliant diamond. Magnified 17×.

Figure 6. In this view of the 25.02 ct diamond, several etch channels have converged to form a rough-surfaced, undulating "cavern." Magnified 20×.

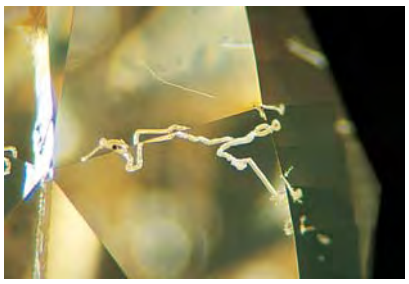

Figure 7. Note the width variations within this single etch channel, which abruptly narrows and turns back on itself, looping in tight curves. Magnified 33×.

for Diffraction Data (formerly JCPDS) reference library. The infrared spectrum included an absorption edge at about 3000 cm^{-1} and peaks at 5828, 5070, 4660, 4464, 4292, about 4000 (strong), 3758, 3590, 3421, 3229, 3179, and 3154 cm^{-1}.

As bastnäsite is an uncommon gem material, it is difficult to say whether it might have been identified without the advanced testing methods. In this case, as all the evidence pointed to bastnäsite for this stone, we were ultimately confident of the identification .

When it was time to write up the conclusion, we had some slight problems concerning what to put on the report. In Fleischer's *Glossary of Mineral Species* 1999 (J. A. Mandarino, Mineralogical Record Inc., Tucson, AZ), this material is identified as "bastnäsite-(Ce)." (There are also lanthanum and yttrium end members.) However, because we were not able to obtain a quantitative chemical analysis, we could not confirm that a predominance of the rare-earth sites were occupied by cerium (as the -Ce notation implies), so we left off this suffix. Also, because our report printing process does not accommodate umlauts, we substituted the archaic "ae" for "ä." Therefore, our report describes this unusual gem as "bastnaesite." *MLJ*

Editor's note: The initials at the end of each item identify the editor(s) or contributing editor(s) who provided that item.

Gems & Gemology, Vol. 35, No. 2, pp. 136-141

DIAMOND, with Abundant Etch Channels

This past spring, staff members at the East Coast laboratory had the opportunity to examine a 25.02 ct brownish yellow round brilliant diamond with a multitude of etch tubes. Figure 5 shows an example of these densely intertwined channels in one area of the girdle. We have previously reported on etch tubes and channels (see, e.g., Gem Trade Lab Notes, Fall 1992, pp. 193–194; Winter 1992, pp. 262–263; Summer 1994, p. 115), but this stone showed much more internal etching than any of us had ever seen in a gem diamond.

Etching—whether it forms tubes, channels, grooves, pits, or other structures—occurs along crystal defects in the diamond (Yu. L. Orlov, *The Mineralogy of the Diamond*, John Wiley & Sons, 1973, pp. 82, 98–99). Like other naturally colored diamonds of similar hue, this round brilliant owes its color—and its distinctive gemological properties—to a variety of crystal defects. We saw medium-to-strong lines in the desk-model spectroscope at 415 nm, 494 nm, and 503 nm. The diamond fluoresced with medium strength in a mixture of blue and yellow colors to both long- and short-wave UV radiation, and it showed a mixture of blue and green fluorescence to strong visible light ("transmission" luminescence). These properties indicate two optical centers in this diamond—the N3 and H3—which are composed of three nitrogen atoms, and two nitrogen atoms with a neutral vacancy, respectively (A. T. Collins, "Colour centres in diamond," *Journal of Gemmology*, Vol. 18, No. 1, 1982, pp. 37–75).

The diamond also showed medium-to-strong phantom graining, with pale brown color along two sets of graining planes; such colored graining is believed to form from dislocations between octahedral planes in the diamond (again, see the A. T. Collins reference given above). However, all colored diamonds contain some crystal defects, and many show defect combinations similar to those observed in this diamond, but relatively few show any etch tubes. The presence of such extensive etching suggests that the original crystal (1) was full of dislocations and other weaknesses, and (2) had an unusually prolonged exposure to the caustic geologic fluids that can chemically oxidize diamond.

The etch features in this diamond formed in a number of interesting shapes (see, e.g., figures 5 and 6), as well as in a range of sizes (see, e.g., figure 7). They serve as a reminder of the many differences between laser drill holes and natural etch tubes or channels (see, e.g., M. L. Johnson et al., "When a drill hole isn't," *Rapaport*

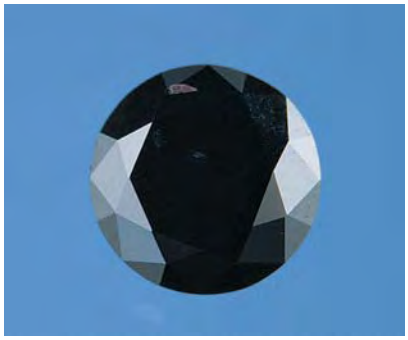

Figure 8. When this 0.29 ct black round brilliant was submitted for identification of its color origin, it was found to be a synthetic diamond.

Figure 9. Magnification and fiber-optic lighting revealed both a dark blue color and a rod-shaped inclusion (typical of a metallic flux) in the synthetic diamond. Magnified 40×.

Diamond Report, Vol. 21, No. 45, December 1998, p. 1). Although the individual tubes in this diamond were rather small in diameter, they showed angular outlines, rather than the round or oval outlines formed by laser drilling. Drill holes are usually straight, but etch tubes rarely are. Most tellingly, drill holes tend to lead to some inclusion, such as a void from which a dark crystal was removed, or a feather, which may be fracture filled. In contrast, etch tubes follow atom-size crystal defects, and thus appear to meander randomly through the diamond. *IR*

SYNTHETIC DIAMOND

Black

As the use of black diamonds in jewelry has increased, we have seen more of them at both laboratories for color-origin determination. In most black diamonds, the overall color appearance is caused by a large number of dark inclusions. We routinely examine black diamonds near the girdle with pinpoint fiber-optic illumination to look for areas of partial transparency (which are typical of natural color) or for a dark green color (which is an indicator of treatment). Such "greenish" black color results from a high dose of radiation, usually in a nuclear reactor, and diamonds treated by this method may be radioactive (see, e.g., Summer 1992 Lab Notes, pp. 124–125).

We were, therefore, somewhat surprised when the strong light revealed a *blue* color in a 0.29 ct "black" round brilliant (figure 8) that was examined last winter in the East Coast lab. The strong electrical conductivity of the sample (100:135 to 120:135) indicated that the blue color was caused by boron impurities (see J. M. King et al., "Characterizing natural-color type IIb blue diamonds," *Gems & Gemology*, Vol. 34, No. 4, 1998, pp. 246–268). The piece was inert to both long- and short-wave UV radiation. It also was heavily included, with only a few relatively transparent areas. One of those areas contained a dark, rod-shaped inclusion (figure 9), which is a common morphology for flux inclusions in synthetic diamond. This prompted us to test the sample for magnetic attraction by suspending it from a thread and bringing a powerful magnet near it. The sample's strong attraction to the magnet provided another indication that it was synthetic.

To confirm this identification and further characterize this unusual specimen, we examined the sample with a De Beers DiamondView™ (see, e.g., C. M. Welbourn et al., "De Beers natural versus synthetic diamond verification instruments," *Gems & Gemology*, Vol. 32, No. 3, 1996, pp. 156–169). We hoped that the greater intensity of this source would stimulate visible fluorescence. Although the reaction was weak and severely interrupted by the many inclusions (which did not fluoresce), we observed a fluorescence pattern that was hexagonal (i.e., reflecting the faces of an octahedron modified by a cube; cubic growth is characteristic of synthetic diamonds), rather than the concentric rectangular pattern typical of natural diamonds. The sample luminesced more strongly to X-rays, revealing a blue, angular pattern typical of synthetic growth. *IR*

Figure 10. These two synthetic diamonds (0.59 and 0.63 ct) illustrate the range of color, from orangy yellow to greenish yellow, that was displayed by a group of 18 synthetic diamonds submitted to the laboratory at one time.

Group of 18 Synthetic Diamonds Submitted at One Time

A regular client submitted a group of 18 round-brilliant and square-modified-brilliant "diamonds" to the East Coast lab for identification and color-origin determination. They ranged from 0.10 to 0.71 ct and exhibited saturated colors that varied from orangy yellow to greenish yellow, as represented by the two samples in figure 10. Standard gemological testing quickly revealed, however, that all 18 samples were synthetic diamonds. All were purchased in Russia, where they were represented as natural, so the client was surprised to hear the results.

Six of the samples contained inclusions that were larger than pinpoints, in the rod- and droplet-shaped morphologies that are typically seen in synthetic diamond. These six also showed obvious attraction to a strong magnet, while the other samples had a very weak or no attraction. We performed EDXRF analyses on two samples, one with large inclusions and one without; both revealed Fe and Ni, the principal elements in the flux that is used to facilitate synthetic diamond growth. All 18 samples exhibited some unevenness of body color, but many showed weak color zoning in which the pattern was difficult to discern. However, their reaction to UV radiation was vividly diagnostic: All showed a yellowish green cross pattern. This pattern was most clearly seen through the crown, but it was strong enough in some samples to be evident through the pavilion as well. Although some natural-color and especially treated-color diamonds fluoresce yellowish green, the cross pattern is diagnostic of synthetic origin (see, e.g., J. E. Shigley et al., "A chart for the separation of natural and synthetic diamonds," *Gems & Gemology*, Vol. 31, No. 4, 1995, pp. 256–264).

The fluorescence ranged from moderate to strong for long-wave UV radiation and from weak to strong for short-wave UV. This general trend of a stronger reaction to long-wave than short-wave UV is unlike that seen in most of the earlier yellow synthetics GIA described (J. E. Shigley et al., "The gemological properties of Russian gem-quality synthetic yellow diamonds," *Gems & Gemology*, Vol. 24, No. 4, 1993, pp. 228–248). It suggests that some of the nitrogen impurities were aggregated at high temperature after growth, forming a type Ia component (A. T. Collins and M. Stanley, "Absorption and luminescence studies of synthetic diamond in which the nitrogen has been aggregated," *Journal of Physics D: Applied Physics*, Vol. 18, 1985, pp. 2537–2545.). Unfortunately, these synthetic diamonds were not available long enough for us to perform the infrared spectroscopy necessary to confirm the diamond type. *IR*

Figure 11. The strong pleochroism of this cobalt-doped synthetic forsterite makes it a convincing tanzanite imitation. The largest cushion mixed cut weighs 6.15 ct and measures 12.29 × 9.85 × 7.06 mm. Courtesy of Tom Chatham.

SYNTHETIC FORSTERITE, A New Tanzanite Imitation

At the April American Gem Society Conclave in New Orleans, Tom Chatham of Chatham Created Gemstones, San Francisco, California, showed contributing editor MLJ four fashioned samples and two rough pieces (figure 11) of a material grown in Russia that had been represented to him as synthetic tanzanite. As this was clearly a "pulled" product, and tanzanite is a variety of the hydrous mineral zoisite, we were skeptical of this claim and agreed to study the material further.

The four fashioned samples included a 6.15 ct cushion mixed cut, a 3.27 ct oval modified brilliant, and two (2.81 and 2.10 ct) modified triangular mixed cuts. The two pieces of rough weighed 5.75 ct and 3.50 ct; portions of these samples showed a smooth curved surface, resembling part of a boule. The fashioned samples had the following properties: color—violet; optic character—biaxial positive; pleochroism—strong, in blue and purplish pink (figure 12); (Chelsea) color-filter reaction—none; refractive indices—1.635 to 1.637, 1.650 (beta), and 1.670 to 1.671; birefringence—0.034 to 0.035; specific gravity (measured hydrostatically)—3.23 to 3.24. The samples fluoresced a moderately chalky, but very weak, orangy yellow to long-wave UV radiation, and a weak greenish yellow to short-wave UV; at both wavelengths, the color was evenly distributed. When viewed with a handheld spectroscope, they showed a 460–470 nm

Figure 12. The two pleochroic colors displayed by the synthetic forsterite, as seen here with polarized light, were blue and purplish pink. Magnified 10×.

band, a 490 nm band, diffuse lines at 510 and 520 nm, and a 570–580 nm band. With magnification, we saw indistinct white inclusions, pinpoint inclusions (possibly gas bubbles), tiny "needles," and stringers (figure 13).

On the basis of the refractive indices and strong pleochroism, in particular, we suspected that the material was synthetic forsterite, Mg_2SiO_4. An EDXRF analysis performed by GTL research associate Sam Muhlmeister on the 6.15 ct cushion mixed cut confirmed this identification. EDXRF revealed major amounts of magnesium and silicon, and traces of cobalt, vanadium, and iron, with the cobalt much more prominent than the other trace elements. A Raman spectrum showed strong orientation effects (i.e., spectra taken from different angular positions had large variations in peak height), with the strongest peaks at 857 and 825 cm^{-1} and others at 965, 919, 607, 591, 547, 435, 307, and 227 (±2) cm^{-1}. An infrared spectrum showed a cutoff at 2000 cm^{-1}, and small peaks at 2497, 2623, and 2985 cm^{-1}; there was no evidence of any significant water present in the sample.

Figure 13. The 6.15 ct synthetic forsterite contained indistinct white inclusions that resemble dust particles, as well as pinpoints, tiny needles, and stringers. Magnified 11×.

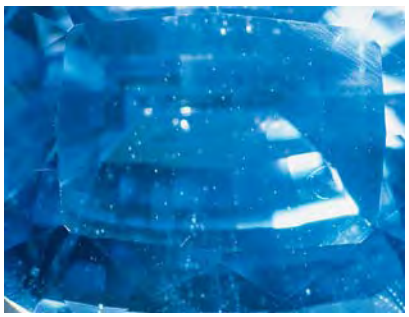

Synthetic forsterite has been described before (see, e.g., K. Nassau, "Synthetic forsterite and synthetic peridot," *Gems & Gemology*, Vol. 30, No. 2, 1994, pp. 102–108); and in an October 1996 personal communication, Dr. Henry Hänni of the SSEF Swiss Gemmological Institute called our attention to Czochralski-pulled synthetic forsterite that had been grown by Solix in Minsk, Russia. In both of these instances, chromium was the only dopant. Dr. Hänni mentioned colorless, blue-green, and "olive green" samples, and Dr. Nassau reported that there was also pink and purple material, in which the chromium could be in various oxidation states. The material we examined, however, contained no chromium, but rather was colored by cobalt (with a possible contribution from vanadium).

A comprehensive article by L. Kiefert and S. Schmidt ("Some tanzanite imitations," *Gems & Gemology*, Vol. 32, No. 4, 1996, pp. 270–276) listed manufactured glass, YAG, and synthetic corundum as tanzanite simulants. Since then, we have also seen treated-color blue beryl represented as tanzanite (Winter 1997 Lab Notes, p. 293). The pronounced pleochroism of synthetic forsterite makes it visually far more convincing as a tanzanite simulant than any we have seen before, although it can be easily distinguished from tanzanite by its refractive indices (1.635–1.670 versus 1.69–1.70 for tanzanite).

MLJ and SFM

PEARL,

Update on Non-nacreous Pearls

In the Winter 1998 Lab Notes section (p. 288), we reported on several banded, light pink and white, non-nacreous "pearls" with a sheen effect. Subsequently, the West Coast lab received samples of the shells (figure 14) that had hosted some of these concretions. Although it was previously thought that the host might be an oyster, we could readily see that the appearance was more like a scallop, of the type commonly known in some areas of the North American Pacific Coast as "lion's paw shells." The characteristic physiognomy, with seven coarsely nodular ribs and two uneven "ears," allowed us to identify the genus as *Chlamys nodosus*. *KH*

Figure 14. These shells, measuring 6 cm across, are from Chlamys nodosus, *a scallop that has produced non-nacreous "pearls" with color banding and a sheen effect (see inset, 14 × 12 mm).*

SYNTHETIC SAPPHIRE

Orangy Pink "Padparadscha"

A narrow range of pinkish orange to orangy pink sapphires are commonly referred to by the trade term *padparadscha*. Although such sapphires have long been highly prized by collectors, the GIA Gem Trade Laboratory does not issue a report using this trade description because of the subjectivity of the term (see R. Crowningshield, "Padparadscha: What's in a name?" *Gems & Gemology*, Vol. 19, No. 1, 1983, pp. 30–36).

A client recently submitted the approximately 9 ct slightly orangy pink cushion mixed cut shown in figure 15 for identification and color description. The client was disappointed that we could not verify if the stone qualified for the term *padparadscha*, but agreed to an identification report that would give an appropriate color description.

The R.I.'s of 1.76–1.77, uniaxial optic character, and absorption spectrum (three lines in the red due to Cr, and a doublet at 460–470 nm) verified that the stone was indeed corundum. In most cases, we can easily determine whether a fancy-colored sapphire is natural or synthetic by the internal features (e.g., the presence of straight or curved color banding). However, this attractive stone was virtually flawless except for a tiny feather near the girdle. Immersion in methylene iodide did not reveal any other internal features; specifically, we could not resolve any color zoning, either straight or curved. The sample fluoresced an equally strong red to both long- and short-wave UV radiation, which also provided no indication as to its origin.

Figure 15. This approximately 9 ct orangy pink cushion mixed cut, which might be called "padparadscha" by the trade, was identified as a synthetic sapphire.

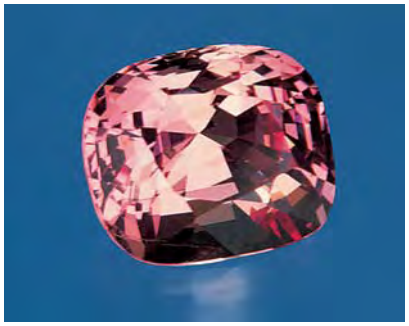

However, EDXRF chemical analysis of the stone showed a significant amount of Ni, in addition to Fe and Cr. Nickel is not found in natural sapphire, but it has been reported in some hydrothermally grown synthetic corundum from Russia (see, e.g., V. Thomas et al., "Tairus hydrothermal synthetic sapphires doped with nickel and chromium," *Gems & Gemology*, Vol. 33, No. 3, 1997, pp. 188–202). Therefore, we concluded that this sample was a synthetic sapphire, although whether it represents Russian hydrothermal growth remains uncertain. *KH*

Early Blue Synthetic Sapphire?

The white metal ring shown in figure 16 is characteristic of jewelry made in the early 1900s. As we have mentioned previously in this section, although it is possible to replicate virtually any style of jewelry, there are often certain features that suggest that a piece is indeed an "original" and was made at the time the style and design indicate. The ring shown here was one such example: Its overall style and the wear, specifically the "burnishing" of the metal around the stones, suggest that the stones had been set in the ring for some time. (A "burnish" implies that the metal has been rubbed over time; that is, it has a polished glossiness that is also somewhat dark from the incorporation of foreign substances. The effect, like that of seasoning a cast-iron skillet, cannot readily be imitated.) Even the synthetic sapphire in the center is consistent with material available in the early part of this century.

Synthetic blue sapphire was first produced by Verneuil in about 1910 (see, e.g., K. Nassau, *Gems Made by Man*, Chilton Book Co., Radnor, PA, 1980). Consequently, the large cabochon in this ring may well date from that time, as its gemological properties were typical for a Verneuil synthetic.

Figure 16. This ring appears to have been manufactured in the early part of this century. The Verneuil synthetic sapphire in the center shows eye-visible concentric circles of color banding.

The noteworthy feature of this cabochon was the eye-visible curved growth banding that was present as concentric circles. Normally, synthetic corundum boules grown by the flame-fusion method are split lengthwise in preparation for fashioning. Once the boule is split, the curved growth bands—or striae—are visible only as a group of nested curves, and not as full circles. One possible explanation for the circular growth banding in this cabochon is that it was cut from a small "button" boule that was not split after growth (see, e.g., D. Elwell, *Man-Made Gemstones*, John Wiley & Sons, New York, 1979).

TM and GRC

PHOTO CREDITS

Vincent Cracco took photos 5, 6, and 7. Maha DeMaggio photographed figures 1, 8, 10, 11, 14, and 15. John King provided figure 16. John Koivula was the photographer for figures 2, 3, and 4. Shane McClure photographed figures 9, 12, and 13.

GEM N·E·W·S

New editorial policy for Gem News. Individual bylines will be published for specific entries prepared primarily by specific contributing editors or other individuals.* Contributing editors will be identified by their initials; all others will be identified by their full names and affiliations. When referencing such entries, please cite them by the name of the person(s) listed in the byline, for example: "Schmetzer K. (1999) Gem news: Twelve-rayed star sapphire from Madagascar. *Gems & Gemology*, Vol. 35, No. 2, pp. 146–147." All entries without bylines are provided by the section editors, and should be cited as being written by Johnson, Koivula, McClure, and DeGhionno.

DIAMONDS

Diamond presentations at the PDAC conference. Since 1992, new developments in diamond exploration have been presented at the annual conferences of the Prospectors and Developers Association of Canada. Consulting geologist A. J. A. (Bram) Janse, of Perth, Australia, attended the 1999 meeting and sent in the following report. This year the meeting was held in Toronto, on March 14–17. Attendance was high (6,200), despite two bad years for the metals and mining industry as a whole. The mood was cautiously optimistic, and diamonds were one of the most popular subjects. The first diamond mine in Canada, Ekati, began operations in October 1998 (see Winter 1998 Gem News, pp. 290–292); and mining at a second deposit, Diavik, is expected to start in 2002.

This year's conference included one technical session on diamonds, and informal diamond talks in the Investors Exchange forum and an "open forum." Mike Jones of Aber Resources, Toronto, presented a design for barrier dams for the Diavik project at Lac de Gras. Roy Spencer, vice president of Denver-based Archangel Diamond Corporation (ADC), outlined the difficulties of operating in Russia, drawing from ADC's experiences with the Grib kimberlite pipe, discovered in February 1996, where development is now at a standstill. John Auston, president of Vancouver-based Ashton Mining of Canada, gave an update on their recent investigations in the Buffalo Hills kimberlite field in Alberta, Canada (see Summer 1998 Gem News, pp. 134–135), where exploration continues although a commercial diamond deposit has not yet been proved.

Ian McGeorge, of MPH Consulting in Toronto, presented a summary of activities in Botswana: Debswana is developing the Martins Drift kimberlite dike prospect, on the border with South Africa's Northern Province (formerly Transvaal), and has applied for a mining license over the Gope 25 prospect in central Botswana. According to Mr. McGeorge, recent research has indicated that the Orapa kimberlite pipe is not located on the Archean basement of the Kalahari Craton, but actually occurs within the surrounding mobile belt of paleo-Proterozoic age. If substantiated, this would upset previously held concepts on the distribution patterns of economic kimberlites (see, e.g., M. B. Kirkley et al., *Gems & Gemology*, Spring 1991, pp. 2–25; and A. J. A. Janse, *Gems & Gemology*, Winter 1995, pp. 228–255, and Spring 1996, pp. 2–30).

Chris Jennings, president of SouthernEra, Toronto, gave one of the most popular presentations, an update on activities at the Klipspringer project (figure 1), which is located near Potgietersrus in South Africa's Northern Province. SouthernEra has discovered a 20 mile (about 33 km) long dike swarm that contains several near-parallel dikes (colloquially called "fissures"); the main ones are the Leopard and Sugarbird fissures, each of which contains one or more "blows" (small pipes). The company experienced a setback in April 1998, when the heirs to the Marsfontein farm, which is centrally located in the dike swarm and contains the M-1 pipe, sold their titles to De Beers. This dispute has now been resolved (see

Anyone interested in contributing a Gem News entry should follow the procedures listed in the "Guidelines for Authors," published on pp. 77–78 of the Spring 1999 issue of Gems & Gemology. *A copy can also be obtained by contacting* Gems & Gemology *senior editor Brendan Laurs at blaurs@gia.edu (e-mail), 760-603-4503 (phone), or 760-603-4595 (fax).*

"Happy families," *Mining Journal, London*, June 19, 1998, pp. 469–470); SouthernEra retained 40% of Marsfontein, while it continues to hold 100% of all other relevant farms. Jennings described the recent development of the Sugarbird blow, for which the payback period for capital expenditure was not the two years usually considered adequate, but only *one week*.

In the Investors Exchange forum, John Kaiser of the *Kaiser Bottom-Fishing Report*, spoke on "understanding the diamond exploration cycle." He explained the lesser significance of microdiamonds recovered from small mineral grain-size fractions, as compared to macrodiamonds from bulk and mini-bulk samples, and the need to restrain enthusiasm until results of all samples are released. Ongoing activities worldwide were highlighted in short talks and displays about diamond exploration and mining in Botswana, Brazil, Canada, Finland, Guinea, Lesotho, Namibia (offshore), and South Africa.

Figure 1. This aerial view (looking east) of part of the Klipsinger project shows the Leopard "fissure." The dike is about 1 m wide, and is visible over a distance of approximately 1 km in this photo; drilling has shown it to be 3 km long. The first underground adit at this fissure is visible in the foreground. Photo courtesy of SouthernEra.

Figure 2. Octahedral diamond crystals are featured in this jewelry, which was designed by Andrew Jordan and manufactured by Steve Fong (both of Vancouver, British Columbia, Canada). The 18k gold ring contains a 2.36 ct diamond crystal and two 0.06 ct faceted yellow diamonds. Each diamond crystal in the earrings weighs about 1.25 ct. Courtesy of Betty Sue King; photo by Maha DeMaggio.

A. J. A. (Bram) Janse
Archon Exploration
Carine, Western Australia

Diamond octahedra in jewelry. In their earliest uses in jewelry, diamonds were left in their distinctive natural shapes, such as octahedra. At the Tucson show this year, Betty Sue King of King's Ransom, Sausalito, California, exhibited contemporary jewelry featuring octahedral diamond crystals from Africa (figure 2). These designs illustrated an interesting use of diamonds that are already attractive as natural crystals. Ms. King later reported that she is expanding this line of jewelry to include pieces featuring flat triangular twinned diamond crystals (macles).

Jo Ellen Cole, GIA

First diamonds from the Merlin project, Australia. Ashton Mining has generated several press releases (see, e.g., those dated October 30 and December 17, 1998, and February 18, 1999) concerning its wholly owned Merlin project in the Northern Territory. Merlin yielded the first production of diamonds in mid-February 1999, including more than 720 carats from one day's production at its Excaliber and Sacramore pipes. This sample, which was taken from low-grade ore at the surface of the two pipes, contained "a large selection" of diamonds 1 ct and larger. A second shipment of Sacramore concentrate yielded a 14.76 ct "white" octahedron (figure 3). Although ore grades have not been specified, Ashton forecasts produc-

tion of 200,000 carats from 500,000 tonnes of ore in the first year (grade 0.4 ct/ton). A commercial-scale trial mining and processing operation is now underway, and will involve taking ore from nine of the 12 pipes on the Merlin property. (For information on the geology of this deposit, see D. C. Lee et al., "The Merlin kimberlites, Northern Territory, Australia," *Proceedings of the Sixth International Kimberlite Conference, Russian Geology and Geophysics*, Vol. 38, No. 1, 1997, pp. 82–96.)

The Merlin diamonds will be sold through Argyle's European sales office in Antwerp, as the production is similar to high-end Argyle material and is "anticipated to appeal to Argyle's established range of customers." Ashton is also mining diamonds at Cuango, in northeastern Angola; more than 61,000 carats from the first three months' production were sold in December to the De Beers Central Selling Organisation (CSO) in Luanda. By agreement, all of the Cuango production will be sold through the CSO.

A review of "GE-processed" diamonds. On March 1, 1999, Lazare Kaplan International Inc. (LKI) sent a press release to the financial press, stating that its new subsidiary, Pegasus Overseas Limited (POL), would be the exclusive agent for selling natural diamonds that had undergone a new process developed by General Electric (GE). According to LKI, the process was permanent and irreversible, and was designed to improve the color, brilliance, and brightness of qualifying diamonds, which they said were a "small fraction of the overall diamond market." Both round and fancy-shaped "processed" diamonds were to be marketed, each with an accompanying grading report from a major laboratory. The release stressed the "all-natural content" of the processed diamonds, and stated that the process did not involve irradiation, laser drilling, surface coating, or fracture filling.

In a March 19 press release, GIA's president Bill Boyajian called for information from the parties involved in the process. The release further noted that GIA researchers had investigated a small sample of diamonds they believed had undergone the GE process, and that they had noted unusual gemological features in some of the diamonds. No specific information as to the nature of these features was provided, and GIA has yet to release any conclusive evidence that will identify that a diamond has undergone the GE process.

Figure 3. This 14.76 ct diamond octahedron was recovered recently from the Sacramore pipe at the Merlin project in Northern Territory, Australia. Photo courtesy of Ashton Mining.

After extensive discussions with GE and LKI, GIA announced the following in a press release dated April 28: LKI will laser-inscribe all GE-processed diamonds on the girdle with the inscription "GE POL" (figure 4). GIA will make the following comment on grading reports for all GE-processed diamonds sent to GIA from POL: " 'GE POL' is present on the girdle. Pegasus Overseas Limited (POL) states that this diamond has been processed to improve its appearance by General Electric (GE)." GIA will move forward with a research project to understand the nature of the process and explore any identifying characteristics of these processed diamonds. It will use its HORIZON laboratory operations and information management system to track and build data on every GE-processed diamond submitted to GIA for grading. Ultimately, GIA intends to publish its findings in *Gems & Gemology*. LKI began selling the GE-processed diamonds—all with "GE POL" inscribed on the girdle—through POL in Antwerp in late May.

During a special June 23 session at the International Gemological Symposium in San Diego, California, Bill Boyajian, GIA Gem Trade Laboratory chief executive officer Tom Yonelunas, GIA Gem Trade Laboratory vice president of identification services Tom Moses, and GIA director of research Jim Shigley provided a "Trade Update" on the GE-processed "Pegasus" diamonds. Although they began by explaining that there was still no "black box" that could identify these diamonds, they did reveal some information based on study of "several hundred" such diamonds that POL had submitted to the laboratory for grading reports. A summary of their findings includes: weight—0.30 to 7 ct, with most in the 1–3 ct range); shapes—most cut in fancy shapes, but some rounds; clarity—IF to I_2, with most IF to SI_1; color—D to light yellow, with most D to H (the majority of all colors are brownish or grayish). The "overwhelming majority" of diamonds were type II's, but some type I's were seen. Mr. Yonelunas, who presented these data, cautioned that the lab had yet to see the "full range" of goods. The best hope to understand this process requires examination of diamonds before and after processing, but these have not yet been available for study.

Dr. Shigley reported that GIA has been conducting its own experiments on treating diamonds using high pressure and high temperature (HPHT) to help develop identification criteria. He noted that one could add or subtract color to diamonds with this technique. Mr. Moses pointed out that HPHT treatment of diamonds has been known in the scientific community since the early

1970s. Although GE has not provided details of the process being used, many people have expressed their opinion that HPHT is involved (see, e.g., K. Schmetzer, "Behandlung natürlicher Diamanten zur Reduzierung der Gelb- oder Braunsättigung" (Treatment of natural diamonds in order to reduce the yellow or brown color), *Goldschmiede Zeitung*, Vol. 97, No. 5, May 1999, pp. 47–48 [in German]), so it is clearly important to know what the starting features of such treated diamonds are.

Mr. Yonelunas stated the belief that at least a portion of the GE-processed diamonds will be recognizable gemologically. In fact, a parcel of GE-processed diamonds from which the inscriptions had been either partially or completely removed had already been resubmitted to the Gem Trade Laboratory, and the diamonds had been noticed using archived data from the laboratory's HORIZON system. A GIA press release dated July 6 indicated how such diamonds would be handled: The company submitting the diamond will be asked to immediately authorize re-inscription of that diamond. Should the company choose otherwise, GIA would be "obligated to report this to the appropriate authorities, including the Jewelers Vigilance Committee (JVC)."

At the World Federation of Diamond Bourses meeting in Moscow in early July, a resolution was proposed regarding the GE-processed diamonds. As quoted on the Internet in *Rapaport News* (and, at our press time, scheduled to appear in the July 30 issue of the *Rapaport Diamond Report*), the resolution states the following:

1. If a diamond has been treated or processed in order to alter or enhance its color, other than by generally accepted procedures of cutting and polishing, this fact must be disclosed in writing when such a diamond is offered for sale or submitted for certification.
2. The removal of a lasered inscription which identifies a diamond as having been treated or processed as above, shall be considered a deceptive process.
3. Any violation of Articles 1 or 2 above shall be regarded as fraudulent and shall be referred to the applicable Bourse for disciplinary action as the Bourse sees fit.
4. If such a treated or processed diamond is sold without disclosure in breach of the above rule, even in good faith, the buyer shall be entitled to cancel the sale, return the diamond and obtain a refund of the purchase price.

COLORED STONES AND ORGANIC MATERIALS

International Colored Gemstone Association Congress. More than 20 countries were represented by 173 participants at ICA's eighth biennial Congress, which was held in Abano Terme, Italy, May 16–19. Dona Dirlam, Director of GIA's Library and Information Center, provided the following report.

The keynote speaker was Rashmikant Durlabhji of India, a founding organizer of ICA, who spoke on the role of colored gemstones in the 21st century. He reminded the audience that ICA is the only organization devoted to colored stones on an international basis, and he pointed out the need to continue to bridge the gaps from miners to cutters to wholesale dealers. He suggested several ideas for promoting jewelry, including the development of a line of jewels for people who wear uniforms. He also encouraged ICA members to be ready to embrace the new paradigm in trading, the Internet.

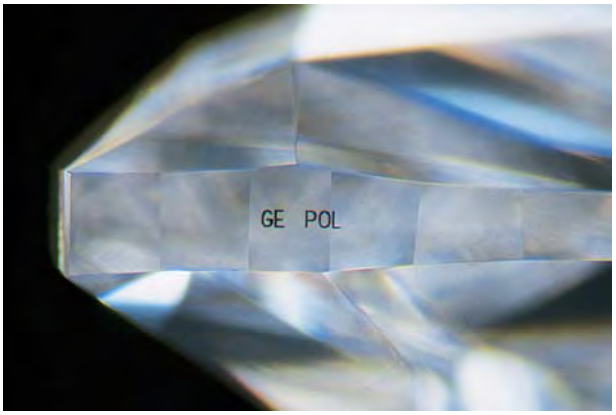

Figure 4. "GE POL" has been inscribed on the girdle of this diamond, which Pegasus Overseas Ltd. stated had been processed by GE. Photomicrograph by Shane McClure; magnified 40×.

Professor Jurgen Kleiber-Wurm of the University of Innsbruck, Austria, spoke on the global marketing of colored stones. What is fundamentally new is the speed at which information travels. Also, new markets will be found by focusing on the concept of selling "desire."

An update on the history, mining techniques, and future prospects of the Paraíba tourmaline mines in Brazil was provided by Marcelo Bernardes. He noted that currently there are three groups working the area, but there has been no recent production. Mr. Bernardes estimated that only 7.65 kg of gem-quality Paraíba tourmaline has reached the trade in 17 years of production, making it one of the rarest of the commercial gemstones.

Mehul Durlabhji, the ICA ambassador to India, gave an update on the commercial ruby localities in India's Orissa and Madhya Pradesh states, on rhodolite garnet mining in Orissa, and on tanzanite mining in Tanzania. In particular, he noted that decreased production combined with steady demand have resulted in sharp price increases for tanzanite. He concluded by suggesting that future mining for colored stones will require more sophisticated techniques and equipment.

Particularly memorable this year was the unveiling of a silver, gold, and platinum sculpture by Ninni Verga called "The Gate of the 2000 Gems" (figure 5). Decorated with 2,000 diamonds and colored gems, the sculpture was presented to the Israeli Ambassador to Italy, Yehuda Millo, by outgoing ICA president Paolo Valentini, as a symbol of peace and hope for the next millennium. After touring countries throughout the world to promote ICA, colored gemstones, and peace, it will be presented to the City of Jerusalem.

A proposal has been submitted to hold the next ICA

Figure 5. The "Gate of the 2000 Gems," an artistic replica of the Lion's Gate of the old city of Jerusalem, symbolizes the crossing from the second to the third millennium. Designed by Ninni Verga, it is made of gold, silver, and platinum and set with 2,000 colored gems weighing 253.13 ct. The sculpture, which stands 36 cm tall, has a 49 × 37 cm base. Photo courtesy of ICA.

Congress in 2001 in Sydney, Australia. The final location will be decided later this year.

Dona Mary Dirlam, GIA

Andradite (including demantoid) from Canada. At the 1999 Tucson show, Brad Wilson, of the Kingston, Ontario, office of Coast-to-Coast Rare Stones, showed *G&G* senior editor Brendan Laurs a 5.8-mm-diameter (0.78 ct) round brilliant andradite garnet that was reportedly from Black Lake, Quebec. Because the color was in the yellow-to-green range, and possibly achieved the green hue necessary to be called demantoid, Mr. Laurs requested the loan of two additional pieces so that their colors could be observed under more controlled conditions. These samples (figure 6) were examined with daylight-equivalent fluorescent lighting in a MacBeth "Judge II" viewing environment. Using Munsell color chips as comparators (see, e.g., J. M. King et al., "Color grading of colored diamonds in the GIA Gem Trade Laboratory," *Gems & Gemology*, Vol. 30, No. 4, 1994, pp. 220–242), we found that one was yellowish green (green enough to be demantoid), but the other was greenish yellow and so not demantoid.

Limited quantities of this andradite were found in 1995 and April 1998 in an asbestos mine at Black Lake, Quebec; this locality was described in the 1940s (J. D. H. Donnay and C. Faessler, "Trisoctahedral garnet from the Black Lake region, Quebec," *University of Toronto Studies, Geological Series*, No. 46, 1941, pp. 19–24). Although most of the stones cut thus far are smaller than 0.5 ct, larger ones have been faceted (e.g., 1.08, 1.38, and 2.74 ct). The properties of this material were reported in a recent article (B. S. Wilson and W. Wight, "Gem andradite garnet from Black Lake, Quebec," *Canadian Gemmologist*, March 1999, pp. 18–19) and include: R.I. of 1.880; S.G. of 3.83–3.94; no "horsetail" inclusions; and low chromium content (less than 0.01 wt.% Cr_2O_3), based on microprobe analysis of a sample for which the color was not specified.

Trapiche cat's-eye emeralds. Most gemologists and jewelers are familiar with trapiche emeralds and their six-spoke, wagon-wheel appearance. What is less well known, however, is that the pie-shaped sections in some of these emeralds may lend themselves to the fashioning of chatoyant gems.

Chatoyancy in emeralds is typically the result of light reflection from fine parallel growth tubes elongated in the c-axis direction. Less commonly, the chatoyancy results from the accidental parallel to subparallel bunching of fibrous mineral inclusions such as amphiboles. Instead of being aligned parallel to the c-axis, as are growth tubes, the fine "bunching" structure that produces chatoyancy in trapiche emeralds is oriented at 90° to the c-axis. This results in cat's-eye cabochons with the optic axis direction oriented through the dome (i.e., perpendicular to the girdle), rather than through the long side, as would be the case in a cat's-eye created by reflection from growth tubes.

Although fine-scale structure has been recognized as a characteristic of trapiche emeralds for many years (see, e.g., K. Nassau and K. A. Jackson, "Trapiche emeralds from Chivor and Muzo, Colombia," *American Mineralogist*, Vol. 55, 1970, pp. 416–427; Spring 1981 Gem Trade Lab Notes, pp. 43–44), the Gem News editors could find no mention of chatoyancy in such gems. At the 1999 Tucson show, however, Michael Gray of Coast-to-Coast Rare Stones, Missoula, Montana, showed

Figure 6. The 0.39 ct pear shaped andradite garnet from Black Lake, Quebec, Canada, is yellowish green, and therefore the variety demantoid; the 0.34 ct oval from the same locality is greenish yellow, and should be referred to simply as andradite. Courtesy of Brad Wilson; photo by Maha DeMaggio.

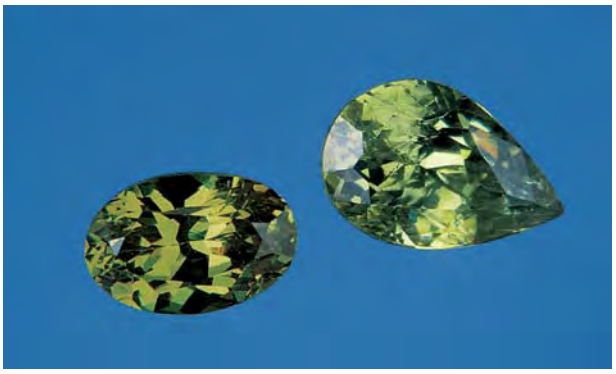

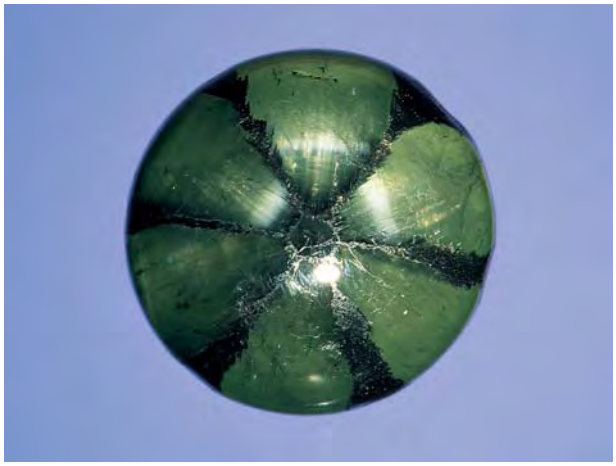

Figure 7. Bright, chatoyant bands are visible near the apexes of several wedge-shaped sections of this 18.37 ct (16.28–15.88 × 9.82 mm) trapiche emerald cabochon. Courtesy of Coast-to-Coast Rare Stones; photo by Maha DeMaggio.

us an 18.37 ct trapiche emerald cabochon (figure 7) that had a chatoyant band in each of the six wedge-shaped sections, near the apex of the cabochon, when viewed with a penlight. Magnification revealed a fibrous-looking structure that was oriented perpendicular to the c-axis. From this observation, it seemed logical that individual emerald cat's-eyes could be cut from the trapiche crystal if the fibrous structure was fine enough, and if the rough was properly oriented during cutting.

As a coincidence to this earlier observation, Roxanne Kremer of Collectors in Rosemead, California, subsequently loaned GIA two cat's-eye emerald cabochons (2.05 and 2.15 ct) that reportedly had been cut from trapiche rough from the Muzo mine (figure 8). Examination with magnification showed that the structure of these two cabochons was identical to that of the much larger, complete trapiche emerald cabochon we had examined previously. The internal structure became even more apparent when the cabochons were examined with polarized light (figure 9). It was also apparent that the fibers did not extend radially from the core (i.e., like the spokes on a bicycle wheel); instead, they maintained a parallel orientation within each trapiche section. Opaque black fringe-like extensions protruding from the spokes also pointed in the same direction as the fibrous structure in the emerald sections.

Natural pearls from the northern Cook Islands. In October 1998, GIA Extension Education manager Eddie Buscher visited the Cook Islands and met with Ben Bergman of Bergman & Sons (on Rarotonga, the capital island), who provided the following information about natural pearls from Penrhyn Island, in the northern Cook Islands.

According to Mr. Bergman, commercial farming of South Sea black (cultured) pearls was established in the Cook Islands 27 years ago. Before then, the enormous

Figure 8. Both of these free-form double cabochons, which were cut from a single trapiche emerald crystal, show chatoyancy. These 2.05 and 2.15 ct samples measure 10.79 × 7.78 × 3.32 and 10.98 × 8.01 × 3.33 mm, respectively. Courtesy of Collectors; photo by Maha DeMaggio.

lagoon at Penrhyn was noted for the small natural pearls found there, which continue to be harvested today. Penrhyn is located 650 miles (about 1,045 km) north of Rarotonga; its lagoon, which is about 50 miles (80 km) in circumference, is the home of the species *Pinctada maculata*, also known as the "Polynesian Pipi Shell." This mollusk, which averages 4 cm in diameter, occasionally produces natural pearls (figure 10). *P. maculata* mollusks cluster underwater, from near the surface to about 2 m deep, on massive coral heads that occur randomly throughout the lagoon. The natural pearls are harvested year-round, mostly by local women who use small outboard-powered boats to reach the pearl beds. Some divers employ a unique technique to determine selection of the shell: They actually look into the naturally gaping shells to see if there is a pearl inside. This approach requires considerable finesse, as the mollusk will close if it

Figure 9. When the two cabochons in figure 8 were viewed in the optic axis direction with cross-polarized light, the parallel fibrous structure that causes the chatoyancy was readily apparent. Notice how the fringed edges of the black spokes taper in the same direction as the fibrous structure. Photomicrograph by John I. Koivula.

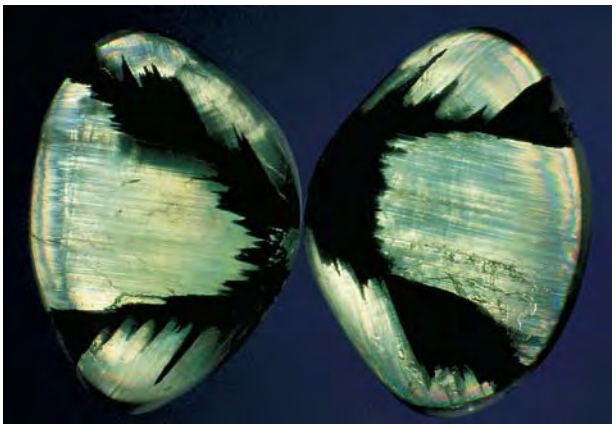

Figure 10. These natural pearls (4.5–5.0 mm) and polished shells (2.5–3.8 cm) are typical of Pinctada maculata*, a small mollusk native to Penrhyn Lagoon in the Cook Islands. Pearls courtesy of Bergman & Sons, and shells courtesy of the Beachcomber, Rarotonga; photo by Maha DeMaggio.*

detects the presence of the diver. In the last decade, Penrhyn has been affected by some unusually low tides (attributed to El Niño), which have left portions of the pearl beds exposed on the surface. The resulting mortality of the mollusks has restricted the availability of these pearls.

According to Mr. Bergman, the pearls produced by *P. maculata* average 4–5 mm in diameter. Although the color can vary considerably, the pearls are predominantly a "soft golden hue." Rarely, pearls are found that could be considered "deep gold," green, "copper," black, gray, pink to orange, or white. Common shapes include baroque, semi-baroque, button, and occasionally round. Blister pearls are referred to locally as "puku." The population of *P. maculata* is insufficient to justify commercial exploitation, and local law forbids foreigners from harvesting them. As a consequence, no official production statistics have been kept. These natural pearls are usually sold to local buyers for use in jewelry manufacturing.

Mr. Bergman noted that Penrhyn and the neighboring island Manihiki also have a large population of "wild" *P. margaritifera* mollusks (about 5 million currently), which have been harvested for the last 100 years. Local legend alludes to fabulous collections of natural pearls from the *P. margaritifera*. Although Mr. Bergman was not able to confirm this, he has seen some notable natural pearls from this mollusk, including a pair of "silver white" egg-shaped pearls about 10 mm in diameter (both said to have come from the same shell) and a single drop-shaped "silver white" pearl that measured 10.2 mm.

Eddie Buscher, GIA

Twelve-rayed star sapphire from Madagascar. Star sapphires from northern Madagascar are frequently fashioned from crystals with colorless transparent cores that are surrounded by milky white to intense blue growth sectors, as described by D. Schwarz and J. Kanis ("Madagaskar: Korund aus Nord und Süd," *extraLapis*, No. 15, 1998, pp. 60–63). In general, the six-rayed star sapphires are cut to remove this colorless core, or to place it at the rim of the cabochon. The latter was the case for a 71.18 ct 12-rayed star sapphire (figure 11) that was recently examined by contributing editor Karl Schmetzer. The stone was reportedly recovered from Antsirañana Province in northern Madagascar, a large region from which blue and yellow sapphires—including six-rayed star sapphires—have been recovered since about 1997 (see, e.g., Summer 1998 Gem News, pp. 140–141).

The flat back of this cabochon revealed that the original crystal had indeed grown around a colorless transparent core (some of which remained on one edge of the cabochon). This core was surrounded by three milky white growth sectors, which were found to be hexagonal dipyramids—probably ω {14 14 $\overline{28}$ 3}. Between two of these milky white growth sectors were narrower, transparent, intense blue rhombohedral *r* {10$\overline{1}$1} growth zones. These forms are consistent with those of sapphire seen from northern Madagascar in recent years; as such, they provided additional evidence that the stone was natural.

The 12-rayed star actually consisted of two six-rayed stars with the same axis on which the rays were offset at

Figure 11. This 12-rayed star sapphire is from Antsirañana Province, in northern Madagascar; the 71.18 ct cabochon measures 26.2 ×18.9 mm. Photo by Maha DeMaggio.

30°. The arms of the most prominent star were oriented perpendicular to the hexagonal dipyramids. (This is the usual orientation of six-rayed star cabochons from northern Madagascar.) The rays of the other star were oriented parallel to the hexagonal dipyramids, between the arms of the first star. The cause of the double star—that is, the identity of the elongated mineral inclusions in two orientations within this stone—has not yet been determined.

KS

Blue, pink, and purple sapphires from Ilakaka, Madagascar. . . . Tom Cushman of Allerton Cushman and Co., Sun Valley, Idaho, recently showed us several sapphires from new production at Ilakaka, in southern Madagascar. According to Mr. Cushman, 30 kg of gem rough were legally exported in November–December 1998; however, the miners probably recovered a great deal more than that, and the rate of production is increasing. He considers several kilograms per week a reasonable estimate, with the majority of the sapphires in pink-to-purple colors. The stones (all alluvial) are being mined principally in two areas (one near the town of Ilakaka) that are about 100 km apart; recently, however, stones also have been recovered from the region between these two areas. Pieces as large as several grams have been found.

The sapphires generally are heat treated after export, and untreated fashioned stones are comparatively rare. Mr. Cushman reports that more than 90% of the Madagascar sapphires he is marketing have been heat treated.

Figure 12. These sapphires came from Ilakaka in southern Madagascar. The long blue oval (bottom right) showed evidence of heat treatment. Courtesy of Tom Cushman; photo by Maha DeMaggio.

We examined five faceted stones (figure 12), ranging from blue to purple to pink. All but the 1.54 ct stone, a modified octagonal brilliant, were oval mixed cuts. The gemological properties are given in table 1. Four of the stones contained tiny birefringent transparent crystals,

TABLE 1. Properties of five sapphires from Ilakaka, Madagascar.

Properties	Orangy pink	Purplish pink	Pinkish purple	Blue	Blue[a]
Weight (ct)	1.99	1.54	2.12	1.72	2.03
Pleochroism	Purple pink Orange pink	Purplish pink Orangy pink	Purple Orange	Violet-blue Blue	Violetish blue Greenish blue
Color filter reaction	Reddish orange	Reddish orange	Red	Weak pink	None
Specific gravity	4.00	3.99	4.00	3.99	3.98
Refractive indices	1.760–1.768	1.760–1.768	1.761–1.769	1.760–1.768	1.761–1.769
UV fluorescence					
Long-wave	Moderate to strong orange	Moderate red-orange	Moderate red-orange	Very weak red	Inert
Short-wave	Very weak orange	Very weak orange	Very weak orange	Inert	Chalky, uneven, mod. yellowish green
Visible luminescence	None	None	None	Weak red	None
Absorption spectrum	Chromium lines (ruby spectrum)	Weak ruby spectrum	Ruby spectrum + 450 Fe line	Very weak ruby spectrum + 450 Fe band	Weak 450 Fe band
Inclusions	Stringers and clusters of tiny transparent near-colorless birefingent crystals, tension cracks around crystals	Tiny individual transparent near-colorless birefringent crystals, tension cracks, partially healed fractures	Tiny transparent near-colorless birefringent crystals, stress haloes, lamellar twinning, residues in surface cavities	Tiny transparent near-colorless birefringent crystals, irregular silk, lamellar twinning, "fingerprints"	Melted crystals, discoid fractures, cloud, "fingerprints"

[a] *Internal features showed evidence of heat treatment.*

Figure 13. This lot of mixed gem rough was recovered from alluvial deposits in the Ilakaka region of Madagascar. The largest pieces measure about 1 cm. Photo courtesy of Henry Hänni.

possibly zircon. Although we were told that two of these samples had been heat treated, only the 2.03 ct blue oval mixed cut showed evidence of this, in the form of melted crystals surrounded by discoid fractures.

. . . and other gems from near Ilakaka. Blue, pink, and purple sapphires are not the only gem materials being found in the Ilakaka area. Contributing editor Henry Hänni examined a 1 kg parcel of gem rough obtained by Werner Spaltenstein of Chanthaburi, Thailand, from the Ilakaka district. The 150-km-long alluvial deposit begins about 50 km beyond the city of Tulear (Toliara) on the southwest coast of Madagascar, along the road to Antananarivo; the village of Ilakaka is currently at the center of the excavations.

The colorful mix of slightly to distinctly rounded pebbles (figure 13) was analyzed with Raman spectroscopy at the SSEF Swiss Gemmological Institute in January 1999. The following gem minerals were identified: blue, pink-to-purple, and brown sapphire; blue, violet, and purple spinel; yellow-to-brown grossular garnets, including orange hessonite; pyralspite garnets, including almandine, rhodolite, violet-blue and "malaia"-type garnets; colorless-to-yellow, greenish yellow, or brownish yellow chrysoberyl, with some cat's-eye material and some alexandrite; colorless, light yellow, and light blue topaz; brown and red tourmaline; andalusite; yellow, brown, and green zircon; grayish blue platy kyanite; and citrine and amethyst, as well as colorless quartz. The parcel was also found to contain one light green pebble of manufactured glass.

It is interesting to note that these gem pebbles were very similar in species and shape to the rough in the parcel from Puchapucha, in the Tunduru area of southern Tanzania, that Dr. Hänni described in the Summer 1995 Gem News section (pp. 133–134). These similarities suggest that the gems may have been derived from a geologically similar source that existed while Madagascar was still attached to the African continent (see, e.g., C. B. Dissanayake and R. Chandrajith, "Sri Lanka–Madagascar Gondwana linkage: Evidence for a Pan-African mineral belt," *Journal of Geology*, Vol. 107, 1999, pp. 223–235, which includes a map showing a possible reconstruction of East Africa, Madagascar, and Sri Lanka). *HAH*

Tanzanite fluorescence: a seldom-noted property. Bill Vance, a Graduate Gemologist and gem dealer from Waldport, Oregon, recently showed the Gem News editors a transparent, 3.46 ct pear-shaped mixed-cut tanzanite that fluoresced to long-wave UV radiation. Since UV fluorescence has not been reported previously for tanzanite (see, e.g., pp. 387–388 of R. Webster's *Gems*, 5th ed., Butterworth-Heinemann, 1994: "There is no noticeable luminescence under ultra-violet light"), we examined the stone in more detail.

The tanzanite was slightly purplish blue face-up, and

Figure 14. Miners emerge from a tunnel at the Merelani mining area in northeast Tanzania. Photo by Angelique Crown.

showed rather typical pleochroism in shades of reddish purple, brownish yellow, and grayish to greenish blue. The refractive indices were 1.691, 1.693, and 1.701, with a birefringence of 0.010 and a biaxial positive optic character; a partial interference figure could also be resolved through the pavilion of the stone. The specific gravity, determined hydrostatically, averaged 3.36 over three measurements. No absorption spectrum was seen through either a diffraction-grating or a prism spectroscope. With magnification, we saw several small scratches and surface abrasions, and a single small, iridescent cleavage extending from the girdle.

The stone showed no reaction to short-wave UV radiation, but it did fluoresce a weak yet definite slightly chalky bluish green to long-wave UV. Three other faceted tanzanites—ranging in tone from very light to very dark purplish blue—were used as comparison stones; all three were inert, and their presence in the ultraviolet testing box made the reaction of the 3.46 ct stone all the more obvious. Since UV fluorescence has apparently not been recognized in tanzanite until now, we do not know if this particular stone represents an anomaly or, because the reaction is weak, if similar fluorescence may have been overlooked in the past. Regardless, this example shows the importance of using "darkroom" conditions when testing gems for their potential reaction to UV radiation.

Tanzanite mining update. GIA instructor Angelique Crown visited the Merelani mining area in northeast Tanzania in late April 1999 (figure 14) and provided the following update. Blocks A, B, and D were being actively mined. Although no activity was noted at Block C (the largest mining area), this Block was acquired in February 1999 by a Tanzanian/South African joint venture from Graphtan International, which had been mining graphite there. African Gem Mining Resources (AFGEM) purchased the Block through its subsidiary, Mererani Mining Ltd. According to Michael Nunn, chief executive officer of AFGEM, 5% of the equity of the mining company will be placed into the Merelani Development Trust, which will be operated for the benefit of the community of Merelani. This company, which is investing $10 million in the project in the short term, is now conducting a comprehensive feasibility study and plans to begin production by the second quarter of 2000.

Meanwhile, the American Gem Trade Association (AGTA) relief program has raised approximately $35,000 to help the tanzanite miners recover from the April 1998 mine disaster (see Summer 1998 Gem News, p. 145), and a shelter for the miners is being built. During the author's visit, Philip Zahm, chairman of the AGTA project, was at the mining site with three professional paramedic and rescue training experts (Jeff Schneider, Larry Bingham, and Rod Shimamoto) from the former Samaritan Training Center based in Vacaville, California. At least 15 miners completed three days of emergency medical and rescue training. Assistance has also been provided to the Arusha Fire Brigade, the emergency responder. *Angelique Crown, GIA*

Figure 15. These stones (approximately 0.50–2.52 ct) are representative of the color range we observed in faceted tsavorites from the new deposit in southern Tanzania. Photo by Maha DeMaggio.

A new source for tsavorite. Dr. Horst Krupp, technical director of Wahuwa Mining Ltd. of Tanzania, recently informed us of a major new primary deposit for tsavorite garnet in southern Tanzania that may radically change the availability of fine–color material. The new locality is about 15 km from the town of Ruangwa in Lindi Province. Word of this new discovery has spread quickly, and miners are flocking to the area. According to Dr. Krupp, mining at Tunduru, about 150 km west of this new deposit, has virtually ceased as a result.

Dr. Krupp told us that the tsavorite is found as cracked masses in pods that may reach as large as 8 kg. The masses yield approximately 10%–15% gem-quality rough, most of which will cut small stones. Dr. Krupp showed us approximately one kilo of gem tsavorite rough and about 40 faceted stones (some of which are shown in figure 15), which were among the largest tsavorites cut to date (most larger than 1 ct, the largest being 3.65 ct). All were a medium dark green with very little or no yellow component, and many were equal in quality to the finest material on the market. According to Dr. Krupp, the new locality is producing this quality of tsavorite by the kilo, with the overall color of the rough being very consistent.

The gemological characteristics of these stones are virtually identical to those of material from other localities in Tanzania. The R.I. is very consistent at 1.74, there were no distinct lines in the spectroscope, and none of the samples fluoresced to UV radiation. Even the inclusions were the same as those in tsavorites from the older deposits, consisting of "sugary"-appearing fingerprints, curved or angled needles or growth tubes, and—identified on the basis of morphology—platy crystals of opaque black graphite and transparent dark brown mica, probably biotite. We also noted some unusual graining in one of the stones. This consisted of fine parallel curved lines that veered off in several directions (figure 16) and was

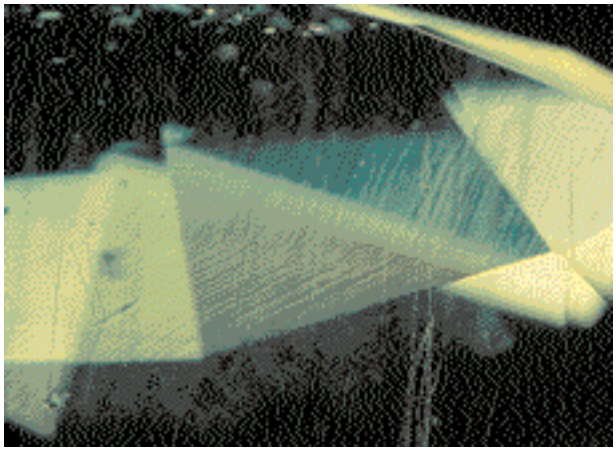

Figure 16. This unusual curved parallel graining, which was observed in one of the faceted tsavorites from the new Tanzanian deposit, is reminiscent of flow lines seen in some types of glass. Photomicrograph by Shane F. McClure; magnified 20×.

reminiscent of the swirled striae that are seen in glass. Indeed, if the stone had not had natural inclusions we would have been suspicious of its origin.

We obtained qualitative chemical analyses of three of the tsavorites using EDXRF spectrometry. The chemistry of these samples was consistent with tsavorite from other localities, with the main chromophore being vanadium. Traces of chromium may have been present, but those peaks would be concealed by overlap with the vanadium spectral peaks.

This deposit appears to be located within the same geologic belt (the Mozambique belt) as the well-known tsavorite mines at Komolo, Tanzania. However, it is almost 800 km to the south, and much of the region between has yet to be thoroughly explored. *SFM*

SYNTHETICS AND SIMULANTS

Synthetic beryl showing zoned pleochroism. Russian laboratories have been growing hydrothermal synthetic beryl in a variety of colors for more than a decade (see, e.g., Winter 1988 Gem News, pp. 252–253; and articles by J. I. Koivula et al. [pp. 32–39] and K. Schmetzer [pp. 40–43] in the Spring 1996 *Gems & Gemology*). Although most of the Russian hydrothermal synthetic beryl is green (i.e., synthetic emerald), colored by chromium, more "exotic" colors also are produced. These include: rich "turquoise" blue, colored by copper; intense pink, colored by manganese; orangy red, resulting from a trace of cobalt; and purple, colored by traces of chromium and manganese in combination. Recently, the Gem News editors received for examination an interesting hydrothermal synthetic beryl crystal with a coloration not previously encountered.

The crystal, grown on a colorless seed plate as is typical for such material, measured 45.7 × 10.5 × 9.3 mm and weighed 42.50 ct. Thomas Hunn of Thomas Hunn Co. in Grand Junction, Colorado, purchased it from the Fersman Mineralogical Museum (Moscow) as a "purple hydrothermal (synthetic) beryl." The crystal was obviously bi-colored when examined through the side in a direction parallel to the plane of the seed plate: The outer rim was dark purplish blue, and the center sections next to the seed plate were intense purplish pink (figure 17, left). When the crystal was examined in a direction perpendicular to the seed plate, or in the optic-axis direction, the mixture of these two hues resulted in an overall purplish color.

When viewed with the spectroscope, the crystal showed a sharp line at 678 nm, weaker lines at 648 and 630 nm, general absorption in the yellow-green to orange region from approximately 540 to 580 nm, and a band in the blue region between 433 and 434 nm. The spectrum did not change as the orientation of the specimen was changed, provided the beam did not pass through the seed plate. The R.I. values obtained on a relatively flat and smooth crystal face were 1.576–1.582 (typical for beryl), yielding a birefringence of 0.006. The crystal was inert to both long- and short-wave UV radiation. Since

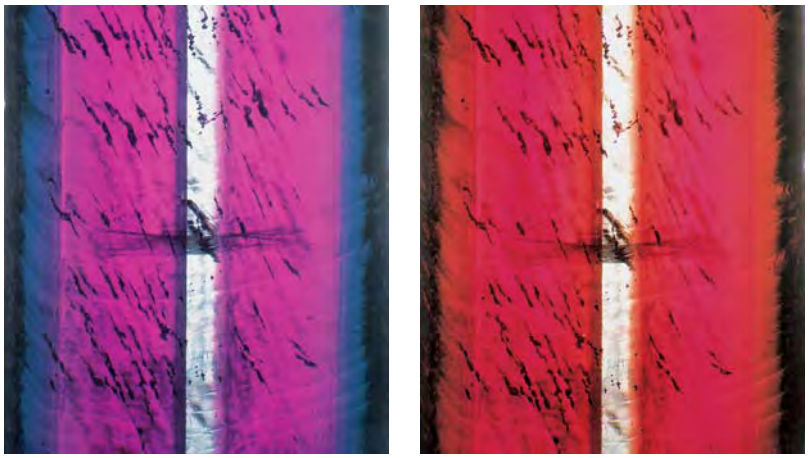

Figure 17. This 9.3-mm-wide crystal of hydrothermal synthetic beryl shows distinct color zoning, with a dark purplish blue rim and a purplish pink central area (left); these are the colors normally seen when observing the crystal. The colorless layer in the middle is the seed plate; the dark horizontal cracks are due to strain. A 90° rotation of the analyzer (right) produces a dramatic shift in the pleochroic colors, resulting in a reddish orange rim and an orangy red center. Photomicrographs by John I. Koivula.

the crystal had metal wires embedded at both ends, no attempt was made to obtain the specific gravity.

When we viewed the sample with a microscope, we saw numerous two-phase fluid inclusions. Most of these were conical- to needle-shaped growth tubes that extend in the c-axis direction. There were a few partially healed fingerprint-type fluid inclusions, particularly around the suspension wires at either end of the crystal. The pleochroism related to the color zones—perhaps the most striking aspect of this crystal—was also most evident with magnification. We observed the sample through the microscope using only the analyzing plate (that is, not the polarizer as well). The colors in each zone shifted dramatically as the plate was rotated through 90°: from dark purplish blue to reddish orange in the rim, and from purplish pink to orangy red in the center section (figure 17).

GIA Gem Trade Laboratory research associate Sam Muhlmeister obtained qualitative chemistry on the crystal using a Tracor Spectrace 5000 EDXRF system. He analyzed two separate surfaces, one parallel and the other perpendicular to the seed plate (i.e., in directions that maximized information from the bulk and the rim of the sample). The major elements detected were aluminum and silicon (light elements such as beryllium cannot be detected using this instrumentation). Phosphorus appeared to be present in minor amounts, and traces of calcium, chromium, copper, gallium, iron, manganese, nickel, sulfur, and zinc were also noted. The dark purplish blue rim contained more chromium and copper than the purplish pink central area. The exact cause of color in the crystal was not determined, but it is logical to speculate that the purplish pink central zone is colored primarily by manganese, as are natural morganite and red beryl, and additional chromium and copper are responsible for the coloration in the rim.

Polymer-impregnated synthetic fire opal from Kyocera. At the 1998 Basel Fair, the Kyocera Corp. of Kyoto, Japan, was offering a new product: "synthetic fire opal." Kyocera had already test marketed several colors of polymer-impregnated synthetic opal (see, e.g., Summer 1995 Gem News, pp. 137–139), including orangy pink, reddish orange, and orangy yellow. However, the product presented in Basel looked somewhat different from these in that it showed green and orange play-of-color against a bright orange bodycolor, similar in appearance to some Mexican fire opal.

A 24.55 ct block of this bright orange synthetic opal (figure 18) was recently studied by contributing editor Emmanuel Fritsch. The columnar structure typical of synthetic opal was clearly visible, with the cells elongated perpendicular to the top and bottom surfaces of the sample. The overall appearance was reminiscent of the atypical Gilson synthetic opal described in the Summer 1985 Gem Trade Lab Notes (pp. 110–111). The R.I. of the block was about 1.46; the S.G. (estimated by volumetric means) was about 1.8, which is low for natural gem-quality opal. The sample fluoresced strong yellow-orange to long-wave UV radiation and very strong orangy yellow to short-wave UV; the orange appearance of this luminescence might be influenced by the sample's bodycolor. The luminescence was evenly distributed (whereas some natural opals have uneven luminescence) and was not followed by phosphorescence (many natural and some synthetic opals, including fire opals, do phosphoresce).

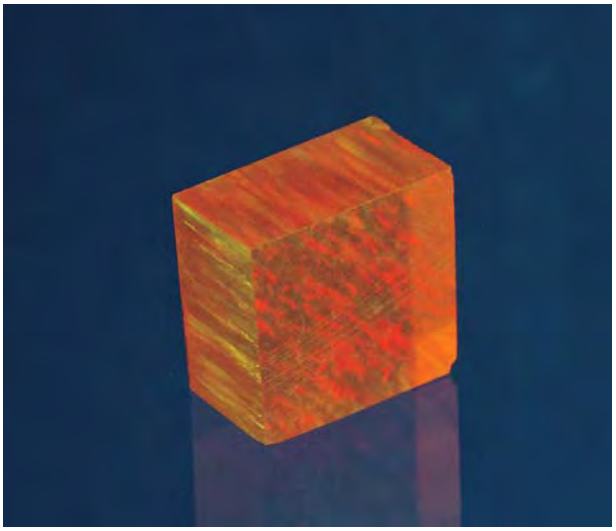

Figure 18. This 24.55 ct block of Kyocera polymer-impregnated synthetic fire opal, introduced at the April 1998 Basel Fair, has properties that are significantly different from those of natural fire opal. The block measures about 16.5 mm in maximum dimension. Photo by A. Cossard.

With magnification, many small fractures perpendicular to the top and bottom surfaces were visible; these extended about 1 mm into the block. The resulting small brownish patches (figure 19) on the top and bottom sur-

Figure 19. A typical "chicken wire" structure was seen within some brown patches on the surface of the synthetic opal shown in figure 18. Photomicrograph by E. Fritsch; magnified 60×.

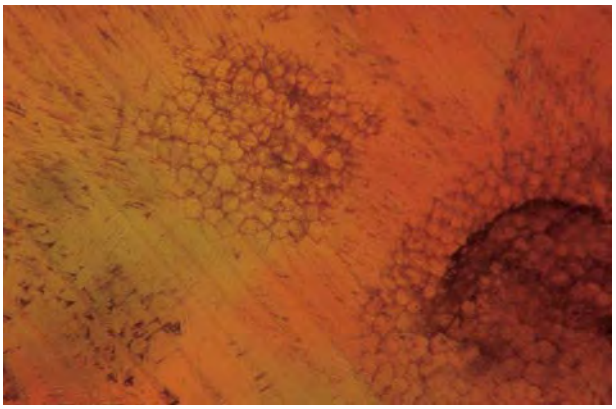

Figure 20. These citrine, tourmaline, and amethyst gemstones (39.46 ct, 6.46 ct, and 4.24 ct, respectively) were fashioned by Guy Couture as Butterfly cuts. Courtesy of Yves Morrier; photo by Maha DeMaggio.

faces showed the "chicken wire" structure that is typical for synthetic opal.

Mid-infrared absorption spectroscopy revealed absorption maxima at about 5950, 5875, 5815, 5800, 5625 (with a shoulder at 5125), 4371, and 4675 cm^{-1}. The sample was opaque at lower wavenumbers due to bulk absorption. These features are reminiscent of those seen in Kyocera's previous generation of colored impregnated synthetic opals—indicating the presence of polymers—but the differences in band positions suggest that a different polymer is being used for this material. A significant concentration of low-S.G. organic materials could account for the low specific gravity value.

Although this synthetic opal appears to be somewhat different from Kyocera's previous material, it still can be readily identified by standard gemological properties (i.e., columnar texture, "chicken wire" pattern, UV luminescence, and low S.G.). *EF*

MISCELLANEOUS

A new cut for colored stones. Gemologist Yves Morrier of Les Gemmologistes Associés OCYM Inc., Montreal, Quebec, Canada has provided the following information about a new cut for colored stones. The "Butterfly" cut features 43 facets (figure 20). Gems fashioned so far with this cut have ranged from 0.27 to 44 ct (with some calibrated goods) and include the quartz varieties amethyst and citrine, tanzanite, rhodolite and almandine garnets, fire opal, topaz, tourmaline, scapolite, and cubic zirconia. Mr. Morrier examined more than one hundred samples that revealed fairly consistent proportions, including an average length-to-width ratio of 1.38:1; an average total depth of 62%; an average crown height-to-pavilion depth ratio of 1:3; and "excellent balance" for all profile views.

The Butterfly cut was created by jewelry designer Guy Couture of Beauport, Quebec, Canada, after two years of experimentation; it debuted in August last year at Expo Prestige 98 (the annual jewelry show of the Quebec Jewellers Corp.). Mr. Couture holds U.S. and Canadian patents on this cut, and a French patent is pending. He plans to produce "butterflies" from ruby, sapphire, and emerald in 1999, and from diamond for the new millennium.

Yves Morrier
Les Gemmologistes Associés OCYM
Montreal, Quebec, Canada

Pearl Branding: "Utopia" cultured pearls. One of the latest entries in the branding of gem materials is the "Utopia pearl." According to Claudio Pagani, international promotion manager for the South Sea Pearl Consortium, each cultured pearl that is branded and marketed as a "Utopia pearl" has not been either treated or polished, and is considered the finest-quality white South Sea cultured pearl. In the patented system, a minute (1 mm × 1 mm) alphanumeric code (figure 21) is placed on each pearl by a gold vaporization method. Although a special sealant is laid over the code for protection, the customer can still remove the code without damaging the nacre. All "Utopia pearls" are accompanied by a certificate that includes a digital photo as well as the dimensions, weight, and form. To date, Mr. Pagani reports, approximately 10,000 cultured pearls in virtually all sizes have been branded "Utopia pearls."

Noted U.S. designer Henry Dunay of New York is creating a special jewelry collection of rings, pendants, earrings, and bracelets fashioned from "Utopia pearls." This collection will be introduced nationwide at the Neiman Marcus department stores this fall.

ANNOUNCEMENTS

Hong Kong Jewellery & Watch Fair '99. This show will be held from September 23 to 27 at the Hong Kong Convention and Exhibition Centre (HKCEC). Specialized

Figure 21. Magnification reveals the alphanumeric code that has been placed on this "Utopia pearl" by a gold vaporization method. Courtesy of Henry Dunay.

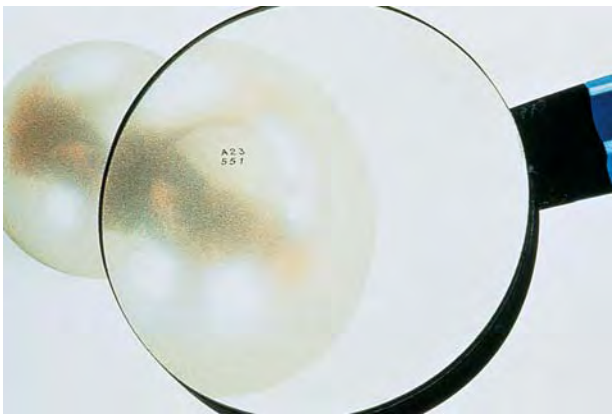

pavilions highlighting new jewelry designs, fine designs, antique and estate jewelry, equipment and packaging products, and design competitions will be featured. Two major pearl auctions, by Paspaley and Robert Wan, will also be held at the HKCEC just before the fair. There will also be professional seminars and workshops. For details, contact Miller Freeman Asia Ltd. at 852-2827-6211 (phone) or 852-2564-5496 (fax), or visit http://www.jewellery-net-asia.com/fair9jw.htm.

***Cartier* at the Field Museum.** The exhibition *Cartier: 1900–1939* will be held at the Field Museum in Chicago from October 2, 1999 to January 16, 2000. Over 200 works will be displayed, including jewelry, clocks, watches, and ornamental accessories. Client order books, idea sketches, and original plaster casts of jewels will provide a behind-the-scenes look into Cartier's creative process during this innovative period. For more information, call the Field Museum at 312-922-9410, or visit the Web site http://www.fmnh.org/exhibits/spec_exhibits.htm.

Gem Conference 99. The 10th annual Canadian Gemmological Association conference will take place October 23–24 at the University of Toronto. Lectures and workshops will cover inclusions, synthetic moissanite, jewelry design and manufacturing, and appraisals. For more information, contact Mary Ellis at 416-785-0962 (phone) or 416-785-9043 (fax).

Jewellery Arabia 99. The 8th Jewellery Arabia exhibition will take place November 9–13, 1999 at the Bahrain International Exhibition Centre. The event is intended to serve jewelry manufacturers, importers, wholesalers, and retailers throughout the Middle East. Visitors will be admitted on the basis of a business card or invitation. For further information, contact the event organizers (based in London) at 44 171-862-2041 (phone), 44 171-862-2049 (fax), or via e-mail at jewellery@montnet.com.

CORRECTIONS:

1. *On page 19 of the Schmetzer and Peretti article "Some Diagnostic Features of Russian Hydrothermal Synthetic Rubies and Sapphires," published in the Spring 1999 issue, the photographer of the main photo in figure 3 was Maha DeMaggio.*

2. *In the Spring 1999 Gem News entry "Cat's-eye andradite from San Benito County, California," the large cat's-eye andradite in figure 4 (p. 48) and the two orangy andradites in figure 5 (p. 49) were courtesy of Rick Kennedy.*

Thank You, Donors

The Treasured Gifts Council, chaired by Richard Greenwood, was established to encourage individual and corporate gifts-in-kind of stones, library materials, and other non-cash assets that can be used directly in GIA's educational and research activities. Gifts-in-kind help GIA serve the gem and jewelry industry world-wide while offering donors significant philanthropic and tax benefits. Treasured Gifts Awards are presented to those who have given gifts valued at $10,000 or more. We extend a sincere thank you to all those who contributed to the Treasured Gifts is Council in 1998.

$100,000 or more
Ramsey Gem Imports, Inc.

$50,000 to $99,999
The Bell Group, Inc.
Japan Pearl Exporters'Association
Dr. Duane Lennartson
Rouben & Mary Varozian
Zvi & Rachel Wertheimer

$10,000 to $49,999
Mr. Gary L. Alexander
Mr. George Brooks
Mr. Martin T. Coeroli
Color Change Empire
G. Robert Crowningshield, G.G.
August & Margaret Hansch
Gary & Sang Leonard
Mr. James Leonard
Nancy B & Company
Mr. Rubin Snyder
Mr. Edward R. Swoboda

$5,000 to $9,999
American Ariana Trading Corp.
Daniel & Bo Banks
Broken Hill Propriety Minerals
Classic Colors
Golay Buchel USA, Ltd.
Susan G. Goldstein, G.G.
H. G. Kazanjian & Sons, Inc.
Mariora Australia Pry. Ltd.
Stephen M. Neely, M.D.
Oro America
Pacific Perles

$1,000 to $4,999
Ms. Audrey Afholter
American Gem Trade Association
Mr. German Ayubi
AZCO Mining, Inc.
Dr. Vladimir S. Balitsky
Ben Bridge Jewelers
C3 Inc.
Chatham Created Gems
Colgem EL 97, Ltd.
Color Masters Gem Corporation
George C. Houston, Inc.
House of Onyx
Jostens
K R Gems & Diamonds International
Ms. Betsy Ross Marcinkus
Marcus Jewelers & Gemologists
Mr. Nick Michailidies
Stone Flower Co.

$500 to $999
All That Glitters
Ashland Press, Inc.
William E. Boyajian, G.G., C.G.
Carlsbad City Library
Constellation Colombian Emerald Co.
Eddie Buscher, G.G.
Frances & Roger Drezek
The Golden Cache
Archie Henderson, G.G.
Henderson Jewelry
Institute of Experimental Mineralogy
Mr. Robert E. LaPrad
Mr. William F. Larson
William Lerner, III, G.G.
Pala International, Inc.
D. Poynter & Co., Inc.
Provockative Gems, Inc.
Mr. William C. Reiman
Ronald H. Ringsrud, G.G.
Mr. Till Schoeffel
Ms. Cri Cri Solak-Eastin
Thomas Hunn Co.

$100 to $499
Christopher Amo, G.G., F.G.A.
Antique Gas & Steam Engine Museum
Mr. K. C. Bell
Mr. Charles L. Bennett
Bergman and Sons
C.P. S. Gems
Donald Clary, Gemologist
Colorado Gem & Mineral Co.
Mr. Ralph T. Davenport
Martin B. de Silva, G.G.
Michael T. Evans, G.G.
Fortunoff Fine Jewelry
Mr. David Frizell
Ms. Carole Johnson
K & K International
Bernard H. Kaplan, G.G.
Mr. George R. Kaplan
Mr. John S. Kerr
John Koivula, G.G., F.G.A.
Gail Brett Levine, G.G.
Mason-Kay, Inc.
Joseph Mayer, G.J.G.
Yianni B. Melas, G.G.
Professor Milan Novák
Mr. Carlos D. Parsons
Mr. Jeffrey E. Patterson
Mr. Gary H. Peterson
Phoenix Gems
Prime Art Jewelry
Tish & Wes Rankin
Ms. Joan Rolls-Gragg
Mr. Henry Shawah
Lewis & Alice Silverberg
John Sinkankas, G.G.
Dr. Iouliia P. Solodova
Ms. Helen L. Stanley
H. Stern Jewellers, Inc.
Richard E. Taylor, G.G.
The World of Science
USAA Alliance Services Co.
Valalan's Jewelers
Mr. Patrick M. Weglarz
E. John Wells, IV
World Wide Golf
Mr. Louis Zara
Ms. Barbara Anne Zinke

Under $100
Ms. Jo Anna Agle
Allerton Cushman & Co.
Boxlee - Applachian Gems & Minerals
Brundage Jewelers
Capalion Enterprises
The Charles Cecil Collection
Jo Ellen Cole, G.G., F.G.A.
Companhia Real Dc Metals
Mr. Vincent Dahlgren
Ms. Jan David
Del Time
Nun Durucu, G.G.
Exclusive Merchandisers, Inc.
Fine Jewelry, LLC
Gemming International Co.
Houston Imperial Crystals
Mr. Richard M. Knox
Mr. Nickolai B. Kuznetsov
Mr. Richard J. LaForge
Brendan Laurs, G.G.
Lawrence Welk Country Club
Mr. Donald B. Lee
Glen Lehrer, G.G.
MB Enterprises
Nebula Stone
Ms. Renée Newman
Ms. Susanne S. Patch
Pearl Museum
Mr. David L. Peterson
Mr. Bill Pinch
Charles R. Richmond Fine Gems
Howard Rubin, G.G.
Ms. Elizabeth Scherer
Jim Shigley, Ph.D.
Mr. Neil A. Sims
Dr. David R. Soller
Elisabeth Strack, G.G., F.G.A.
Tahiti Perles
Thai Lanka Trading Ltd.
Mr. Randy Thill
Daniel E. Weddle, G.G.

In its efforts to serve the gem and jewelry industry, GIA can use a wide variety of gifts. These include natural untreated and treated stones, as well as synthetics and simulants, media resources for the Richard T. Liddicoat Library, and equipment and instruments for ongoing research support. If you are interested in making a donation, and receiving tax deduction information, please call (800) 421-7250, ext. 4155. From outside the U.S. call (760) 603-4155, fax (760) 603-4199. Every effort has been made to avoid errors in this listing. If we have accidentally omitted or misprinted your name, please notify us at one of the above numbers.

Book Reviews

Susan B. Johnson & Jana E. Miyahira-Smith, Editors

THE COMPLETE HANDBOOK FOR GEMSTONE WEIGHT ESTIMATION

By Charles I. Carmona, 427 pp., illus., publ. by Gemania Publishing, Los Angeles, CA, 1998. US$59.95 (softbound)*

The Complete Handbook for Gemstone Weight Estimation is a compendium of formulas, tables, and other pertinent data for estimating the weight of mounted gemstones of all sizes, shapes, and types—from the mundane to the arcane.

The author has devised a clever methodology for organizing and presenting his approach to weight estimation. He first assigned gemstones into eight categories based on specific gravity. This premise allowed for the presentation of voluminous information in a relatively compact set of tables that are conveniently indexed by the 24 most common shapes encountered in the trade today. Weight calculation formulas for an additional 48 less-common shapes are also provided. These formulas, combined with the author's explanation of applicable correction factors, allow the reader to estimate weights for even the most esoteric gemstone shapes. Because diamond cutting criteria and pearl shapes are unique among gem materials, separate sections detail weight estimation information for diamonds and pearls.

The value of this handbook, however, extends far beyond a rote system of tables, charts, and formulas, as the author provides special insight into the effect of gemstone shape on weight variations. His premise is that gemstone shape is not limited to a simple finite set of profiles; rather, it is a continuum, which he illustrates by showing how weight correction factors vary as a gem's shape transitions from round to oval to square and so on.

Whether you appraise, buy, or sell mounted gems, this handbook is a valuable resource. Tabular data are presented in a concise and easy-to-access format. Ancillary discussions are straightforward and well illustrated. An expansive list of formulas and an extensive glossary of gemstone cuts (which includes more than 200 trade and proprietary names) complete this repository of weight estimation information. In short, the *Complete Handbook for Gemstone Weight Estimation* delivers on the author's stated promise "to guide both novice and professional in estimating the weight of mounted gemstones with a high degree of accuracy."

SHARON WAKEFIELD
Northwest Gem Lab
Boise, Idaho

GEMMOLOGISTS' COMPENDIUM, 7th Edition

*By Robert Webster, revised by E. Alan Jobbins, 240 pp., illus., publ. by N.A.G. Press, London, US$35.00**

The seventh edition of the *Gemmologists' Compendium* continues the excellent tradition of earlier editions by enabling quick and easy access to a vast amount of valuable gemstone data and information that even the most experienced gemologist will appreciate.

The first part of the *Compendium* is an extensive alphabetical glossary of names and terms that covers several subject areas rarely offered in other compilations, such as testing liquids and plastic gem simulants. Minor problems include the fact that some minor, past, or non-gem localities are listed, while other very important current localities (e.g., Afghanistan for spodumene and tourmaline) are conspicuously absent. Also, the book describes tourmaline species according to their color: Brown tourmaline must be dravite, and green, blue, yellow-green, "honey" yellow, or pale-colored tourmaline must be elbaite. What about liddicoatite with its palette of colors, or uvite in red and green?

In addition to standard tables such as refractive index and specific gravity, the second part of the *Compendium* contains information on such subjects as transparency of gemstones to X-rays, liquids for refractive index determination, and the important current topics of gemstone treatment and disclosure. One page covers country name changes. The 32 color plates show microscopic features of various gems, as well as timely illustrations of Russian hydrothermal synthetic emerald, heat-treated Mong Hsu ruby, diffusion-treated sapphire, heat-treated Thai ruby, and fracture-filled diamonds. These are complimented by old favorites such as "byssolite" in demantoid and "lily-pad" inclusions in peridot. Mr. Jobbins took many of these excellent photos specifically for this edition.

**This book is available for purchase through the GIA Bookstore, 5345 Armada Drive, Carlsbad, CA 92008. Telephone: (800) 421-7250, ext. 4200; outside the U.S. (760) 603-4200. Fax: (760) 603-4266.*

Despite some discrepancies and omissions, the *Gemmologists' Compendium* is highly useful for gemologists, bench jewelers, and lapidaries. For gemologists trained in North America, it provides valuable exposure to British gemology at a reasonable price.

MICHAEL T. EVANS
Gemological Institute of America
Carlsbad, California

CHRISTMAS JEWELRY

By Mary Morrison, 158 pp., illus., publ. by Schiffer Books for Collectors, Atglen, PA, 1998. US$18.95.

Ms. Morrison provides an intimate journey into the pleasure of small details that only a dedicated collector of Christmas jewelry would notice. Page after page of crisp photos cover an unbelievable array of holiday themes. On the surface it looks like jumbled kitsch, but nine orderly chapters soon dispel that apprehension.

A chronicle of costume jewelry's little-known history, which started in the 1940s, provides unexpected depth. The chapter on signed Christmas tree jewelry is particularly helpful, as it places these pieces in the context of the early years, when costume jewelry was in its heyday. The thumbnail biographical sketches of major and minor manufacturers, however, leave you wanting more.

The conversational tone, personal notations, and observations within the body of the explanatory paragraphs introduce the reader to characteristics that make these pieces collectible. Small details are given to help differentiate a piece's time period and manufacturer. Unfortunately, jewelry items in the photos are not numbered to coordinate with the text, which created minor frustration. A glossary of costume jewelry terminology would be immensely helpful—I still don't know what "japanned" means.

The prices cited are, in the words of the author, "a reflection of real prices paid for these pieces in the mid-1990s in the United States." As a gemologist I was aghast, but independent research and interviews revealed that even though we are talking about rhinestones and nonprecious metals, Christmas jewelry is highly sought after: It is a viable market that fully supports the prices and ranges given.

GAIL BRETT LEVINE, G.G.
Auction Market Resource
Rego Park, New York

GLOSSARY OF MINERAL SYNONYMS

By Jeffrey de Fourestier, 442 pp., illus., Special Publication 2 of The Canadian Mineralogist, publ. by the Mineralogical Association of Canada, Ottawa, Canada, 1999. US$50.00

With this book, the author has succeeded in compiling a glossary of undeniable utility for his intended audience of "private collectors, museum curators, researchers, and those in the gem trade." The more than 35,000 entries include an eclectic mix of synonyms, variety names, names of discredited minerals, names for synthetics, trade names, and more—a much-appreciated resource for those of us who have had to deal with cryptic mineral or gem names that eluded all of our deciphering efforts.

Entries are organized in alphabetical order. In most cases, the synonym is linked to the currently accepted mineral species name, occasionally with brief modifying or explanatory information. The author has made a conscientious effort to follow the nomenclature guidelines of the Commission on New Minerals and Mineral Names (CNMMN) of the International Mineralogical Association (IMA). The book is well printed and bound, and nicely (though sparingly) decorated with attractive black-and-white drawings of minerals. It is evident that the text has been carefully screened for typographical errors.

The compilation is surprisingly inclusive. The bibliography lists many of the publications that the author scoured for names, which date from 1260 to 1998 AD; besides English, it also include texts in German, French, Spanish, and Latin, among other languages. When a name has been applied to several different materials, all are listed, and virtually every variation in spelling of a name is provided.

Overall, this book is a marvelous resource, but it does have a few shortcomings. The conciseness of each entry makes it an excellent quick reference, but it often leaves the reader in want of more information. In particular, the significance and full meaning of some terms is not provided. *Amethyst*, for example, is equated with quartz, but with no mention of color. *Amethyst* is also noted as being a synonym for corundum and beryl, but there is no mention of the fact that this usage is old and obsolete. Although I wanted to learn more about this, unfortunately no bibliographic references are provided for specific entries. It would also have been useful to include *all* accepted mineral species names as separate entries, regardless of whether they have synonyms. Thus, there is no entry for "painite," an accepted name for a mineral species (and rare gem material) without a synonym.

In reviewing this book, I was reminded of a joke I heard many years ago. A young man, asked about the last book he read, responds, "There wasn't much plot, but the cast of characters was tremendous." Although he was actually talking about a telephone directory, he might just as well have been referring to the *Glossary of Mineral Synonyms*. However, you can probably get by without a telephone directory—there is always directory assistance—but anyone interested in gems and min-

erals will quickly come to rely on this book as an essential reference.

ANTHONY R. KAMPF
Los Angeles County Museum of Natural History
Los Angeles, California

THE PHOTO-ATLAS OF MINERALS [CD-ROM]

*Developed by Anthony R. Kampf and George Gerhold, produced by The Gem & Mineral Council, Los Angeles County Museum of Natural History, Los Angeles, 1998. US$49.95.**

The Photo-Atlas of Minerals is a thoughtful, sophisticated product, in CD-ROM format, that uses the capabilities of computer technology to provide exciting features. To put the *Photo-Atlas* in perspective, I spent $40 on the *Encyclopedia of Minerals* by W. L. Roberts, G. R. Rapp, Jr., and J. Weber (Van Nostrand Reinhold, New York) when it was first published in 1974. It was an extravagance for a struggling graduate student, but I bought it for two reasons: First, it had entries for 2,200 mineral species, the most comprehensive reference then available. More importantly, the *Encyclopedia* was the first standard reference in mineralogy to be extensively illustrated in color, with almost 1,000 color photographs of an unusually wide variety of species. Now, a generation later, *The Photo-Atlas of Minerals* serves the same purpose even better, and at a much cheaper price.

The *Photo-Atlas* is easy and fun to use. Clear instructions are provided, but they really are not needed. The core of the product is 6,500 color images of more than 800 mineral species. Most of these are the work of Wendell E. Wilson and Louis Perloff, two of the very best mineral photographers. Some species, especially the gem minerals, are represented by dozens of illustrations. There are occasional images of gemstones, as well as inclusions. These are all linked to a database of mineral properties that covers 3,600 species and an extensive glossary. The user can search and view minerals by name, chemistry, locality, crystal class, or physical properties. For users who are wired for sound, click on the name of a mineral and it is pronounced! The CD also can be used to play an identification game or create a slide show. *The Photo-Atlas of Minerals* provides an unparalleled collection of excellent mineral images with supporting text, and a search capability that can be used and enjoyed by a wide audience.

CARL FRANCIS
Harvard Mineralogical Museum
Cambridge, Massachusetts

OTHER BOOKS RECEIVED

Mani-Mala, or A Treatise on Gems, *by Sourindro Mohun Tagore, reprinted by Nandishkor R. Barot, 1,046 pp., illus., publ. by Mehul Barot, Philadelphia, PA, 1996, US$200.* It is always a cause for celebration whenever a much-esteemed historical gemological book, hitherto inaccessible to most persons because of rarity, is reprinted. The basic worth of Tagore's treatise, first published in 1879, remains unchanged from my evaluation in *Gemology: An Annotated Bibliography* (Scarecrow Press, Metuchen, New Jersey, 1993), entry no. 6475: "On all counts one of the most remarkable and important works on gems ever published, particularly so because its Indian author stresses the knowledge of gems and their cultural significance in the Indian lands. For information on Indian gems, one must ultimately seek out and consult this splendid work. It is the product of many years research in locating and extracting the ancient literature of India. . . .[Readers are given] the opportunity to compare directly this translation to the originals in native languages which are conveniently placed in parallel [Bengali, Hindi, and Sanskrit]."

In this reprint, a number of original lithographic illustrations are poorly reproduced, but the text is sharp and easily legible. Although the binding leaves much to be desired, nevertheless the volumes should hold together and wear well. It is interesting to note the meteoric rise in price of an original *Mani-Mala*, beginning with an auction sale at $85 in 1971, to $4,000 at Christie's in 1987, and an astonishing $8,625 paid in the Swann auction of 1994. Given those astronomical sums, perhaps $200 isn't too much after all.

JOHN SINKANKAS
Peri-Lithon
San Diego, California

Edelsteine: Symbole der Schönheit und der Macht (Gemstones: Symbols of Beauty and Power), *by Edward J. Gübelin and Franz-Xaver Erni, 240 pp., illus., publ. by Verlag Hans Schöner GmbH, Königsbach-Stein, 1999 [in German], US$43.00.* Forming the core of this large (30.5 × 24.5 cm), richly illustrated volume are more than 110 pages devoted to 26 different gemstones. Discussions of each gemstone are accompanied by the photographs of Harold and Erica Van Pelt, among others. Remaining chapters contain general overviews of origins and characteristics, symbolism, production, processing, inclusions, and synthesis of gemstones. Tables, charts, and other graphics supplement the text throughout. *Edelsteine* closes with a glossary and a bibliography. An English version is forthcoming.

STUART D. OVERLIN
Gemological Institute of America
Carlsbad, California

Gemological ABSTRACTS

COLORED STONES AND ORGANIC MATERIALS

Amber specimen yields another link to the past. C. Fenelle, *National Jeweler*, Vol. 42, No. 20, October 16, 1998, p. 20.

A new species of mayfly estimated to be more than 25 million years old was found in a piece of Mexican amber recently unveiled at Britain's Natural History Museum. Mayflies are rarely found in amber, because the insects only live above water for a few hours and die shortly after mating. Other insect and plant remains contained in amber are spiders, ants, gnats, flies, wasps, bees, flowers, mushroom caps, seeds, leaves, and stems. The most common plant remains found in amber are pine needles and pine cones. *MM*

Crystal, quartz, or what? S. Frazier and A. Frazier, *Lapidary Journal*, Vol. 52, No. 6, September 1998, pp. 26–31, 62.

Fourteen different meanings of the word *crystal* are presented in this article. More common uses of the term include any mineral with natural faces, transparent quartz, clear cut glass of superior quality, the colorless cover of a watch face, or any material with an orderly internal arrangement of atoms. *Crystal* may also refer to an early diamond grading term corresponding to GIA color grade J, a clarity grade for opal, or any material that

This section is designed to provide as complete a record as practical of the recent literature on gems and gemology. Articles are selected for abstracting solely at the discretion of the section editor and his reviewers, and space limitations may require that we include only those articles that we feel will be of greatest interest to our readership.

Requests for reprints of articles abstracted must be addressed to the author or publisher of the original material.

The reviewer of each article is identified by his or her initials at the end of each abstract. Guest reviewers are identified by their full names. Opinions expressed in an abstract belong to the abstracter and in no way reflect the position of Gems & Gemology or GIA.

has particular transparency or purity. However it is used, the word *crystal* stems from the Greek *krystallos*, or "clear ice." For 2,000 years, the main source for quartz crystals was cavities in rocks in the higher elevations of the Alps. The cavities also contained clear ice crystals during the cold months, so that, at times, quartz crystals would appear to be growing out of the ice. Quartz was considered permanently frozen ice; thus, *krystallos* also became synonymous with clear quartz. The various other meanings of the word *crystal* evolved over time as a result of such factors as the apparent similarity of quartz to glass and other minerals, and the adaptation of the word through the Latin, French, and Middle English languages. *MD*

Demantoid garnet enjoys market transformation. *ICA Gazette*, November–December 1998, pp. 1, 7.

Demantoid (andradite) garnet was first discovered in 1854 in Russia's Central Ural Mountains, where it is still being mined. The rarest of all gem garnet varieties, it was found as a by-product of platinum mining in the Bobrovka River. Demantoid was originally thought to be peridot, based on its color resemblance. In 1878, the stone was identified as a garnet and named *demantoid* (from the Dutch *demant*, meaning "diamond") because of its extremely high dispersion. A second deposit of vivid green demantoid garnet was discovered at the Chusovaya River near Ekaterinburg in 1879. Demantoid was popular in the early part of the 20th century, particularly among royalty, and was frequently used in Peter Carl Fabergé's intricately crafted objects.

More recently, demantoid has enjoyed limited popularity because of the relatively small quantities and faceted sizes available. In 1997, a new deposit of demantoid was discovered at Usakos in central Namibia. The Namibian material shows a beautiful brilliance, and occurs in larger sizes, but it does not contain the characteristic "horse-tail" inclusions found in the Russian material. Production is expected to increase in both Russia and Namibia, perhaps enabling demantoid to regain its popularity with jewelers, designers, and gem collectors. *MM*

The gemological identification of emeralds and blue sapphires. J. E. Shigley, *CIM* [Canadian Institute of Mining and Metallurgy] *Bulletin*, Vol. 91, No. 1025, Nov. 1, 1998, pp. 91–96.

The gemological properties of natural emeralds and sapphires, and ways of differentiating them from other gemstones and from their synthetic counterparts, are reviewed for a geologic audience. In addition to tables of gemological properties and distinctive features observed with a gemological microscope, the following topics are discussed for both emeralds and sapphires: types of geologic occurrence, methods of synthesis, treatments, and means of identifying synthetic and treated stones using both standard (e.g., microscopic) and advanced (e.g., infrared and Raman spectroscopic) techniques.

An underlying theme of the article is that ethical business practices on the part of the entire jewelry industry are essential to maintain consumer confidence. Thus, synthetic stones must be identified and treatments disclosed. Ethical failures at the jewelry counter, for example, eventually will have negative consequences throughout the industry. One possible result could be reduced exploration and mining of natural stones. *MD*

Investigation of the intracrystalline Cr^{3+} distribution in natural and synthetic alexandrites. H. Rager, A. Bakhshandeh-Khiri, and K. Schmetzer, *Neues Jahrbuch für Mineralogie Monatshefte*, Vol. 12, December 1998, pp. 545–557.

The substitution of Cr for Al in chrysoberyl (ideally $BeAl_2O_4$) produces the phenomenal gem, alexandrite. The intensity of the color-change effect in alexandrite is directly proportional to Cr content. Electron Paramagnetic Resonance (EPR) was used on eight samples (five natural and three synthetic) to establish which of two different Al crystallographic lattice sites (designated Al_I and Al_{II}) controls Cr distribution in alexandrite.

The data suggest that Cr is mostly concentrated in the larger of the two Al sites (Al_{II}), contrary to the conclusions of several previous studies. The influence of Fe on the Cr distribution was minimal. The amount of Cr in the larger sites increases with overall Cr content, but the Cr fraction in the smaller sites either remains constant or increases minutely. Therefore, it was concluded that the larger Al site is host to the Cr that causes the color change in alexandrite. *JL*

Investigation of the stability conditions and structural-chemical transformations of Baikal lazurite. V. L. Tauson, V. V. Akimov, A. N. Sapozhnikov, and K. E. Kuznetsov, *Geochemistry International*, Vol. 36, No. 8, 1998, pp. 717–733.

Lazurite, the main constituent of lapis lazuli, is part of the sodalite mineral group (along with sodalite, nosean, and haüyne). This in-depth geochemical study of lazurite from the Baikal region of Siberia was undertaken to establish the causes of structural modulations at the crystal lattice-atomic level. Samples were annealed according to three different experimental methods. The first two were "dry" runs that used gold or quartz ampoules to hold ~50 mg of lazurite powder and chemical reaction indicators. The third group of experiments was designed to mimic hydrothermal conditions, using aqueous solutions at higher pressures. On the basis of the results, the authors constructed a crystallization phase diagram.

Since the Baikal lazurite is inferred to have formed over the narrow temperature range of about 500°–600°C, the experimental data suggest that the microstructural

modulations depend more on the partial pressure (fugacity) of the sulfur dioxide (i.e., fSO_2) gas phase than on the temperature at the time of crystallization. In the experiments, the lazurite was transformed into complex sulfate and oxide phases at high fSO_2. At low fSO_2, sodalite was formed. The lazurite that formed at moderately high fSO_2 showed a modulated structure. The blue lazurite color is attributed to the fugacities of sulfur and hydrogen gas phases during formation, as well as to the size of the crystals. *JL*

Is opal . . . ? S. Frazier and A. Frazier, *Lapidary Journal*, Vol. 52, No. 5, August 1998, pp. 16–25.

This article, which answers 12 commonly asked questions about opal, establishes the distinction between the different types, including precious (has play-of-color), common (lacks play-of-color), boulder (cut with matrix as part of the gem), and fire (has a "fiery" body color). The distinction between play-of-color (a flash of different colors) and opalescence (a milky body color) is explained. The formation of fire opal requires an unusual combination of geologic conditions, hence the rarity of fine specimens, with the most valuable coming from Querétaro, Mexico. Although Australia is the best-known source of precious opal, gem-quality material is also found in Brazil, Honduras, Mexico, the U.S. (Nevada, Idaho, and Oregon), Canada (British Columbia), and Slovakia. Particular attention is paid to Brazil as a source: Six types of opal (precious, green, black, hyalite, greenish yellow cat's-eye, and fire) are mined there, though none in large quantities. Historical aspects of opal, such as its appeal to the Aztecs and Mayans, and practical aspects, such as crazing of opal from some localities, also are noted.

Like other gemstones, opal has simulants (e.g., plastics introduced in the 1970s, which are easily detected). In 1964, John Slocum produced what is known as "Slocum Stone," a glass showing apparent play-of-color that imitates precious opal. It is harder, tougher, and much more stable than natural opal. Pierre Gilson of France perfected the manufacture of material marketed as (Gilson) synthetic opal. Today, synthetic opals are produced in Japan and Russia. *MD*

Marketing high quality Chinese freshwater pearls. B. Sheung, *Jewellery News Asia*, No. 169, September 1998, pp. 124, 126.

Of the companies that supply Chinese freshwater cultured pearls, a few now seek to upgrade the product's image by focusing on quality rather than quantity. By concentrating on pearls that have been cultivated over a longer time period and selecting only the largest, highest quality specimens, these dealers are able to sell loose pearls and strands at prices closer to those usually seen for Akoya and South Sea cultured pearls.

Chinese freshwater cultured pearls can be as large as 15 mm, but the ones sold by high-end dealers typically range from 9 to 11 mm. Among these are treated black freshwater cultured pearls that offer an affordable alternative to natural-color Tahitian cultured pearls. Natural colors in Chinese freshwater cultured pearls include white, "champagne," orange, and purple. The article includes several company profiles; some Chinese freshwater cultured pearl processors in Hong Kong and Japan focus on the favored pinkish tint rather than a bleached yellowish white. *Doug Fiske*

Mined in America: Five stones to watch (Part Two). D. Yonick, *American Jewelry Manufacturer*, Vol. 43, No. 12, December 1998, pp. 18–19, 21.

Part two of this series focuses on Arizona "Anthill" garnet and Montana sapphire. (Part one, published in October 1998, featured Oregon sunstone, California benitoite, and Utah red beryl.) Red pyrope garnet is mined from an alluvial deposit on Navajo land in northeast Arizona, with 90% of the material marketed by Tucker Gems of Homedale, Idaho. The mine could produce about 1 million carats of rough a year. However, there is a limited supply of cut material over 1 ct. Meanwhile, American Gem Corp. (AGC) of Helena, Montana is expected to achieve full-scale production of Montana blue and fancy-colored sapphires from its alluvial deposits in southwestern Montana in 1999. Once plagued by financial difficulties, environmental liabilities, and internal problems, the company restructured in 1997. By the end of 1998, AGC had processed about 2 million carats of rough, which is expected to yield approximately 200,000 carats of cut stones. *MM*

Models of corundum origin from alkali basaltic terrains: A reappraisal. F. L. Sutherland, P. W. O. Hoskin, C. M. Fanning, and R. R. Coenraads, *Contributions to Mineralogy and Petrology*, Vol. 133, 1998, pp. 356–372.

Corundum from basalt fields, particularly in Australia and Southeast Asia, has been the subject of numerous geologic studies. Two types, "magmatic" and "metamorphic," are recognized based on their trace-element characteristics, mineral inclusions, and likely geologic origin within the earth's crust and mantle. This paper is concerned only with magmatic corundum, designated as "BGY" for the dominant blue, green, and yellow colors. BGY corundum shows distinctive trace-element contents (up to 0.04 wt.% Ga_2O_3 and low Cr/Ga and Ti/Ga ratios); 20 different primary mineral inclusions, including several reported here for the first time, have been identified within them.

Detailed examination was made of the crystallization characteristics (e.g., temperature of formation and intergrowth relationships) of several primary inclusions, particularly zircon, columbite, and feldspar. The authors evaluated these data in light of the tectonic setting of the deposits, and performed thermodynamic modeling of the crystallization of igneous melts of various compositions, to reach the following conclusion: The BGY corundum

crystallized from a low-volume silicate melt derived from amphibole-bearing mantle assemblages at temperatures of 720°–880°C and pressures of 0.7–1.1 GPa (about 25–40 km depths). The corundum was subsequently brought to the surface as xenocrysts in alkali basalts. The seven previously published origins that have been suggested for magmatic corundum from alkali basalts are reviewed in light of the conclusions reached in this paper. *AAL*

Prevalence and origin of birefringence in 48 garnets from the pyrope-almandine-grossularite-spessartine quaternary. A. M. Hofmeister, R. B. Schaal, K. R. Campbell, S. L. Berry, and T. J. Fagan. *American Mineralogist*, Vol. 83, No. 11–12, Part 1, November–December 1998, pp. 1293–1301.

Of 48 samples of garnet with pyrope-almandine-grossular-spessartine chemical compositions, 40 were anisotropic and the other eight samples were too thin to determine anisotropy. The birefringence (δ) of the garnets ranged from 0.0001 to 0.0006 (26 were only marginally birefringent, with $\delta \leq 0.0002$), and was generally undulatory in appearance. Hence, weak and undulatory birefringence is apparently widespread in garnets. A relationship between birefringence and geologic setting was recognized. Specifically, there is an inverse relationship between the degree of birefringence and the stress encountered during a garnet's geologic history. Thus, the greatest birefringence occurs in garnets from xenocrysts of mantle origin and in garnets from eclogite xenoliths in kimberlite pipes, as these are farthest from their conditions of formation.

It is suggested that most of the optical anomalies (i.e., birefringence and undulatory extinction) result from internal strain within the garnets, although other possible origins are acknowledged for a few specimens, such as those with sector twinning. Retention of internal strain is compounded by a mismatch in size between Ca^{2+} and Mg^{2+} within the crystal structure. Four previous models that explain the origin of birefringence are reviewed.

Kyaw Soe Moe

World jade resources. F. Ward, *Arts of Asia*, Vol. 29, No. 1, 1999, pp. 68–71.

There is more "jade" available today than at any other time in history. This is due primarily to three newly discovered deposits in the Western Hemisphere: two are nephrite (in Canada and the U.S.), and one is jadeite (in Guatemala). The Polar mine in northern British Columbia, Canada, produces an attractive translucent, bright, intense green nephrite that is reportedly harder than any other nephrite. It has found a market of its own because of its distinctive characteristics and beauty. The Blue Moon mine in California produces two beautiful varieties of botryoidal nephrite ("Mint in Snow" and "Blossom Jade") that are highly sought by collectors and jewelry manufacturers. "Galactic Gold" is the name given to a newly discovered black jadeite from Guatemala that has bright metallic inclusions of undetermined mineralogy (they may be pyrite). Worldwide, nephrite is much more abundant than jadeite.

The history and uses of jade, and the differences between nephrite and jadeite, are reviewed. Value factors for the different colors and physical properties (e.g., ability to take a good polish) of both types of jade are noted, along with the high esteem in which jade is held in Asia. A brief market overview is presented for all major nephrite and jadeite producing countries (China, Russia, Canada, U.S., Australia, New Zealand, Guatemala, and Myanmar).

It is encouraging that in this age of ever-diminishing deposits and reserves, a gem of such historical importance and renown continues to be discovered in exciting new forms. *JEC*

DIAMONDS

Of diamonds, dinosaurs and diastrophism: 150 million years of landscape evolution in southern Africa. T. C. Partridge, *South African Journal of Geology*, Vol. 101, No. 3, September 1998, pp. 167–184.

This article chronicles and interrelates the geomorphologic and geologic history of southern Africa starting with the breakup of Gondwanaland 150 million years ago, which led to the separation of Africa, South America, Antarctica, Australia, and India. At that time, southern Africa had a high elevation, but 1–3 km of the surface was subsequently eroded. Also, from 150 million years ago to the present, southern Africa has experienced extreme and/or rapid climatic changes (ranging from desert to tropical rainforest to grassland), fluctuations in sea level, volcanism (including two episodes of diamondiferous kimberlite emplacement at approximately 120 and 90–60 million years ago), and the enormous meteorite impact at the Cretaceous–Tertiary boundary that caused major extinctions of plant and animal life (most prominently the dinosaurs). During this time, the major rivers in southern Africa (Orange and Vaal) carried gem diamonds from their kimberlite hosts in the central part of South Africa to the sea.

Using details from all these geomorphic, geologic, climatic, and biological events, the continually changing landscape of southern Africa is reconstructed. One aim of this review is to explain and predict the locations of the important secondary (alluvial, beach, marine) diamond deposits of South Africa and Namibia. *AAL*

Diamonds from kimberlite diatreme 50, Liaoning Province, China: Microtextural, mineralogical, geochemical, and genetic characteristics. S. F. Vinokurov, A. I. Gorshkov, Y. N. Bao, I. D. Ryabchikov, L. V. Bershov, and M. I. Lapina, *Geochemistry International*, Vol. 36, No. 8, 1998, pp. 676–683.

Diamonds from pipe 50 in Liaoning Province show several textural, mineralogical, and geochemical features

related to their primary crystallization conditions and later explosive events that occurred in the lower part of the kimberlite diatreme. Of special interest are unique "inverse coated" diamonds, which have a transparent outer zone and a black inclusion-rich inner zone; normally, coated diamonds have the black inclusion zone on the outside. The black inclusion-rich zone contains a diverse population of submicron-size inclusions, including native metals, alloys, sulfides, oxides, chlorides, and the like. On the basis of the texture, composition, and inclusion distribution within the zones of an "inverse coated" diamond, the authors suggest that these diamonds most likely crystallized via "secretion" (i.e., from the outside inward). *TB*

Eclogitic diamond formation at Jwaneng: No room for a recycled component. P. Cartigny, J. W. Harris, and M. Javoy, *Science*, Vol. 280, No. 5368, May 29, 1998, pp. 1421–1424.

Geologists recognize two major groups of diamonds based on their distinctive mineral inclusions: peridotitic (P-type) and eclogitic (E-type). Diamonds of both types are generally believed to form in the earth's mantle, the P-type from mantle materials and the E-type as a consequence of the transformation of subducted biospheric carbon (i.e., a recycled organic component from the earth's surface). Support for the different origins is found in the carbon isotopic compositions ($\delta^{13}C$) of diamonds. P-type diamonds have a narrow "mantle range," ($\delta^{13}C$ = about –5‰), whereas E-type diamonds have a broad range ($\delta^{13}C$ = –34.5 to +2.7‰) that is characteristic of carbon compounds in the earth's near-surface environment.

Diamonds from Jwaneng, Botswana, contain small amounts of nitrogen (average 380 ppm) as is characteristic of E-type diamonds; based on a study of their nitrogen isotopic compositions ($\delta^{15}N$), the authors question the theory outlined above, at least for E-type diamonds from this particular locality. Specifically, the mean $\delta^{15}N$ value (–5.5‰) for Jwaneng E-type diamonds is essentially identical to that of P-type diamonds worldwide, but the authors believe that this value should be more positive if these diamonds crystallized from recycled carbon that originated from organic matter (which has a small nitrogen component).

The authors suggest that the carbon in E-type diamonds, like that in P-type diamonds, also comes from the mantle (and not from a recycled surface component). They believe that the broad range of $\delta^{13}C$ values in E-type diamonds is the result of a fractionation process of carbonatitic melts (involving such processes as the escape of CO_2), which undergo different evolutions before diamond precipitation when percolating through a peridotite or eclogite in the mantle. These different evolutions depend mainly on the presence or absence of olivine (in peridotite and eclogite, respectively), and can account for the respective $\delta^{13}C$ distributions. *AAL*

The Merlin kimberlites, Northern Territory, Australia. D. C. Lee, H. J. Milledge, T. H. Reddicliffe, B. H. S. Smith, W. R. Taylor, and L. M. Ward. In *Proceedings of the Sixth International Kimberlite Conference, Russian Geology and Geophysics*, Vol. 38, No. 1, 1997, pp. 82–96.

The Merlin field (10 × 5 km) consists of 11 diamondiferous kimberlites, which are located in four clusters in the Batten region of Australia's Northern Territory (about 800 km southeast of Darwin). The kimberlites were emplaced about 367 million years ago. They are all small (the largest is only 125 m in diameter), and all have a constant diameter to a depth exceeding 100 m. None of the kimberlites was exposed at the surface at the time of discovery.

The extensively altered kimberlite rocks are mainly diatreme-facies (that part of the pipe filled with angular broken fragments resulting from gaseous explosions), with some hypabyssal rocks (nonbroken kimberlite characteristic of the root zone). The trace-element chemistry resembles micaceous kimberlites and also some phlogopite lamprophyres (dark-colored, mafic intrusive igneous rocks) from the Kimberley region of Western Australia; their trace-element patterns are different from those of South African kimberlites or of the Argyle lamproite.

Chrome spinel, pyrope, chrome clinopyroxene (diopside), apatite, and sulfides were identified in heavy mineral concentrates of the kimberlites. Only limited information was available on the macrodiamonds, which occur in dodecahedral and resorbed shapes in about equal proportions. Most showed no visible evidence of plastic deformation. Microdiamonds (0.1–0.8 mm) were abundant; from a study of 40 samples, at least three different populations were defined based on nitrogen content and aggregation state: (1) predominantly type IaA and type IaAB, (2) type IIa (two microdiamonds), and (3) partially type Ib (one microdiamond). Three nitrogen-rich (>1,500 ppm N) microdiamonds had "exceptionally high" hydrogen contents (actual H content not stated), while the rest had no hydrogen. Carbon and nitrogen isotopes indicate that the microdiamonds originated by mixing between a mantle source of these elements and either a SiC-derived or a recycled crustal source. The abundance of twins and aggregates in the microdiamonds indicate that there was a plentiful supply of carbon in the source region. The diamonds were interpreted to have crystallized 1.65 billion years ago.

[*Editor's note:* The *1998 Annual Report of Ashton Mining Ltd.* (p. 10) states that mining operations at the Merlin Diamond Project commenced in November 1998, at the southern cluster of four kimberlites with an inferred resource base of 0.4 ct/tonne. The diamonds have a weighted average value of approximately US$75 per carat.] *MLJ*

The problem of the diamond potential of the northwestern Russian Plate. A. A. Konstantinovskii and T. E. Shcherbakova, *Lithology and Mineral Resources*, Vol. 33, No. 3, 1998, pp. 226–234.

A potential new diamond-producing region has been recognized in Russia. Located in the "Latvian Saddle," on the northwestern part of the Russian Plate, it is centered in the vicinity of Borovichi (about halfway between St. Petersburg and Moscow). Although kimberlite pipes have not been located, a few octahedral diamonds and numerous kimberlite indicator minerals—mainly pyrope garnet, but also chrome spinel and picroilmenite—have been found in alluvium and stream sediments in the region.

The diamond indicator minerals have been traced to two specific Devonian and Lower Cretaceous sedimentary formations (secondary sources), in which they occur as accessory heavy minerals. These heavy minerals arrived at their present sites as a result of the weathering of a primary (presumably kimberlite) source that has yet to be found. By plotting the distribution of the indicator minerals in alluvium and in stream sediments eroded from the sedimentary formations, and determining that these minerals did not travel far from either their primary or secondary sources, geologists have identified a relatively small potential kimberlite area (the Borovichi Uplift). The favorable potential of this area is confirmed by geophysical data (e.g., the earth's crust is thick in this area, and basement faulting is present) and geologic features (e.g., an Archean-age basement, regional folding, and local dome-shaped uplift).

AAL

Rare and unusual mineral inclusions in diamonds from Mwadui, Tanzania. T. Stachel, J. W. Harris, and G. P. Brey, *Contributions to Mineralogy and Petrology*, Vol. 132, No. 1, 1998, pp. 34–47.

Diamonds form in the earth's mantle and have a complex history of crystallization. Mineral inclusions in diamonds can give insight into the conditions under which the diamonds formed. One hundred diamonds from the Mwadui mine in Tanzania were crushed, and 91 of these yielded inclusions that were analyzed for geochemical data. Most of the inclusions were minerals common in the upper mantle, such as olivine, garnet, and pyroxenes. However, rare mineral inclusions also were found, such as ilmenite with an unusual chromium content, magnetite with a silicate exsolution phase, native iron, and dolomite.

The associations of minerals that formed under different conditions in the same diamond suggest to the authors that strong and variable geochemical compositional gradients were present during diamond formation at Mwadui. Different oxidation states of coexisting iron minerals (magnetite, wüstite, and native iron) imply that the diamonds grew along oxidation boundaries. On the basis of these data, the authors conclude that the Mwadui diamonds formed from carbon that was released from methane-rich gas phases during mantle recrystallization and mineralogic changes. *JL*

A rift model for the sedimentary diamond deposits of Brazil. R. Fleischer, *Mineralium Deposita*, Vol. 33, 1998, pp. 238–254.

Essentially all the diamonds found in Brazil are secondary in origin, obtained from either diamond-bearing conglomerates or recent alluvials derived from them; their primary sources have never been found. Although several hundred kimberlites have been discovered within the Brazilian diamond districts in recent years, almost all are barren and thus cannot be the primary diamond source. In this article, a new "rift model" proposes where the diamond-bearing rocks (presumably kimberlites) may have been emplaced and why they have not been found.

The model is based on the observation that although the diamond-bearing conglomerates are of four vastly different ages (Proterozoic, Devonian, Carboniferous, and Cretaceous), they all have geologic features in common that have recurred through time. First, the diamond-bearing conglomerates are always found in small graben-like troughs (basins) formed during successive rifting events. Second, a short transport distance is inferred for the conglomerates, and the diamonds occur above the basal member of each sequence (i.e., diamond deposition took place after each basin formed). Therefore, the volcanic events are adjacent to the faults that form the basins. Third, volcanic debris in the sedimentary sequences indicates that, for the most part, volcanic events (including possible emplacement of kimberlites or lamproites) occurred after the rifting.

These general observations link diamond-bearing volcanic sources to rift basins. The diamond-bearing kimberlites proximal to the basins supplied diamonds to the conglomerates within the basins and, in the process, have been eroded or buried by post-rift material. Those noneconomic kimberlites that have been found are farther from the basins and probably represent different volcanic events. *AAL*

Unusual upper mantle beneath Guaniamo, Guyana shield, Venezuela: Evidence from diamond inclusions. N. V. Sobolev, E. S. Yefimova, D. M. DeR. Channer, P. F. N. Anderson, and K. M. Barron, *Geology*, Vol. 26, No. 11, 1998, pp. 971–974.

The mineral inclusions in industrial-quality diamonds from alluvial and primary deposits of the Guaniamo region of Venezuela were examined to study the environments of diamond genesis. Diamonds form deep beneath the continental lithosphere in the mantle, which has different zones with distinct mineralogies. Populations of diamonds mined from any one region will have a dominant proportion of crystals from one mantle source over another. Most of the diamond occurrences in

the world are associated with a peridotite mineralogy, which includes such minerals as olivine and pyroxenes. In some locales, mineral inclusions and source rock characteristics suggest an eclogite source, with a mineralogy that includes omphacite (a clinopyroxene) and pyrope garnet.

During this study, the existence of transparent garnet and clinopyroxene inclusions, as well as opaque sulfides and other minerals, was microscopically established in 329 alluvial and 53 kimberlite diamonds. The chemistry of inclusions extracted from 124 alluvial and 53 kimberlite diamonds was measured by electron microprobe analysis. The authors determined that 99% of the diamonds were eclogitic. The coexistence of coesite (a high-pressure quartz polymorph) and corundum, combined with the variability of the garnet and clinopyroxene compositions, suggests a highly variable source composition. The unique characteristics of the Guaniamo diamonds and associated rocks imply that the mantle source under the Guyana shield in Venezuela has an unusual composition. *JL*

Why pink diamonds are special. R. Weldon, *Professional Jeweler*, Vol. 1, No. 11, December 1998, p. 22.

Although Australia's Argyle mine is the most consistent producer of pink and red diamonds, these gems are by no means plentiful. Only some 700 carats (rough) out of the millions of carats mined each year from Argyle qualify as "pinks" or "reds." Fancy pink diamonds were once reserved for royalty, but now anyone who can afford the price—some polished stones sell for hundreds of thousands of dollars per carat—has the opportunity to acquire one. The origin of the pink and red colors is a mystery, although in the book *The Nature of Diamonds*, Dr. Emmanuel Fritsch suggests that "the color is due totally or in part to a color center resulting from deformation." The supply of pink diamonds is decreasing, in spite of the recent decision to continue mining at Argyle. *MM*

GEM LOCALITIES

Arizona andradite debuts. *Jewelers' Circular Keystone*, Vol. 169, No. 12, December 1998, p. 28.

Fine-quality andradite garnet, including a limited amount of demantoid, is being mined near San Carlos, Arizona. The recently discovered deposits are located near the well-known peridot mines; they are mined by hand, as the gems are found near the surface. The andradite ranges from golden yellow to greenish yellow to reddish brown. Compared to the highly regarded Russian demantoid, the Arizona material has lower saturation, attributed to its lower chromium content, but also higher dispersion. Similarly, the other colors of andradite from this locality are not overly saturated and also are highly dispersive. Thus far, the San Carlos production has yielded only small faceted gems that have been used as side stones to accent larger gems. *MM*

City of pearls. L. Werner, *Aramco World*, Vol. 49, No. 5, September/October 1998, pp. 10–19.

Founded in 1591, Hyderabad has been India's pearl-trading capital for more than 400 years. The city developed and sustained a robust jewelry industry to support the formidable demands of the wealthy dynastic rulers. From the early 18th century until 1948, when the last ruler was forcibly removed from power by the Indian army, untold quantities of gems and pearls passed through Hyderabad's jewel shops on Patthargatti Road. Although the formerly important diamond trading center at Golconda is only 12 miles (20 km) away, pearls have left the boldest mark on Hyderabadi culture and trade over the years. Today it is the city's pearl merchants who occupy premier positions in the jewelry industry.

Hyderabad is an unlikely candidate to be at the center of the pearl trade. The ocean is 200 miles distant and, commercially speaking, the city is less advanced than, say, Bombay or Bangalore. One local jeweler attributes Hyderabad's position to "the high quality and low cost of labor." Indeed, behind almost every door on Patthargatti Road there are pearl sorters, drillers, and stringers, each with hundreds of years of family experience. This cumulative experience in the pearl trade has firmly established Hyderabad as India's city of pearls. *SW*

Contribuição ao estudo mineralógico dos cristais de esmeralda do distrito mineiro de Campos Verdes, Estado de Goiás [Contribution to the mineralogical study of emerald crystals from the Campos Verdes mining district, Goiás State]. G. M. Pulz, T. M. M. Brum, P. L. Juchem, L. J. H. DeR. Silva, L. B. Neto, and P. Barreto, *Pesquisas*, Vol. 25, No. 2, 1998, pp. 11–19 [in Portuguese with English abstract].

Five emerald crystals from the Campos Verdes mining district in Brazil were analyzed by inductively coupled plasma mass spectrometry (ICP-MS) and Fourier-transform infrared (FTIR) spectroscopy. The samples contained relatively high Fe (e.g., 1.77 wt.% Fe_2O_3 and 0.25 wt.% FeO) and high weight loss on ignition (2.92–4.62 wt.%), and low alkali contents (with Na>>Cs>Li). The FTIR spectra indicate type-II H_2O vibrations. By combining the chemical data with optical and physical properties, and comparing these to published literature, the authors were able to distinguish these Campos Verdes emeralds from those of the Swat district (Pakistan), Franqueira (Spain), Itabira (Brazil), and Colombia, as well as from synthetic emeralds. *RAH*

Compositional variation of tourmaline in the granitic pegmatite dykes of the Cruzeiro mine, Minas Gerais, Brazil. M. Federico, G. B. Andreozzi, S. Lucchesi, G. Graziani and J. César-Mendes, *Canadian Mineralogist*, Vol. 36, Part 2, 1998, pp. 415–431.

The complex granitic pegmatite dikes of the Cruzeiro mine contain several species of tourmaline (schorl, dravite, and elbaite) in well-defined zones. Because of its

sensitivity to the concentrations of Fe, Mg, Al, and Mn in the melt, tourmaline can be used as a recorder of the internal evolution of granitic pegmatites. Thus, differences in the chemical compositions of the tourmalines found at Cruzeiro enabled the authors to reconstruct the various stages in the crystallization of the pegmatite dikes.

The evolutionary features shown by the compositions of these tourmalines suggest the following: (1) Al was abundant in the melt; (2) Mg, Fe, Zn, Mn, and Li each reached their maximum concentrations at different stages of pegmatite evolution; and (3) there was a limited amount of F in the volatile phase and in the melt. The removal of large amounts of boron from the melt is responsible for the formation of tourmaline-rich pockets and the late crystallization of OH-rich tourmaline.

TB

Gem corundums and zircons from the Primorye placers. S. A. Ananyev, T. A. Ananyeva, V. K. Garanin, and G. P. Kudryavtseva, *Proceedings of the Russian Mineralogical Society*, Vol. 127, No. 4, 1998, pp. 120–124 [in Russian with English abstract].

Descriptions are given of gem-quality sapphire and "hyacinth" zircon—and the associated chrome spinel, magnetite, and enstatite—found at Primorye in heavy-mineral concentrates that were ultimately derived from alkali basalts. Transparent blue, blue-green, green, and occasional multicolored sapphires are found as rounded pebbles (2 to 30 mm in size); some star sapphires are recovered. Chemical analyses and visible absorption spectra show that the sapphire coloration is related to the presence of Fe (0.72–1.75 wt.% FeO) and Ti (0.02–0.20 wt.% TiO_2). Inclusions of hercynite and ferrocolumbite were identified in some of these corundums.

The zircon also is found as rounded pebbles (1 to 25 mm in size). They are transparent orange, orange-yellow, or brown-red, and become colorless on heating. Their chemical compositions correspond to those of the rare zircon variety naegite, with 4.59–6.14 wt.% Ta_2O_5, 3.22–3.59 wt.% Nb_2O_5, and 3.98–4.09 wt.% ThO_2. [*Editor's note:* The terms *hyacinth* and *naegite* are not used in most modern gemology and mineralogy references in English.] *RAH*

Gemstones of New England. G. B. Webb and F. L. Sutherland, *Australian Journal of Mineralogy*, Vol. 4, No. 2, December 1998, pp. 115–121.

Brief details are given of the occurrence of diamond, sapphire, beryl, topaz, quartz, garnet, zircon, feldspar, rhodonite, nephrite, peridot, and fluorite from this area of northeastern New South Wales. More than 500,000 carats of diamonds have been produced, and two distinct categories are recognized: (1) yellow, rounded crystals with a high, uniform nitrogen content; and (2) white, internally complex crystals with low, variable nitrogen content. Most of the diamonds have been substantially resorbed; with cathodoluminescence, one showed octahedral growth zones on a resorbed surface. Fine blue sapphires are produced with a medium to dark hue, but greenish blue, yellow, and green varieties also are found; color zoning down the c-axis is a prominent feature. Beryl with emerald "stripes" perpendicular to the c-axis is illustrated. Colorless (rarely blue) topaz occurs in alluvium derived from the granitic rocks of the area. Zircon—in yellow, brown, and pink—is derived from basalts and often is encountered in the sapphire workings. *RAH*

A note on Buttala and Okkampitiya gem fields in Sri Lanka. R. Chandrajith, C. B. Dissanayake, and H. J. Tobschall, *Zeitschrift der Deutschen Gemmologischen Gesellschaft*, Vol. 47, No. 2, June 1998, pp. 69–76 (in English with German abstract).

The adjacent Buttala and Okkampitiya gem-producing areas in southeastern Sri Lanka are relatively small and have received little geologic or mineralogic attention. Geologically, they are located near the boundary between two metamorphic terrains, the Highland-Southwest Complex (which contains most of the gem deposits in Sri Lanka) and the Vijayan Complex. This preliminary report indicates their present gem production and future potential.

Both areas produce a wide variety of fine-quality gems, including blue, yellow, and pink sapphires, as well as spinel, hessonite and other garnets, and tourmaline. There is also some geuda (heat-treatable) sapphire. The gems are mined from "residual" deposits that are characterized by layers of alternating sands, clays, and laterites containing large boulders of marble. The authors note that expansion of mining activities for such residual deposits has increased the damage to forest reserves on the island. *MM*

Philippine pearl report: The Philippines gathers strength for 21st century. B. Sheung, *Jewellery News Asia*, No. 169, September 1998, pp. 112–122 passim.

Mastery of oyster hatchery techniques should allow Philippine cultured pearl producers to increase their annual volume from the present estimate of 100–150 kan to more than 200 kan by the year 2000 [1 kan = 1,000 momme; 1 momme = 3.75 grams]. Of the 23 pearl farms in the Philippines, most of which are in Palawan Province, 15 are of commercial scale. Neither the number of farms nor the number of pearls cultivated is restricted by the government.

The cultivation period for Philippine South Sea pearls ranges from 18 to 24 months. Sizes range from 9 to 16 mm, with most falling between 10 and 12 mm. Colors "vary from silver, white, cream, champagne to golden" for pearls from white-lipped oysters, and "blue to black" for pearls from black-lipped oysters.

A prominent pearl industry figure predicts that South Sea cultured pearls, including those produced in the Philippines, will play a major role in the jewelry scene in the 21st century. *Doug Fiske*

Polar jade. F. Ward, *Lapidary Journal*, Vol. 52, No. 8, November 1998, pp. 22–26.

The Canadian province of British Columbia is the world's largest supplier of nephrite, and it has huge reserves. Geologically, British Columbia's nephrite is found in association with serpentinite. At present, the two major producing mines are Kutcho and Polar, located about 25 miles (40 km) apart east of Dease Lake in the northern part of the province. Current annual production from each mine is about 80 tons. Nephrite from each mine is characteristic, with that from the Polar mine being particularly desirable because it is brighter green (highly saturated) in color, more translucent, and somewhat "harder" than Kutcho nephrite. Boulders as large as 20 tons have been found recently at the Polar mine.

Both mines are owned by Kirk Makepeace, who currently produces about 85% of the world's gem-quality nephrite. Since entering the business in about 1980, he has sold approximately 2,400 tons of material. During the last decade, the main market for nephrite has shifted from Taiwan to China, where it is used for souvenir carvings and inexpensive jewelry. Rough nephrite currently sells for a few dollars a pound. *MM*

Ruby-bearing mineralization in Sljudjansky complex of the south-western Baikal region. V. I. Levitsky and L. A. Pavlova, *Proceedings of the Russian Mineralogical Society*, Vol. 127, No. 6, 1998, pp. 84–88 [in Russian with English abstract].

Ruby-bearing rocks are hosted by dolomite marbles in two separate areas of the Sljudjansky complex in Siberia. Near the town of Sljudjanka, corundum has been found locally within zoned magnesian skarns, where it is associated with forsterite, spinel, phlogopite, amphibole, and calcite. Two varieties of corundum are recognized: (1) translucent pink and grayish pink, and (2) "water-clear" pink and ruby-red. In the Tunkinsky district (Buryat Republic), corundum-bearing rocks occur as vein-like and pocket-like bodies with rare disseminated forsterite, red and pink spinel, and "water-clear" pink and red corundum. At both localities, the spinel is characterized by low amounts of iron and appreciable Cr_2O_3 and V_2O_3 contents. Electron microprobe analyses are reported for 10 spinels, five rubies (Cr_2O_3 0.01–0.22 wt.%, TiO_2 0.01–0.08 wt.%, V_2O_5 0.01–0.15 wt.%), and a single phlogopite sample. In general, the ruby mineralization is related to postmetamorphic alteration of the precursor skarns and calc-silicate rocks by deep (mantle) fluids. *RAH*

INSTRUMENTS AND TECHNIQUES

Fourier transform-Raman spectroscopy of ivory: A nondestructive diagnostic technique. H. G. M. Edwards, D. W. Farwell, J. M. Holder, and E. E. Lawson, *Studies in Conservation*, Vol. 43, No. 1, 1998, pp. 9-16.

Because of the declining elephant population and the resultant worldwide ban on trade in elephant ivory, it is essential to distinguish nondestructively between true elephant ivory and non-elephant ivory. Fourier transform-Raman (FT-R) spectra obtained from seven African elephant tusks seized by British Customs in London were identical, regardless of the color of the ivory or the age of the elephant from which the tusks were obtained (i.e., the spectra are not subject to intra- or inter-tusk variations). Spectra were also obtained for ivory from an Asian elephant and from the extinct woolly mammoth, as well as for non-ivory samples of human and animal origin (including an adult incisor tooth and an animal bone). Characteristic vibrational features were found that enabled each ivory and non-ivory sample to be identified by its FT-R spectrum. Thus, FT-R spectroscopy is a viable and nondestructive technique for distinguishing genuine elephant ivory from specific regions (Africa and Asia) from other types of ivory (woolly mammoth) and from imitations. At present, this type of identification is not achievable by any other method. For large samples that cannot be accommodated in the FT-R instrument, a remote sensing probe (1 m long) was adapted successfully. *MM*

JEWELRY HISTORY

Fabulous fakes. L. Grant, *Antiques & Collecting*, Vol. 103, No. 12, February 1999, pp. 38-43.

The use of fakes or costume jewelry as inexpensive alternatives to fine jewelry dates back to the ancient Egyptians, who first coated glass beads to make them resemble precious stones. Subsequent milestones include the production of glass beads in Czechoslovakia in the 14th century and the advent of a clear glass known as "cristallo" (crystal) in the 15th century, at a locality near Venice. In 18th century France, George Stras developed a high-quality lead glass known as "paste" or "rhinestones," which he cut and set into spectacular jewelry creations. Late in the 19th century, Swarovski produced small "brilliant-cut" crystal "stones" of exceptional quality; the company remains the premier manufacturer of crystal used by costume jewelers today. During the same era, René Lalique created imaginative pieces using colored stones and a variety of unusual materials, including plastic.

The golden era of costume jewelry was between 1930 and 1970, with fashion designers such as Schiaparelli and Coco Chanel developing their own styles. Whereas Schiaparelli captured the market with unexpected and humorous pieces (including earrings shaped like telephones and bracelets made with porcelain vegetables), Chanel's fashions reflected timelessness and elegance. She broke all conventions by mixing real gem materials with fake ones and made it acceptable to wear jewelry on informal occasions. Today, Coco Chanel's stylish designs continue to look contemporary, and they are widely sought by collectors. Other designers who have embraced costume jewelry include Miriam Haskell, Cartier, Trifari, Christian Dior, Yves Saint Laurent, and Donna Karan. While costume jewelry was first accepted in Europe, it

became a thriving industry in the U.S., where it was sold at boutiques and department stores. Vintage costume jewelry pieces produced during the 20th century are now collectibles, although early examples of Schiaparelli, Chanel, and Haskell are difficult to find. *MD*

René Lalique, Art Nouveau genius. C. L. E. Benesh, *Ornament*, Vol. 22, No. 2, Winter 1998, pp. 71–74.

René Lalique (1860–1945) was one of the world's greatest Art Nouveau jewelry designers. This article chronicles the development of Lalique's career, as well as the Art Nouveau artistic movement. This design style of the late 19th century was characterized especially by winding lines and foliate forms.

After an apprenticeship to a Paris goldsmith at the age of 16 and additional studies in London, Lalique returned to Paris as a designer and freelance illustrator. His creativity exploded in 1885, when he purchased his own studio and progressed from design to jewelry making. Within a few years, his creations—which emphasized nature and femininity— were being avidly collected by wealthy aristocrats and celebrities. Lalique's stature as a great artist was sealed after an astonishing display at the Universal Exhibition in Paris in 1900. Because his pieces emphasized the beauty of the design over the intrinsic value of the materials in which the design was executed, he championed the use of inexpensive gem materials such as amber, ivory, horn, opal, and carnelian. He also made exquisite use of glass and enamel. Art Nouveau achieved prominence in the 15-year period from 1895 to 1910. In 1912, Lalique abandoned jewelry altogether and devoted himself entirely to glass. *MM*

JEWELRY MANUFACTURING

Thermal and microchemical characterisations of $CaSO_4$-SiO_2 investment materials for casting jewellery alloys. G. M. Ingo, G. Chiozzini, V. Faccenda, E. Bemporad, and C. Riccucci, *Thermochimica Acta*, Vol. 321, No. 1/2, 1998, pp. 175–183.

The decomposition of calcium sulfate in the commonly used calcium sulfate-silica ($CaSO_4$-SiO_2) investment (an "investment" is a material, such as plaster of paris, that is used in casting gold-based alloys in jewelry) method can cause what is known as the gas porosity defect. This defect, seen in gold alloy jewelry as tiny surface pores, can reduce the value of the piece. The authors simulated numerous temperature and atmosphere (e.g., air, argon) casting conditions to assess the potential for $CaSO_4$ decomposition.

The decomposition temperature of pure anhydrous $CaSO_4$ determined in this study ranged from 1240° to 1450°C. In conjunction with silica, the decomposition temperature was lowered to a range of 990° to 1260°C. The decomposition temperature is lowered further in reducing or inert atmospheres, or with oxides of other alloy metals, especially Cu_2O and ZnO. Since the melting temperature of commercial gold alloys ranges from 960° to 1200°C, the authors suggest that decomposition of $CaSO_4$ in the $CaSO_4$-SiO_2 investment method is a valid concern. *JL*

JEWELRY RETAILING

Consumers seek gems that change colors. C. Fenelle, *National Jeweler*, Vol. 42, No. 22, November 16, 1998, pp. 16, 18.

Color-change gemstones are experiencing an increase in popularity, especially as color-change synthetics become more available. The most popular are alexandrite, sapphire, and garnet. The most valuable color-change stones are those in which the change is to a completely unrelated color, such as from red to blue or green, when viewed with fluorescent (sun) versus incandescent light. The attractiveness and saturation of each color are also factors that should be considered. Many gemstones commonly show a slight difference in color when examined under different lighting conditions, an effect known as metamerism. Such stones have been labeled as "color-shift," but they do not justify a premium over their regular gem counterparts. *MD*

Designing a successful business. M. Z. Epstein, *American Jewelry Manufacturer*, Vol. 43, No. 6, June 1998, pp. 40–43, 45–48.

Jewelry designers may get noticed for their artistic talent, but their companies grow only when they combine artistic skills with financial planning and acumen. This article presents seven ways to turn a design shop into a successful business:

1. *Be nice to people.* The importance of interactions with manufacturers, other designers, and retailers is often underestimated. As much as their jewelry, it is the artists themselves who are on display anywhere they meet other professionals or the public.
2. *Do your market research.* Knowing what customers want is critical. A large component of market research is determining customer demographics. Such information can help you choose the materials for designs, and possibly the way you design.
3. *Pinpoint profitable price points.* Jewelry has to be sold at a profit, which means that the pricing must be correct. This requires accurate knowledge of material, manufacturing, and overhead costs. The suggested retail selling price of custom jewelry is 1.5–2.5 times total costs; for designer jewelry, the factor is 2.2–3.0.
4. *Give your jewelry "wow" power.* Educating retailers to be enthusiastic about your jewelry is necessary to increase sales. This is accomplished in several ways, such as using a combination of rare stones in designs, or creating pieces with cultural significance.
5. *Build a cohesive image.* Name recognition is crucial for developing a cohesive image. Press releases are a good first step. Establishing a working relationship with editors of trade and consumer publications, attending trade

shows, and using direct mail for niche markets are three more ways to build an image.

6. *Hire and keep good employees.* Hiring the best people, treating them well, and giving them the skills they need (whether it be order filling or selling) will be profitable in the long term.

7. *Develop a business plan.* Financial consultants can be of great value in assisting with a business plan. There is no substitute for professional advice from someone experienced in business, especially "your" business.

Lorrie Ames

Fixed flaws. D. A. Yonick, *American Jewelry Manufacturer*, Vol. 43, No. 9, September 1998, pp. 62–69, 71, 73.

Today's gemstone treatments enhance clarity, increase durability, reduce porosity, improve and stabilize color, and produce colors not found in nature. There is nothing wrong with using treatments to improve on or fix what nature has produced, provided consumers are advised of the enhancements and their stability/durability characteristics. This article admonishes jewelry manufacturers to require full disclosure of treatments from their suppliers and to pass this information along to retailers, who ultimately inform the consumers.

To help the manufacturer understand the most common treatments being used today, this article explains the following terms: heat treatment, irradiation, diffusion treatment, fracture filling, infilling, stabilization, oiling, impregnation, infusion, lasering, bleaching, dyeing, and coating. Examples of each process are given, along with the gemstones that are likely to be enhanced by that process, the improvement that usually results, and the stability or durability of each enhancement. *MD*

Technology and the retail jeweller. J. Lawrence, *Diamond International*, No. 55, September/October 1998, pp. 67–68.

Many consumers are confused by the subtle differences in the "4Cs" that affect the price of diamonds. To explain these differences and instill confidence in the jeweler's explanations, affordable instrumentation is readily available to jewelers. In the hands of trained staff, these instruments are very effective.

The microscope is the essential instrument, and recently it has become especially important for reading laser-inscribed certificate numbers. A TV camera attachment enables the retailer to explain clarity, at least in qualitative terms. Effective for unmounted stones are TV image processing systems, such as the "Brilliant-Eye" produced by Sarin, which measure the proportions of a polished stone and compute its weight to within 0.01 ct (1 pt). Some of them also have the ability to print a customized certificate with a proposed cut grade. Color also can be graded by attaching a colorimeter to a port on some proportion machines. It is reported that such systems are selling at a rate of more than one a day in the U.S.

These instruments appear to have great appeal to the public because "seeing is believing." From the jeweler's perspective, they can support or verify a certificate at the retail counter. *AAL*

12 hot tips: The inside scoop on what consumers want to see. R. Weldon, *Professional Jeweler*, Vol. 1, No. 11, December 1998, p. 87.

A prominent New York jeweler predicts increased demand for: (1) yellow gold jewelry; (2) unusual colored stones (e.g., fire opals and brown- or gray-colored gems to harmonize with clothing fashions); (3) fancy colored diamonds—especially pinks and yellows; (4) bold and geometric shapes—particularly chunky pieces in yellow gold; (5) fancy cut diamonds (e.g., oval, emerald, princess, star); (6) solitaire diamond jewelry; (7) pearls—especially cultured Tahitian black pearls and pearl solitaires; (8) antique appearance in jewelry—specifically, delicate and feminine pieces in platinum and white gold set with diamonds and colored gems; (9) romantic and colorful nature-inspired pieces (e.g., dragonflies and butterflies); (10) well-made charms accented with diamonds; (11) diamonds, pearls and other gems set in white or yellow gold, and suspended from clear "invisible" filaments; and (12) wrap necklaces with exotic colored gems (e.g., apatite and tanzanite). *MM*

PRECIOUS METALS

A sterling moment for silver. C. Soucy, *National Jeweler*, Vol. 42, No. 13, July 1, 1998, pp. 28, 30, 32–33.

The growing popularity of white metals has stimulated the sales of platinum, white gold, and sterling silver. Sixty million pieces of silver jewelry were sold in 1997. A longtime favorite in boutiques and fashion-oriented retail stores, sterling silver jewelry now appears alongside platinum and gold jewelry at the high-end jewelry stores. Lower-priced pieces targeted to the teen market are also selling well. The hottest item in white metals is neckwear—especially chokers—followed by earrings, rings, and bracelets. Silver is easily worked into intricate filigree and cut-out designs, and it offers the option of using its oxidation characteristics in the creation of designs. Because it is lighter than platinum or gold, larger pieces can be designed (especially earrings), without the added weight. *MD*

SYNTHETICS AND SIMULANTS

China company produces hydrothermal rubies. *Jewellery News Asia*, No. 169, September 1998, p. 50.

Hydrothermal synthetic rubies marketed under the name "JL synthetic rubies" are available from Guangxi Jewelry Co. Ltd. in Guilin, China (Guangxi Province). The material ranges from red to orange-red in color, with some displaying purple hues. The synthetic rubies fluoresce strong red to long-wave ultraviolet radiation; the fluores-

cence is less intense to short-wave UV. Colorless "net-like" inclusions are reported. The synthetic rubies have R.I. values of 1.759–1.769, and an S.G. of 4.01. They are incorporated into gold rings, pendants, earrings, and bracelets. *MM*

Growth conditions and real structure of synthetic diamond crystals. Y. N. Pal'yanov, A. F. Khokhryakov, Y. M. Borzdov, A. G. Sokol, V. A. Gusev, G. M. Rylov, and N. V. Sobolev, *Russian Geology and Geophysics*, Vol. 38, No. 5, 1997, pp. 920–945.

This comprehensive article describes the growth of synthetic diamond crystals at the Institute of Mineralogy and Petrography in Novosibirsk, Russia. The authors are leading researchers in the area of diamond synthesis at high temperatures and pressures using the multianvil apparatus (also known as the "split sphere" or "BARS" apparatus). Synthetic diamond crystals have been produced at this institute since the early 1990s.

The article begins with a review of the ways to grow single-crystal synthetic diamonds, and explains details of the growth of crystals from a molten metal alloy flux by the temperature-gradient method. The types of inclusions and other kinds of growth defects, as well as the crystal shapes and surface features of these synthetic diamonds, are described and photographically documented. Last, the article reviews the physical conditions under which the various diamond types (e.g., type Ib, type IIa, etc.) are produced. An extensive reference list is provided. *James E. Shigley*

TREATMENTS

Behandlung natürlicher Diamanten zur Reduzierung der Gelb- oder Braunsättigung (Treatment of natural diamonds in order to reduce the yellow or brown color saturation). K. Schmetzer, *Goldschmiede Zeitung*, Vol. 97, No. 5, May 1999, pp. 47–48 [in German].

This brief article, written for a German trade journal, identifies nine patents that involve changing the color of diamond. These U.S. patents (4,124,690; 4,174,380; 4,399,364; 5,523,071), as well as German (2 732 793), European (0 014 528; 0 638 670; 0 668 377), and Japanese (63-291895) published patent applications, all available publicly, are from the period 1978–1996, and involve research work on both natural and synthetic diamonds. They were filed by General Electric Company, De Beers Industrial Diamond Division (Pty.) Ltd., and Sumitomo Electric Industries Ltd. The General Electric patents describe treatments at high pressure and high temperature, whereas the De Beers and the Sumitomo patents describe two-step treatment processes: (1) irradiation and (2) high-pressure and high-temperature annealing. The experimental conditions outlined in these documents show that atomically dispersed nitrogen atoms (i.e., type Ib) are forced to migrate and form clusters or aggregates (i.e., type Ia), thereby reducing the influence of the color-causing (yellow or brownish yellow) type Ib nitrogen atoms. Although other decoloration mechanisms (e.g., for brown diamonds) are imaginable, they are not discussed in these patent documents.

This article is a response to the recent announcement by Lazare Kaplan International Inc. of a new General Electric "process" that improves the appearance of certain (presumably brown) natural diamonds. This announcement, along with uncertainties regarding the identification and disclosure of GE-processed diamonds, have produced great concerns in the jewelry trade. While GE has not revealed the details of their process, the patents cited here suggest that various kinds of color change can be produced by treating natural diamonds at high temperatures and pressures. *James E. Shigley*

Belgium diamond report: Enhancing low quality coloured diamonds. *Jewellery News Asia*, No. 169, September 1998, pp. 320, 322.

Russian scientists are using BARS-autoclave technology to enhance the color of low-quality, fancy-color diamonds. The treatment involves hyperbaric heating (i.e., at pressures high enough to prevent conversion from diamond to graphite). The effect of the heating on color depends on two factors: the original color of the diamond and the duration of treatment, which determines the number of former color centers that are destroyed and replaced by new ones.

Characteristics of these treated fancy-colored diamonds include: a greenish overcast effect visible in daylight; a strong green fluorescence related to growth lines; color zoning; greenish, yellowish, or brownish body color; prominent graining; cracks and cleavages at the rim of the table and around the girdle; and corrosion marks, particularly around the girdle. Photos of treated diamonds showing many of these characteristics are provided. *MM*

Ein neuer Typ farbbehandelter Diamanten (A new type of colour-treated diamonds). U. Henn and C. C. Milisenda, *Zeitschrift der Deutschen Gemmologischen Gesellschaft*, Vol. 48, No. 1, 1999, pp. 43-45 [in German with English abstract].

A new type of color-treated greenish yellow to brownish yellow fancy-color diamond, with a saturated yellow body color and a strong green fluorescence partly related to growth lines, is described. Other identifying features seen under magnification include strong graining, fine cracks and cleavages under the table and at the girdle, as well as burn marks. The absorption spectrum shows lines at 415, 495, 503, and 985 nm, and a broad band between 450 and 500 nm; this spectrum is distinctly different from natural colored or irradiated diamonds of these colors. An important feature of these heat-treated diamonds is their fluorescence to long-wave ultraviolet radiation. Natural-color greenish yellow diamonds have a chalky

fluorescence, whereas these diamonds show a mixture of greenish yellow and blue fluorescence, with distinct green fluorescing zones following growth lines.

These diamonds were initially offered as Russian treated synthetic diamonds, but a closer investigation revealed that they are natural diamonds that obtained their enhanced color through a special heat treatment process at high temperature and pressure that uses the Russian BARS system (a belt-type apparatus normally used in the production of synthetic diamond). The raw material consists mainly of low-quality diamonds from the Argyle mine (Australia), but diamonds from Russian and Central African sources are used as well. [*Editor's note:* Similar color-treated yellow diamonds were described in the Summer 1997 Gem Trade Lab Notes, p. 136.] *PRB*

Observation of the H2 defect in gem-quality type Ia diamond. P. R. Buerki, I. M. Reinitz, S. Muhlmeister, and S. Elen, *Diamond and Related Materials*, Vol. 8, No. 6, 1999, pp. 1061–1066.

The authors define "H2 diamonds" as diamonds with a 986 nm absorption band. They typically have a greenish yellow, yellow, or brownish orangy yellow color and show strong green luminescence to visible light, associated with brownish yellow graining, and "burns" on the surface and in fractures. Other absorption bands include H3 (503 nm) and H4 (496 nm). The vast majority of H2 diamonds are treated, having been produced from natural type Ia diamonds (probably brownish hues) by a new process that most likely consists of irradiation with high-energy electrons, followed by high-temperature (about 1,400°C) heating in air, possibly at a stabilizing pressure of about 5 GPa. About 50 such diamonds were received at the GIA Gem Trade Laboratory (GTL) in a one-month period in 1996, and since then another 100 have been seen and characterized at GTL. Natural type Ia diamonds with the same or similar colors and luminescence and a 986 nm (H2) band are suspected to be very rare (only 11 had been identified by GTL in the previous 12 years) and are possibly formed when type Ia diamonds are subjected to natural radiation and temperatures above 1,000°C. The distinction between diamond with natural H2 characteristics from those described herein is extremely difficult, and is dependent on such features as a very low intensity 986 nm band, or evidence of laboratory treatment (e.g., burn marks, certain IR absorption bands).

Out of a total of 510 greenish yellow diamonds with green luminescence examined at GTL in the last 12 years, 90 showed all the typical characteristics of H2 diamonds *except* the H2 band. This raises the question: Does a method exist to destroy the H2 center after its formation? If possible, such a method would have major implications for determining whether any specific diamond owes its color to natural or artificial processes. [*Editor's note:* Many questions about color-treated greenish yellow diamonds remain unanswered. The previous two abstracts report on similar (probably identical) material and illustrate the importance of this topic.] *AAL*

MISCELLANEOUS

Reach for the sky. M. Z. Epstein, *American Jewelry Manufacturer*, Vol. 43, No. 10, October 1998, pp. 57–65.

Jewelry manufacturers, like other workers subject to repetitive stress injuries, are aggressively taking steps to apply the science of ergonomics (the study of human abilities and characteristics) to eliminate workplace injuries. This article describes nine steps to improve the ergonomic efficiency of the jewelry manufacturing environment, where there is high risk for repetitive stress injuries: acknowledge the problem(s), evaluate work positions, analyze tool design, improve workspace layout, check environmental conditions, develop ergonomic solutions, train workers in safety, perform ergonomic checkups and, if necessary, seek out ergonomics experts. Companies that have taken proactive measures have benefited from fewer injuries and illnesses. For instance, one company found that simply providing employees with $5 wrist supports reduced the incidence of carpal tunnel syndrome. A list of body parts and the repetitive motions that can injure them is included. *JEM-S*

The right image. G. Dawson, *American Jewelry Manufacturer*, Vol. 43, No. 5, May 1998, pp. 92–96.

Photographing jewelry and gemstones is especially difficult because of their highly reflective surfaces and the problems associated with capturing subtle colors. To overcome these challenges, the author (a goldsmith-photographer) has developed several photographic techniques. He recommends using interchangeable lenses and a camera body that allows complete manual operation. A long macro lens permits a greater working distance, which is useful in avoiding reflections from metals or gemstones. A diffusion tent can also be helpful in this regard. Another suggestion is to use an off-camera flash with a warming filter to bring out the richness of gold. A light meter is essential, and several exposures bracketing the meter reading in half-stop increments should be taken. A multitude of shots of the same object, with subtle variations in lighting or angle, is recommended for important pieces. *MD*